2016

Effects of Mammalian Target of Rapamycin Inhibition on Circuitry Changes in the Dentate Gyrus of Mice after Focal Brain Injury

Corwin R. Butler
University of Kentucky, crbu222@uky.edu
Digital Object Identifier: http://dx.doi.org/10.13023/ETD.2016.182

STUDENT AGREEMENT:

I represent that my thesis or dissertation and abstract are my original work. Proper attribution has been given to all outside sources. I understand that I am solely responsible for obtaining any needed copyright permissions. I have obtained needed written permission statement(s) from the owner(s) of each third-party copyrighted matter to be included in my work, allowing electronic distribution (if such use is not permitted by the fair use doctrine) which will be submitted to UKnowledge as Additional File.

I hereby grant to The University of Kentucky and its agents the irrevocable, non-exclusive, and royalty-free license to archive and make accessible my work in whole or in part in all forms of media, now or hereafter known. I agree that the document mentioned above may be made available immediately for worldwide access unless an embargo applies.

I retain all other ownership rights to the copyright of my work. I also retain the right to use in future works (such as articles or books) all or part of my work. I understand that I am free to register the copyright to my work.

REVIEW, APPROVAL AND ACCEPTANCE

The document mentioned above has been reviewed and accepted by the student's advisor, on behalf of the advisory committee, and by the Director of Graduate Studies (DGS), on behalf of the program; we verify that this is the final, approved version of the student's thesis including all changes required by the advisory committee. The undersigned agree to abide by the statements above.

Corwin R. Butler, Student

Dr. Bret N. Smith, Major Professor

Dr. Bret N. Smith, Director of Graduate Studies

EFFECTS OF MAMMALIAN TARGET OF RAPAMYCIN INHIBITION ON CIRCUITRY CHANGES IN THE DENTATE GYRUS OF MICE AFTER FOCAL BRAIN INJURY

DISSERTATION

A dissertation submitted in partial fulfillment of the requirements for the degree of Doctor of Philosophy in the College of Medicine at the University of Kentucky

By:

Corwin Randall Butler

Director: Bret N. Smith, Professor of Physiology

Lexington, KY

2015

ABSTRACT OF DISSERTATION

EFFECTS OF MAMMALIAN TARGET OF RAPAMYCIN INHIBITION ON CIRCUITRY CHANGES IN THE DENTATE GYRUS OF MICE AFTER FOCAL BRAIN INJURY

Post-traumatic epilepsy is a common outcome of severe traumatic brain injury (TBI). The development of spontaneous seizures after traumatic brain injury generally follows a latent period of little to no symptoms. The series of events occurring in this latent period are not well understood. Additionally, there is no current treatment to prevent the development of epilepsy after TBI (i.e. antiepileptogenics). One cell signaling pathway activated in models of TBI and in models of epilepsy is the mammalian target of rapamycin (mTOR). mTOR activity is sustained for weeks after the initial insult in models of TBI, and the inhibition of mTOR using rapamycin has shown promising pre-clinical outcomes in rodent models. This makes rapamycin an ideal therapeutic to test various outcomes associated with epileptogenesis after TBI. The results from this study suggest that rapamycin treatment after controlled cortical impact reduces aberrant axonal sprouting of ipsilateral dentate granule cells, prevents increased neurogenesis in the subgranular zone, and differentially alters phasic and tonic inhibition in dentate granule cells. However, rapamycin treatment did not prevent all forms of axon sprouting in the dentate gyrus or cell loss in selected regions of the hippocampus. Collectively these results support a role of mTOR activity in both excitatory and inhibitory plasticity in the mouse dentate gyrus after TBI.

KEYWORDS: Traumatic Brain Injury, Epilepsy, Mammalian Target of Rapamycin

_____Corwin R Butler_____

_____Date_____

EFFECTS OF MAMMALIAN TARGET OF RAPAMYCIN INHIBITION ON CIRCUITRY CHANGES IN THE DENTATE GYRUS OF MICE AFTER FOCAL BRAIN INJURY

By

Corwin Randall Butler

Bret N. Smith

(Director of Dissertation)

Bret N. Smith

(Director of Graduate Studies)

(3/9/14)

For my wife, Annabelle, and my

parents, Randy and Donna Butler

ACKNOWLEDGEMENTS

The following thesis, while an individual work, benefited from the insights and direction of several people. First, my Thesis Chair, Dr. Bret N Smith, who gave me the opportunity to pursue my research questions with guided freedom. I owe a great amount of the knowledge I have learned over the last 5 years to Bret and am very thankful to have had him as my mentor. My dissertation advisory committee which consisted of Drs. Steve Estus, Kathy Saatman, and Eric Blalock, did not give me an easy route through graduate school and I am thankful for the challenging and thoughtful questions given to me when we met. Due to their constant demand for improvement I became a much better scientist and will be ever thankful for pushing me to attempt to fulfill my potential as a scientist.

In addition, Drs. Jeffery and Carie Boychuk provided timely and instructive comments and evaluation at every stage of the thesis process, since arriving in Bret Smith's lab. I want to thank them for the many hours, days, and weeks of time that they spent helping me to better present my data and understanding of the field of research I was interested in. Before the two of them joined the lab, I did not have a post-doctoral mentor to help guide me along the way, and ever since they joined the lab my progress has exponentially improved. Next, I wish to thank the other members of the Smith lab, who were there with helpful criticisms during lab meetings or other practice presentations to improve my work. Each individual provided insights that guided and challenged my thinking, substantially improving the finished product.

Additionally, I would like to thank my friends and family for providing support and care over the course of this dissertation process. My parents, Randy and Donna Butler, called every week to make sure that I was ok, and even though it was not always something they understood or I would not always do a good job of explaining what it was that I was working on at that time, they were always there to listen. Also, I would like to thank my brother, Cameron, and his wife, Anna, for the support and encouragement they not only provided me during this process, but also for the support they gave to my wife, Annabelle. My wife's family, John, Carla, Drake, and Hope, was also important to both me and my wife during this time. They not only helped support Annabelle and I during

this process but have been a wonderful and welcoming second family in Lexington for me while not always able to visit my own family. Last but most important of all, I would like to thank my wife, Annabelle. Not only was she able to withstand our first conversation in which I attempted to impress her with neuroscience information that any other girl would have likely found annoying or weird, but she has put up with me in all the highs and lows of this dissertation process being the loving wonderful woman she is! I am also forever in her debt because of her assistance during some of my data analysis, as she was willing to randomly assort the data and blind me to experimental groups in several of the data collections presented in this dissertation. I love you and do not know how you are able to put up with me sometimes, but one day I hope to help you just as much as you have helped me over the years.

TABLE OF CONTENTS

LIST OF TABLES

LIST OF FIGURES

Chapter 1

Introduction

1.1 Historical perspective

Epilepsy is a disorder which has been qualitatively described dating back to the Babylonian empire around 700 BC in the *Sakkiku* text (York III, 2005). Although the concept of the brain had anatomically been described in 1700 BC by the ancient Egyptians in the *Edwin Smith Surgical Papyrus* (Hughes, 1988), the association of epilepsy as a brain disorder was not made until 400 BC by Hippocrates, a Greek physician (Magiorkinis et al., 2010). At the time of the initial description of epilepsy, the disorder was more commonly attributed to demonic or ghostly possession, in large part due to the nature of physical uncontrollable convulsions and non-recollection of the events in the patients after their seizures (York III, 2005). At the turn of the 18^{th} and 19^{th} centuries there was a shift in mindset regarding epilepsy as a spiritual or demonic possession disorder to a medical disorder associated with the brain (Magiorkinis et al., 2010;Sidiropoulou et al., 2010). One of the most prominent physicians associated with this shift in mindset is John Hughlings Jackson, whose insights have been credited as the beginnings of modern epileptology. The most common medical practice during this period for the treatment of seizures was the use of surgical procedures, and it was not until the early 1900's that pharmaceutical therapies were discovered and used to treat patients with epilepsy (Hauptmann, 1912;Magiorkinis et al., 2014). Seizure medications were developed as anticonvulsants and to this day all seizure medications, while improved in tolerability and safety for the patient can only be classified as anticonvulsants. Although surgical procedures are available in some cases for patients

with epilepsy, this treatment strategy is considered a last resort due to the damage caused during tissue resection. The complete lack of treatments that block or reverse the development of epilepsy continues to be the most glaring need in the field of epilepsy therapeutics.

1.2 Clinical perspective

Epilepsy is defined by the International League Against Epilepsy (ILAE) as the occurrence of two unprovoked seizures more than 24 hours apart. Today, epilepsy is the 4th most common neurological disorder, affecting ~2.2 million people in the United States of America. Epilepsy is now classified as a spectrum of seizure disorders (Jensen, 2011) commonly divided into two classes, idiopathic and symptomatic (Mody et al., 1992b). The Commission on Classification and Terminology of the ILAE defines idiopathic epilepsy as a seizure syndrome in which there is no known cause, but has been generally linked with genetic disorders; while symptomatic epilepsy, a seizure syndrome in which the cause is known, is generally caused by a physical or environmental insult to the brain in a previously healthy patient. In many cases of symptomatic epilepsy there is a latent period, typically months to years, following the initial insult to the brain and prior to the development of spontaneous seizures in which potential remodeling of the brain could be responsible for increased spontaneous seizures. Epileptogenesis is defined as the cascade of events from the initial insult to development of spontaneous seizures and epilepsy. The neurological processes during this latent period prior to seizure generation are still not well understood and their identification is critical in our understanding of epileptogenesis following brain injury.

The overarching problem with all of the current treatment strategies for patients with epilepsy is that none of the treatments available prevent or reverse the development of epilepsy in these patients. All of our current medications for epilepsy patients could therefore be categorized as anticonvulsants, with no current treatment which could be considered an antiepileptogenic. This is a serious concern in particular for patients which acquire epilepsy as a result of some form of brain trauma. These patients will have to continue anticonvulsant therapy, assuming they are not part of the ~30% of patients with acquired epilepsy which is resistant to seizure medication, for the rest of their lives.

Most of the trials done in humans to test antiepileptogenic effects of various pharmacological agents have been done using anticonvulsant seizure medications developed before the 1980's (Temkin et al., 2009). Additionally, many of these first trials were performed with no experimental models of posttraumatic epilepsy (PTE) available, and therefore were done with little or no guidance from the basic science perspective. The drugs that have been used in attempting to treat PTE include phenytoin, phenobarbital, carbamazepine, and valproate. The first attempt at an antiepileptogenic trial was performed in the 1940's using phenytoin (Hoff and Hoff, 1947). This initial study reported that phenytoin treatment reduced development of seizures to 6% of patients compared to the 51% of patients which developed seizures without treatment. However this study had many flaws in its design, such as lack of proper controls and biased treatment groups. Therefore, studies using more rigorous designs and current standards for clinical trials, such as random assignment to treatment, followed up this work. These trials determined that phenytoin treatment following traumatic brain injury (TBI) reduced the early seizure development (<1 week post-injury), but did not affect

development of late seizures (McQueen et al., 1983;Young et al., 1983;Temkin et al., 1990;Temkin et al., 1998). The use of phenobarbital, the first seizure medication, as an antiepileptogenic did not result in positive outcomes (Manaka, 1992;Temkin et al., 1998). Combining phenytoin and phenobarbital in some reports were encouraging, but sample sizes for these studies were small and therefore it is unclear if these results are meaningful or not (Popek and Musil, 1969;Penry and Newmark, 1979;Temkin et al., 1995). The use of carbamazepine in one study demonstrated similar results as phenytoin treatment alone, with a reduction in early seizures but no effect on late seizures (Glotzner et al., 1983). Similarly, valproate treatment as an antiepileptogenic therapy showed no positive effects on late seizures (Temkin et al., 1999). Magnesium, though not a common treatment strategy for patients with seizure disorders, was also used in a clinical trial for TBI patients. Unfortunately, there was no effect on seizure frequency in patients which received magnesium treatment in either the early or late seizure development (Temkin et al., 2007). The lack of positive results from previous human trials on potential antiepileptogenic treatments further underscores the point that antiepileptogenic therapies are in desperate need. Additionally the development of animal models of PTE in the last 20 years has given researchers tools to begin investigation of potential antiepileptogenic treatment strategies which can benefit future clinical trials in humans.

The recent development of rodent models of PTE has allowed the potential to begin testing of therapeutic strategies for the possible mechanisms underlying the development of PTE. Although recent pre-clinical trials involving potential antiepileptic drugs are currently underway, none have proven effective yet. Therefore, the primary course of treatment for patients with epilepsy continues to be a regimen of broad

spectrum anticonvulsants such as levetiracetam and gabapentin. The exact mechanism of action for levetiracetam is not known, but this drug does interact with synaptic binding proteins involved in exocytosis in the rat brain and is thought to be part of its anticonvulsant effects (Abou-Khalil, 2008). The mechanism of action for gabapentin is thought to involve increased production of GABA in neurons based on spectroscopy studies in human and rat tissue indicating increased GABA synthesis, although the exact process by which this occurs remains unclear (Taylor, 1997). These drugs in general are used as anticonvulsants, but neither address the underlying mechanisms of action related to epileptogenesis in patients with symptomatic epilepsies. Consequently, most patients must stay on these drugs for the rest of their lives, and generally need increased dosage over time due to reduced drug efficacy (Löscher and Schmidt, 2006). Additionally, these drugs can cause a multitude of side effects ranging from loss of appetite to severe depression. The lack of reversion from disease state and potential for severe side effects with current pharmacologic treatment strategies again underscores the importance of research for antiepileptogenic therapies.

There are data to support focusing on the temporal lobe structures for temporal lobe epilepsy (TLE) and PTE (Caveness et al., 1979;Cronin et al., 1992;Buckmaster and Schwartzkroin, 1994;Annegers et al., 1998;Diaz-Arrastia et al., 2000;Englander et al., 2003;Winokur et al., 2004;Epsztein et al., 2005). Identifying the region(s) of maladaptive neuronal reorganization may be fundamental to our treatment of TBI and seizure development. In the human patient population, seizure foci are characterized based on their location in partial seizures, but there are also complex/global seizure syndromes. Most typical foci after TBI involve either cortical or temporal lobe structures (Diaz-

Arrastia et al., 2000;Hudak et al., 2004). Temporal lobe structures include the amygdala, auditory cortex, entorhinal cortex, and hippocampus. Of structures within the temporal lobe, the hippocampus is one of the most effected regions in both the TBI animal models and PTE patient population (Newcomb et al., 1997;Annegers et al., 1998;Englander et al., 2003;Hudak et al., 2004;Hall et al., 2005;Saatman et al., 2006). In patients with TLE, several structural and functional changes have been observed in human resected tissue, which has given basic scientists points of emphasis to focus on in modeling this disease as well as areas of focus for therapeutic targeting. Some of the noted changes in hippocampal structure and function in TLE patients are regional cell loss (i.e. hilus, CA3, and CA1), axon sprouting of dentate granule cells back into dendritic field of neighboring dentate granule cells (i.e. mossy fiber sprouting), and imbalanced excitatory and inhibitory circuitry (de Lanerolle et al., 1989;Sutula et al., 1989;Lehmann et al., 2000). Ideal models of TLE and PTE should have these features in order to test effects of antiepileptogenic therapy strategies and to help delineate causal features of epilepsy versus correlative features.

One theory of epileptogenesis postulates that the reorganization of neuronal circuitry within specific brain regions is central to the development of the disease. Several classical examples of reorganization for this theory have been cell loss, synaptic reorganization, axonal sprouting, and neurogenesis as contributing factors to the epileptogenic process. According to the Epilepsy Foundation, approximately 1% of the population has epilepsy (i.e. 65 million people worldwide), of which 30-40% are patients with acquired epilepsy. In a population study of acquired epilepsy patients, a group out of Rochester demonstrated that 6% of acquired epilepsy is due to traumatic brain injury (i.e.

PTE), which was the second highest of the known causes category (Hauser et al., 1993). Additionally, ~30% of these epilepsy patients are unresponsive to current medical interventions. This dissertation focuses on PTE among all of the epilepsies because it is a prominent source of acquired epilepsy and comprises a significant portion of the drug-resistant epilepsy population (Caveness et al., 1979;Annegers et al., 1998;Semah et al., 1998;Englander et al., 2003;Chepreganova-Changovska et al., 2014). It may be possible to block the epileptogenetic process in symptomatic epilepsy by giving appropriately timed treatment, if the precipitating event is known, such as in the case of individuals who suffer TBI. The focus of this dissertation is on how one intracellular cell signaling pathway, the mammalian target of rapamycin (mTOR) pathway, regulates these cell circuitry changes in the hippocampus following brain insult. mTOR signaling was selected for these studies because it has a demonstrated role in excitatory synaptic reorganization after brain insult and is currently being considered as an antiepileptogenic treatment for tuberous sclerosis and PTE (Zeng et al., 2008;Buckmaster et al., 2009;Zeng et al., 2009;Guo et al., 2013;Heng et al., 2013).

1.3 Basic Science Perspective

1.3.1 Modeling PTE in animals

The use of animal models for epilepsy syndromes has advanced the collective understanding of cellular mechanisms associated with the development of epilepsy. Additionally the development of these animal models can contribute to the identification of different therapeutic strategies for various seizure disorders. This section discusses frameworks for evaluating animal models of disease, reviews the 2 major animal models

of PTE, and discusses the types of cell biology changes observed in models of TLE in order to both support a role for temporal structures in epilepsy and discuss several candidate cellular mechanisms of epilepsy.

There are several important considerations for modeling human disease in animals, including types of epilepsy such as PTE. Some of the considerations for use of animal models for human disease include construct, face and predictive validity (Willner, 1984).Construct validity is the ability to reproduce cellular features or mechanisms of the human condition. Face validity is assessed by the similarity to behavioral outcomes of the model to the human condition. Predictive validity is assessed by the ability of the model to mimic clinical outcomes and potency of therapeutic interventions. Animal models to induce experimental seizures include administration of chemical convulsants, mechanical injury, and electrical stimulation. This dissertation focuses on PTE so has avoided use of the chemical convulsant and electrical stimulation approaches to seizure generation. Three of the most commonly used mechanical injury models used for modeling TBI are fluid percussion injury (FPI), weight drop, and controlled cortical impact (CCI). However, of these models only FPI and CCI have demonstrated occurrence of spontaneous seizure generation (i.e. PTE) following a latent period after injury (D'Ambrosio et al., 2004;D'Ambrosio et al., 2005;Kharatishvili et al., 2006;D'Ambrosio et al., 2009;Hunt et al., 2009;Statler et al., 2009;Bolkvadze and Pitkanen, 2012;Guo et al., 2013;Kelly et al., 2015). This dissertation used the CCI model, as opposed to the FPI model, for several reasons. The main reasons for selecting CCI were: shorter latency to seizure generation, better injury severity management, and better reproducibility of focal injury. These are discussed in detail in the following sections. These sections are

followed by more complete descriptions of the most studied cell circuitry mechanisms of epilepsy.

1.3.2 Fluid percussion injury

FPI is a diffuse neuronal injury during which a craniotomy is made and saline fluid is injected from a device pressurized by the strike of a hammer swung on a pendulum, and was initially developed for cats and rabbits (Hayes et al., 1987;Stalhammar et al., 1987). This is one of the most well characterized brain injury models and demonstrates many of the hallmark features of TBI in human patients such as neuron loss, diffuse axonal injury, and cognitive impairment (Cortez et al., 1989;Lowenstein et al., 1992;Hicks et al., 1993;Rink et al., 1995;Bramlett et al., 1997;Hicks et al., 1997;Saatman et al., 1997;Conti et al., 1998;Pierce et al., 1998;Saatman et al., 1998;Knoblach and Faden, 2002). This injury has been most commonly done either as a midline FPI (Dixon et al., 1987;McIntosh et al., 1987) or a lateral FPI (i.e. injury focal to one hemisphere) (McIntosh et al., 1989). The use of FPI as an injury model for PTE has primarily focused on the lateral FPI method. Additionally, the use of lateral FPI as a model of PTE has generally involved a severe injury model in which the pressure of fluid injected into the epidural space creates a focal lesion at the site of injection. This has commonly led to the interpretation of this injury model being one of focal and diffuse injury. Using this severe lateral FPI model, rats (up to 50%) and mice (3%) have demonstrated spontaneous seizures by 12 months following injury (D'Ambrosio et al., 2004;D'Ambrosio et al., 2005;Kharatishvili et al., 2006;D'Ambrosio et al., 2009;Bolkvadze and Pitkanen, 2012).

However, the seizures generated using this model are generally low in frequency and latency to the first seizure generation is 6-7 months, making this model very labor intensive. The prolonged latency between the initial injury and seizure generation makes this model of TBI difficult to determine cellular mechanisms associated with epileptogenesis. Spontaneous seizure development in the FPI model of TBI with less severe impact forces (impact forces from 2-2.2 atmospheres (atm)) has not been demonstrated currently (Kharatishvili et al., 2006;Echegoyen et al., 2009;Gurkoff et al., 2009). Subtle behavioral changes associated with brief electrographic abnormalities have been defined as a new category of seizure in recent work using a variation of lateral fluid percussion injury (D'Ambrosio et al., 2004;D'Ambrosio et al., 2005;D'Ambrosio et al., 2009). This new category of seizures, however, is largely debated, and has even been noted in non-injured animals (Pearce et al., 2014;Rodgers et al., 2015). FPI injury with greater impact forces (>3 atm) in rodents does result in spontaneous seizure development (Kharatishvili et al., 2006;Bolkvadze and Pitkanen, 2012). The variability in fluid pressures used for the injury severity makes comparison of studies difficult. As previously mentioned, the forces necessary to generate spontaneous seizures after FPI generally result in both a focal lesion in the cortex as well as a diffuse injury. The combination of a focal and diffuse injury in the severe FPI injury makes interpretation of the cause of epileptogenesis difficult in this model. Due to these concerns with modeling, FPI injury was not used to model PTE in this dissertation.

1.3.3 Controlled cortical impact

The use of controlled cortical impact to model TBI was originally developed for ferrets (Lighthall, 1988), and has since been modified for both rats and mice (Dixon et

al., 1991;Smith et al., 1995;Scheff et al., 1997;Hall et al., 2005). This injury model uses a computer controlled pneumatically driven impactor, which can be adjusted for impact depth, velocity, and dwell time. A craniotomy is performed so as to leave to underlying dura intact and the resulting cortical compression creates a contusion injury without lacerating the dura. The ability to modify injury parameters such as injury depth, velocity and dwell time allow for a consistent and reproducible injury which can also be scaled for different injury severities and different animal models. The use of this injury model has generated both electrographically measured and observed spontaneous behavioral seizures in mice and rats following a latent period after injury in a subset of rodents ranging from 20-50% (Hunt et al., 2009;Statler et al., 2009;Bolkvadze and Pitkanen, 2012;Guo et al., 2013;Butler et al., 2015;Kelly et al., 2015). Additionally the seizures generated in this model occur at a shorter latency compared to FPI models, ~8 weeks in CCI compared to 6-7 months in FPI. However, there are strain differences in PTE development latency for this model (Hunt et al., 2009;Bolkvadze and Pitkanen, 2012). The rodents which undergo epileptogenesis in this model also demonstrate many of the hallmark cell circuitry changes associated with established models of TLE such as regional cell loss, hyperexcitability of dentate granule cells, synaptic and tonic inhibitory plasticity of dentate granule cells, and axon sprouting in the ipsilateral hemisphere after CCI injury. Additionally, use of isoflurane for anesthesia in the CCI model, as was used in this work, can have neuroprotective outcomes in this TBI model compared to another anesthetic (fentanyl; (Statler et al., 2006). However, in this study all mice were equally treated with isoflurane, therefore changes in cell loss or neuroprotection from use of isoflurane should be equivalent across experimental groups. As a result, these reported

cell circuitry changes can be evaluated with CCI in the context of drug development. These circuitry changes are described below.

1.4 Candidate cell circuit mechanisms of PTE

Within the hippocampus, the dentate gyrus is an important site of excitability regulation and one of the most well understood circuits involved in seizures and epilepsy (Danscher et al., 1975;Heinemann et al., 1991;Franck et al., 1995). The hippocampus is comprised of a tri-synaptic circuit (Andersen et al., 1971;Lothman et al., 1991;Freund and Buzsaki, 1996). Information is sent from perforant path inputs of the entorhinal cortex to the dendrites of dentate granule cells. Dentate granule cells, through mossy fiber inputs, synapse onto CA3 pyramidal neurons, which in turn synapse onto CA1 pyramidal neurons. CA1 neurons then project back to the entorhinal cortex in addition to non-hippocampal targets (Franck et al., 1995). The hippocampus maintains a delicate balance of excitation and inhibition for appropriate information processing. It has been theorized that the dentate granule cells play a critical role in preserving this balance by acting as a "dentate gate" (Heinemann et al., 1991). The "dentate gate" theory is derived from both the physiology and input to dentate granule cells. For example, the resting membrane potential of dentate granule cells is hyperpolarized (~-70mV) compared to many of the other cell types in the hippocampus and throughout the brain (Cronin et al., 1992;Mody et al., 1992a;Mody et al., 1992b;Staley and Mody, 1992;Staley et al., 1992). This hyperpolarized resting membrane potential requires greater depolarizing currents to reach action potential threshold. Additionally, there are multiple inhibitory inputs to dentate granule cells largely arising from inhibitory interneurons in the hilus of the dentate gyrus, which are believed to also contribute to the "dentate gate". Many of these inhibitory

neurons are activated by either dentate granule cells or perforant path inputs causing a feedback inhibitory circuit onto dentate granule cells (Zipp et al., 1989;Han et al., 1993).

Hilar inhibitory interneurons are divided into several classes of cell types synapsing at dendritic, somatic, and axonic locations of dentate granule cells. This means under normal conditions inhibitory synapses on dentate granule cells are located along the entirety of their somatodendritic axis. Some of the more prominent hilar inhibitory interneurons are basket cells and hilar perforant path associated (HIPP) cells. Basket cells are mostly located along the border between the subgranular zone of the dentate granule cells and the hilus (Houser, 2007). These neurons provide somatic inhibition of dentate granule cells and based on the positioning of their apical dendrites receive synaptic input from dentate granule cells and potentially perforant path input from the entorhinal cortex (Zipp et al., 1989;Blasco-Ibanez et al., 2000). Basket cells project to neighboring dentate granule cells in somatic regions (Han et al., 1993). Input from dentate granule cells onto basket cells provides feedback inhibition onto neighboring dentate granule cells, while perforant path input onto basket cells provides a mechanism for feed forward inhibition of dentate granule cells. The HIPP cells have cell bodies located in the hilus and receive the majority of synaptic input from dentate granule cells (Halasy and Somogyi, 1993;Han et al., 1993). These neurons project and synapse into the outer two-thirds of the inner molecular layer of the dentate gryus, the dendritic field of dentate granule cells. One subset of the HIPP neurons is the somatostatin-positive hilar neurons which have been noted to project onto dentate granule cell dendrites directly across from entorhinal cortex excitatory inputs (Buckmaster et al., 1994). Due to the placement of these inhibitory synapses from somatostatin-positive hilar interneurons onto dentate granule cells and

activation of these hilar inhibitory interneurons by dentate granule cells, somatostatin-positive hilar interneurons are believed to provide feedback inhibition to dentate granule cells and shunt potential burst firing from the entorhinal cortex onto dentate granule cells. This role is potentially important to preventing over-excitation of dentate granule cells in normal physiology. Figure 1.1 gives a general representation of the local dentate gyrus circuitry highlighting the primary cell groups discussed in this dissertation; dentate granule cells, hilar inhibitory interneurons, and CA3 pyramidal neurons.

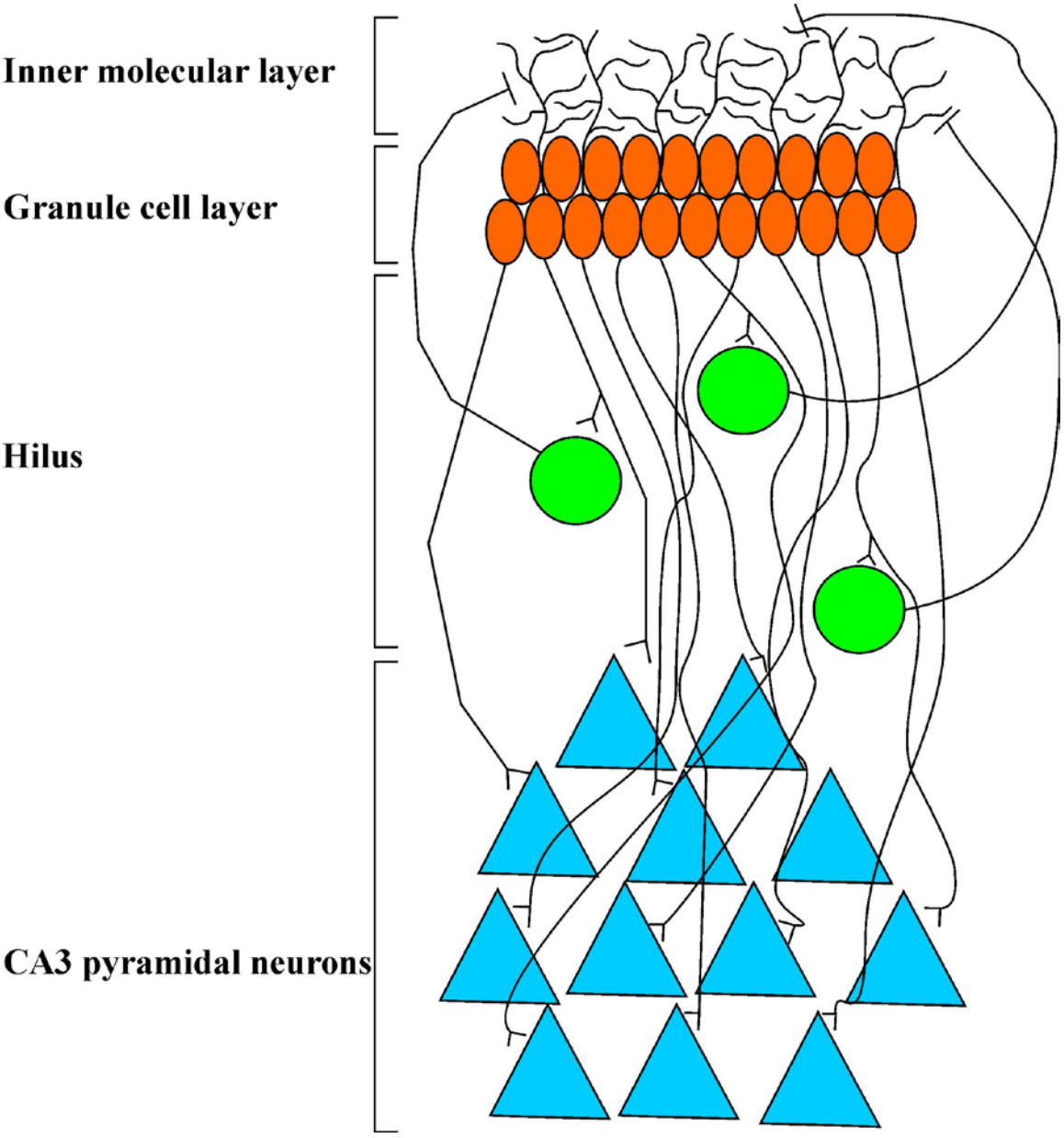

Figure 1.1. Representation of local circuit of dentate gyrus of the hippocampus in normal conditions. Normal information flow involves the excitation of dentate granule cells from perforant path inputs of the entorhinal cortex. Dentate granule cells synapse onto hilar inhibitory interneurons for feedback inhibition and CA3 pyramidal neurons to propagate information flow through the hippocampus.

1.4.1 Alterations to dentate gyrus in TLE and PTE

As previously mentioned, alterations of hippocampal structure and function have been observed in human resected tissue from patients with TLE and PTE, and animal

models of PTE should ideally capture these cell circuitry changes associated with PTE. Using the CCI model of TBI in rodents to model the development of PTE many hippocampal cell circuitry changes have been observed. However, it remains unclear which of these functions is most important to the development of seizures and epilepsy following TBI. Observed changes to hippocampal structure associated with the epileptogenic process include: regional cell loss (Anderson et al., 2005;Guo et al., 2013), enhanced neurogenesis (Dash et al., 2001;Chirumamilla et al., 2002;Villasana et al., 2014;Villasana et al., 2015), altered inhibitory control of dentate granule cells (Mtchedlishvili et al., 2010;Hunt et al., 2011;Boychuk et al., 2016), and axon sprouting (Hunt et al., 2009;Statler et al., 2009;Hunt et al., 2010;Hunt et al., 2012;Guo et al., 2013;Kelly et al., 2015). Many of these changes relate to the common theory of epilepsy, that a brain region such as the dentate gyrus/hippocampus following an insult becomes the center of imbalanced excitation and inhibition (Cronin et al., 1992;Buckmaster and Schwartzkroin, 1994;Dudek and Spitz, 1997;McCormick and Contreras, 2001;Buckmaster et al., 2002;Nadler, 2003;Hunt et al., 2009; 2010;Hunt et al., 2012;Hunt et al., 2013a). These mechanisms were the focus of this dissertation work and are discussed in more detail below.

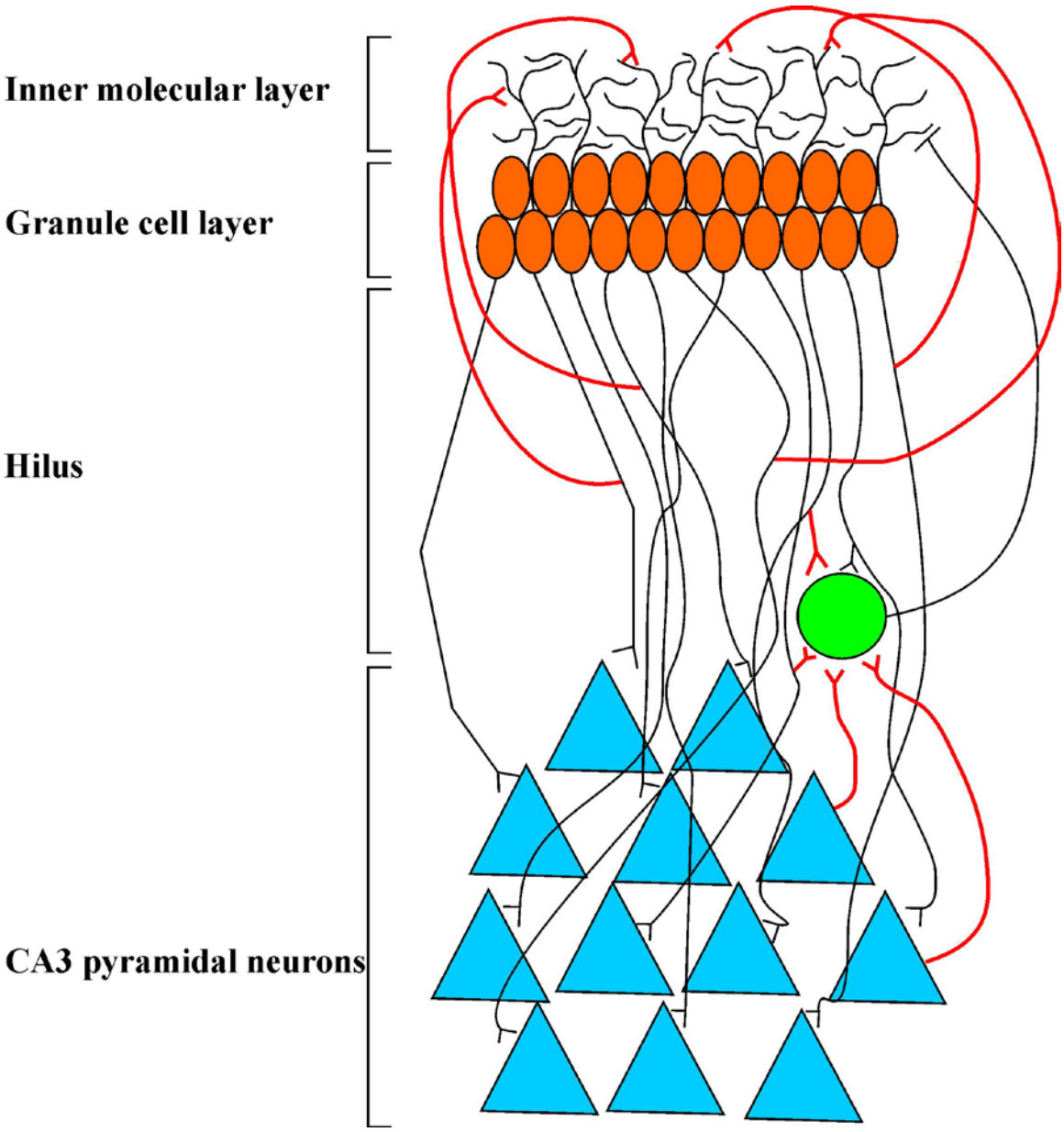

Figure 1.2: Representative image of altered local dentate gyrus circuit of hippocampus after TBI. This illustration demonstrates cell loss in hilus as well as axonal plasticity of both dentate granule cells and CA3 pyramidal neurons which have been observed in the ipsilateral hemisphere of CCI injured mice. These changes to cell circuitry may lead to hyperexcitability of the dentate gyrus and potentially seizure generation.

1.4.2 Cell loss

Following TBI, regional and selective cell loss is observed in the cortex and hippocampus of the injured hemisphere (Lowenstein et al., 1992;Hicks et al., 1993;Smith

et al., 1995;Anderson et al., 2005;Saatman et al., 2006). Regions of hippocampal cell loss following TBI injury include the dentate gyrus, CA3 pyramidal cell layer, and CA1 pyramidal cell layer. Cell death can be broken down into two phases after TBI (Werner and Engelhard, 2007). The first phase occurs in the minutes and hours after injury due to the mechanical forces of the injury causing death of cells, generally leading to necrosis. Necrotic cell death is different than programmed cell death (i.e. apoptosis) and can be characterized by loss of membrane integrity, early organelle damage, cell swelling, mitochondrial swelling, and cell lysis (Graham et al., 2006). In the CCI injury model, the primary region affected by this form of cell death is in the cortex due to the compression forces generated by the CCI device (Pleasant et al., 2011). The injury depth of most CCI-induced models of PTE, including the one used in this dissertation, does not reach the subcortical structures such as the hippocampus, but one report used a more severe CCI injury with increased injury depths, which affected hippocampal integrity (Mtchedlishvili et al., 2010). The secondary phase of cell death following injury is generally due to a cascade of cellular signaling factors associated with delayed tissue damage and often involves apoptosis (i.e. programmed cell death) of damaged neurons in the surrounding tissue, such as the hippocampus. This cell death is on the order of days to weeks following injury due to extracellular signaling which activates apoptosis in the surrounding damaged tissue.

In addition to cell death in the dentate granule cell layer, one of the most common features of both seizures and TBI is the loss of neurons in the hilus of the dentate gyrus (Lowenstein et al., 1992;Smith et al., 1995;Buckmaster and Dudek, 1997b). This cell loss generally peaks within the first three days after injury and gradually diminishes over the

following days until 7 days post-injury (Anderson et al., 2005). The neurons in this area of the hippocampus are prominently GABAergic interneurons and tend to form either somatic or dendritic inhibitory connections to dentate granule cells. One subset of hilar GABAergic interneurons is the somatostatin positive neuron. As previously mentioned, the cell bodies of somatostatin-positive interneurons are predominately in the hilus of the dentate gyrus and project axons into the outer two-thirds of the molecular layer of the dentate gyrus where dendrites of dentate granule cells reside (Bakst et al., 1986;Katona et al., 1999). The development of the FVB-TgN(GadGFP)45704Swn/J (i.e. GIN) mice (Oliva et al., 2000) created a model system in which this subset of somatostatin-positive interneurons produce enhanced green fluorescent protein (eGFP) so they could be selectively studied. Using these GIN mice and Sprague-Dawley rats, somatostatin-positive neurons have indeed been shown to be lost after pilocarpine-induced status epilepticus and TBI (Lowenstein et al., 1992;Buckmaster and Dudek, 1997b;Buckmaster and Wen, 2011). As stated previously, the synaptic connections of these hilar inhibitory interneurons are unique, and this has given rise to the hypothesis that these neurons could directly inhibit excitatory synaptic input onto dentate granule cells from perforant path projections of the entorhinal cortex. If this hypothesis is correct, the loss of these somatostin-positive interneurons in both models of TLE and TBI would dramatically alter the balance of excitatory and inhibitory input to dentate granule cells. Therefore, the loss of these neurons could be part of the epileptogenic process of PTE.

Cell loss is common to other regions of the hippocampus as well. Pyramidal neurons in both the CA3 and CA1 regions of the hippocampus are commonly lost in the ipsilateral hemisphere following TBI (Hicks et al., 1993;Smith et al., 1995;Saatman et al.,

2006). Most of the research on TBI and epilepsy has been performed with a tri-synaptic circuit understanding of hippocampal function. While this view of hippocampal circuitry and function is accurate, it is not the only circuit in the hippocampus. CA3 pyramidal neurons are likely part of another circuit in the hippocampus due to the excitatory input received by CA3 neurons from areas outside of the dentate gyrus and projection onto various neurons aside from CA1 pyramidal neurons, such as hilar inhibitory interneurons, mossy cells, and other regions outside the hippocampus. It remains unclear what effect cell loss in the CA3 region has on hippocampal circuitry, or if cell loss in this region contributes to the epileptogenesis process following TBI. This region is also prone to axon sprouting in the ipsilateral hemisphere, similar to dentate granule cells, which is discussed in later sections.

In the CA1 region both pyramidal neurons and inhibitory interneurons are lost following TBI and seizures (Hicks et al., 1993;Smith et al., 1995;Houser and Esclapez, 1996;Saatman et al., 2006;Peng et al., 2013). The loss of pyramidal neurons could impact the output of the tri-synaptic circuit of the hippocampus. Loss of inhibitory interneurons could also impact the excitatory and inhibitory balance of this region as well. Interestingly, there is evidence from the pilocarpine induced status epilepticus model of TLE that some of the surviving interneurons in the CA1 region sprout into the dentate gyrus (Peng et al., 2013). It is unclear what role this sprouting has in hippocampal remodeling or if this feature is even an effect of TBI or epileptogenesis. However, this data indicates modification of the hippocampus is not restricted to the dentate gyrus and changes in other regions could also contribute to the process of epileptogenesis.

1.4.3 Targeting cell loss as antiepileptogenic therapy

Reduction of cell loss following TBI has been a staple of targeted therapeutic strategies in the TBI field. Using the search words traumatic brain injury and neuroprotection in Pubmed, 1533 studies related to these topics have been performed over the last 20 years. Due to cell loss in epilepsy and TBI, neuroprotection is also a common treatment strategy for PTE. Most studies on therapeutic strategies following TBI have targeted the secondary/delayed tissue damage phase. These studies have generally attempted to enhance neuroprotection through the use of pharmacological treatment strategies including: 3-hydroxy-3-methylglutaryl coenzyme A reductase inhibitors, progesterone, allopregnanolone, erythropoietin, simvastatin, atorvastatin, and cyclosporine A (Zacco et al., 2003;Djebaili et al., 2005;Lu et al., 2007;Wang et al., 2007;Mazzeo et al., 2009). However, none of these potential pharmacological treatments have been proven effective in humans yet.

Another pharmacological treatment which has shown promise as an antiepileptogenic therapy and appears to function through neuroprotection is levetiracetam. Levetiracetam is a seizure medication which is commonly used for the treatment of partial onset and generalized seizures. The use of levetiracetam in a closed head injury and stroke model has shown neuroprotective properties of this drug (Wang et al., 2006;Zou et al., 2013). Although neither of these studies investigated seizure development, studies using chemical convulsant and electrical kindling models of status epilepticus have demonstrated potential for levetiracetam having anticonvulsant and/or antiepileptogenic properties (Loscher et al., 1998;Sugaya et al., 2010;Shetty, 2013). However, levetriacetam's effect on spontaneous seizures is controversial in the chemical

convulsant models of status epilepticus (Yan et al., 2005;Brandt et al., 2007), and it is unclear what the primary mechanism of action is for levetriacetam (Oliveira et al., 2007;Matveeva et al., 2008;Surges et al., 2008;Christensen et al., 2010;Kim et al., 2010). Further testing of this drug using a known PTE animal model and the effects of levetriacetam on spontaneous seizure development in the latent phase are necessary information to determine the potential of this drug as an antiepileptogenic.

Due to the lack of positive results in human testing of many pharmacological treatment strategies for neuroprotection after TBI, alternative therapies could prove useful. One alternative to pharmacological treatment strategies is the use of hypothermia after TBI for neuroprotection. The clinical use of hypothermia in TBI patients has resulted in a variety of outcomes likely due to variability in hypothermia parameters, experimental design, and small sample sizes for some studies (Clifton et al., 1993;Taft et al., 1993;Marion et al., 1997;Clifton et al., 2001). The use of hypothermia has demonstrated some potential as an antiepileptogenic strategy in an experimental animal model of TBI (Atkins et al., 2010). Blowing cool air on the exposed brain to reduce temperature to 33-33.6^{o}C resulted in a reduction of seizure susceptibility to PTZ-induced seizures 12 weeks after FPI injury (Atkins et al., 2010). Although this does not confirm hypothermia as an antiepileptogenic treatment option, it does demonstrate the potential for use of this treatment.

1.4.4 Neurogenesis

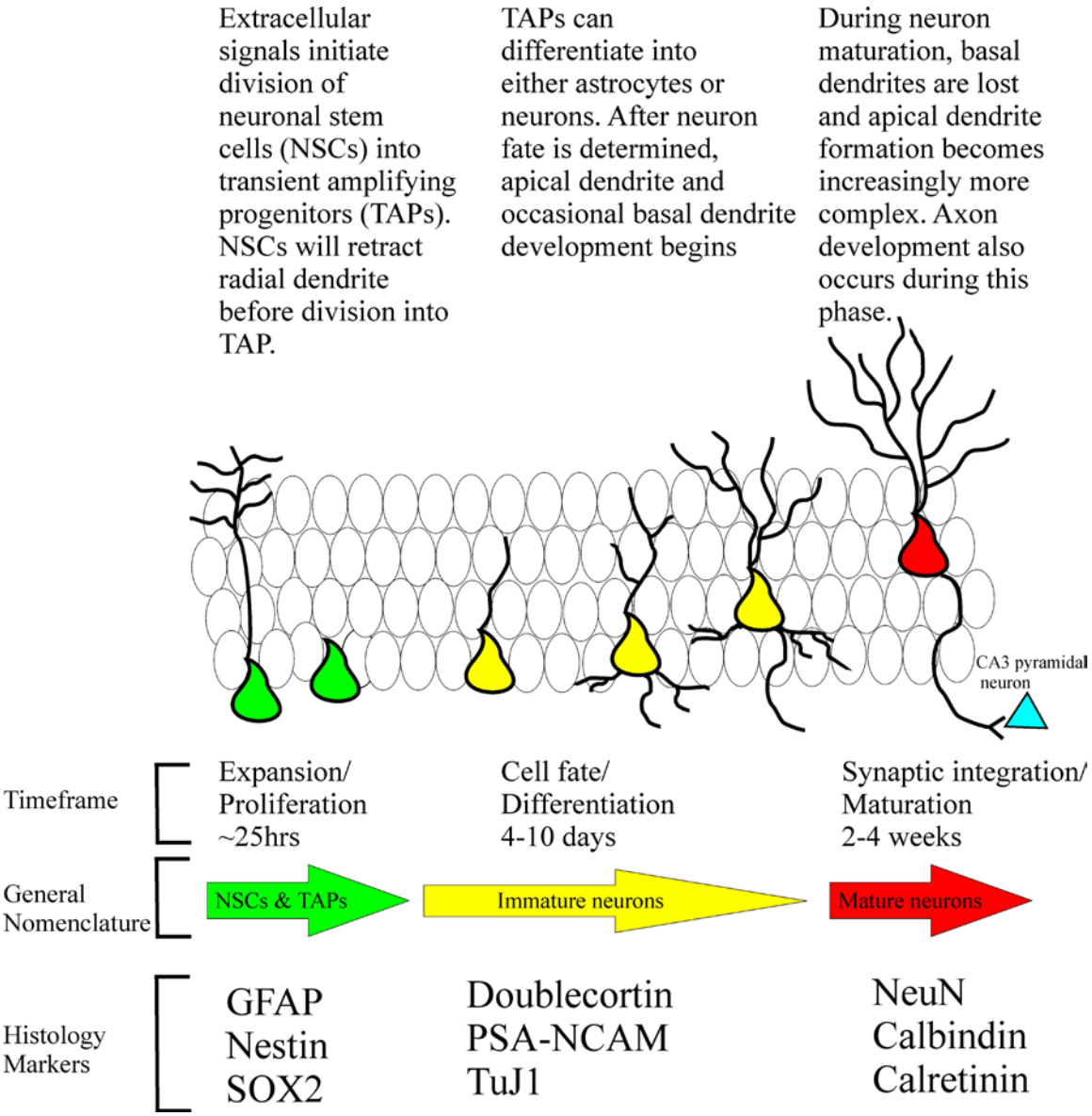

Figure 1.3. Representation of neurogenesis progression in subgranular zone of hippocampus. This illustration demonstrates morphological changes in dendrite and axon formation from progenitor neurons to mature neurons in the subgranular zone. It also depicts some of the signaling proteins expressed by the neurons at various points in development and approximate timeframe of these changes.

Two regions of the brain, the subventricular and subgranular zones, contain progenitor neurons which can differentiate into newborn neurons during adulthood (Altman and Das, 1965b;a;Gueneau et al., 1982;Eckenhoff and Rakic, 1988). The role of

these newborn neurons in the adult brain is still unclear in normal conditions, but in injury states such as seizures and TBI production of newborn neurons from the subgranular zone increases in the injured hemisphere relative to controls (Parent et al., 1998;Dash et al., 2001;Chirumamilla et al., 2002;Kron et al., 2010;Villasana et al., 2014;Villasana et al., 2015). Neurogenesis in the subgranular zone mimics the neurogenic process in the subventricular zone and neurogenesis during embryonic development. In the adult mammalian brain these neural progenitors are asymmetric self-renewing stem cells, which will divide into a cell that is fated to either become a postmitotc neuron or glia and the other cell will maintain the ability to self-renew. However, there are some distinctions between these different processes of neurogenesis.

In the subgranular zone, proliferating neuronal stem cells can be divided into two classes; type 1 and type 2 cells (Zhao et al., 2008). Type 1 neuronal stem cells morphologically resemble the radial glial cells, present during embryonic development, containing a single radial process with a ramified structure at its end (Kempermann et al., 2004). These type 1 neuronal stem cells express GFAP, Nestin, Blbp, and Sox2 (Duan et al., 2008). Type 2 neuronal stem cells do not exhibit the radial process of type 1 neuronal stem cells and are most commonly labeled with GFAP and Sox2 (Duan et al., 2008). Cell ablation studies have suggested a relationship of these two neuronal stem cell populations with mitotic activity levels. The acute ablation of dividing cells using antimitotic drugs or genetic manipulation resulted in suppression of neurogenesis. However, in the subgranular zone GFAP-positive neurons survived, and after the transient suppression of neurogenesis, new granule neurons were produced (Seri et al., 2004). These results suggest that neuronal stem cells contain both actively dividing neurons (i.e. type 2

neuronal stem cells) and infrequently dividing neurons(i.e. type 1 neuronal stem cells). The infrequently dividing neurons survive use of antimitotic drugs and are capable of repopulating the cells lost after cessation of ablation experiments. Both extrinsic and intrinsic cues assist in fating newly generated cells from the neuronal progenitors into either granule neurons or astrocytes in the hippocampus. Newly generated cells fated to become granule neurons express doublecortin (DCX), PSA-NCAM, and TuJ1 (Kempermann et al., 2004;Duan et al., 2008;Suh et al., 2009). Having been fated for granule neurons, these cells will begin developing apical and basal dendrites and an axon. In rodents the basal dendrites are lost during development into mature granule neurons and the axon will project and synapse onto CA3 pyramidal neurons. Mature dentate granule neurons express NeuN.

The role of newborn neurons in normal physiology continues to be poorly understood. Based on ablation studies, one of the more prominent theories associated with newborn neurons in the hippocampus is that these neurons contribute to learning and memory (van Praag et al., 2002;Doetsch and Hen, 2005;Ming and Song, 2005;Aimone et al., 2006). However, recent evidence suggests that increased production of newborn neurons correlates to epilepsy generation (Pun et al., 2012;Hester and Danzer, 2013;LaSarge et al., 2015). In fact, using a genetic mouse model to promote increased neurogenesis in ~5-10% of genetically targeted dentate granule cells was sufficient to promote behavioral seizures after a latent period (LaSarge et al., 2015).

1.4.5 Targeting neurogenesis for antiepileptogenic therapy

Neurogenesis continues to be one of the least understood forms of experience dependent plasticity events in the brain. Due to this lack of knowledge, little is known about the potential of this mechanism for antiepileptogenic therapy. In disease states such as TBI and epilepsy, rodent models have exhibited increased production of newborn neurons at 2 weeks after the initial insult (Parent et al., 1997;Parent et al., 1998;Dash et al., 2001;Chirumamilla et al., 2002;Kron et al., 2010;Villasana et al., 2014;Butler et al., 2015;Villasana et al., 2015). This increase in production is theorized as a mechanism for endogenous cell replacement in this region, and TBI literature supports a hypothesis that increased newborn neurons after TBI leads to improved cognition (Lu et al., 2005;Sun et al., 2009;Xiong et al., 2012;Carlson et al., 2014). However, the production of newborn neurons is also increased in models of epilepsy (Pun et al., 2012;Hester and Danzer, 2013;LaSarge et al., 2015). Considering the relationship of PTE as a consequence of a significant portion of the TBI population, targeting neurogenesis as an antiepileptogenic treatment strategy is of particular interest. However before neurogenesis is targeted for antiepileptogenic therapies, much needs to be clarified in regard to the relationship of neurogenesis to improved cognitive recovery and potential mechanism of epileptogenesis after TBI. Currently, a report claims that newborn neurons in the ipsilateral hemisphere of CCI injured mice will integrate normally compared to age-matched cotnrols (Villasana et al., 2015). However, this study was done at a time (4 weeks post-injury) when cellular circuit changes have not been noted. The newly born ipsilateral dentate granule cells did display abnormal dendritic morphology, so further studies of changes to newborn dentate

granule cell function and connectivity are required to assess the contribution of this process in epileptogenesis.

1.4.6 GABAergic plasticity of dentate granule cells

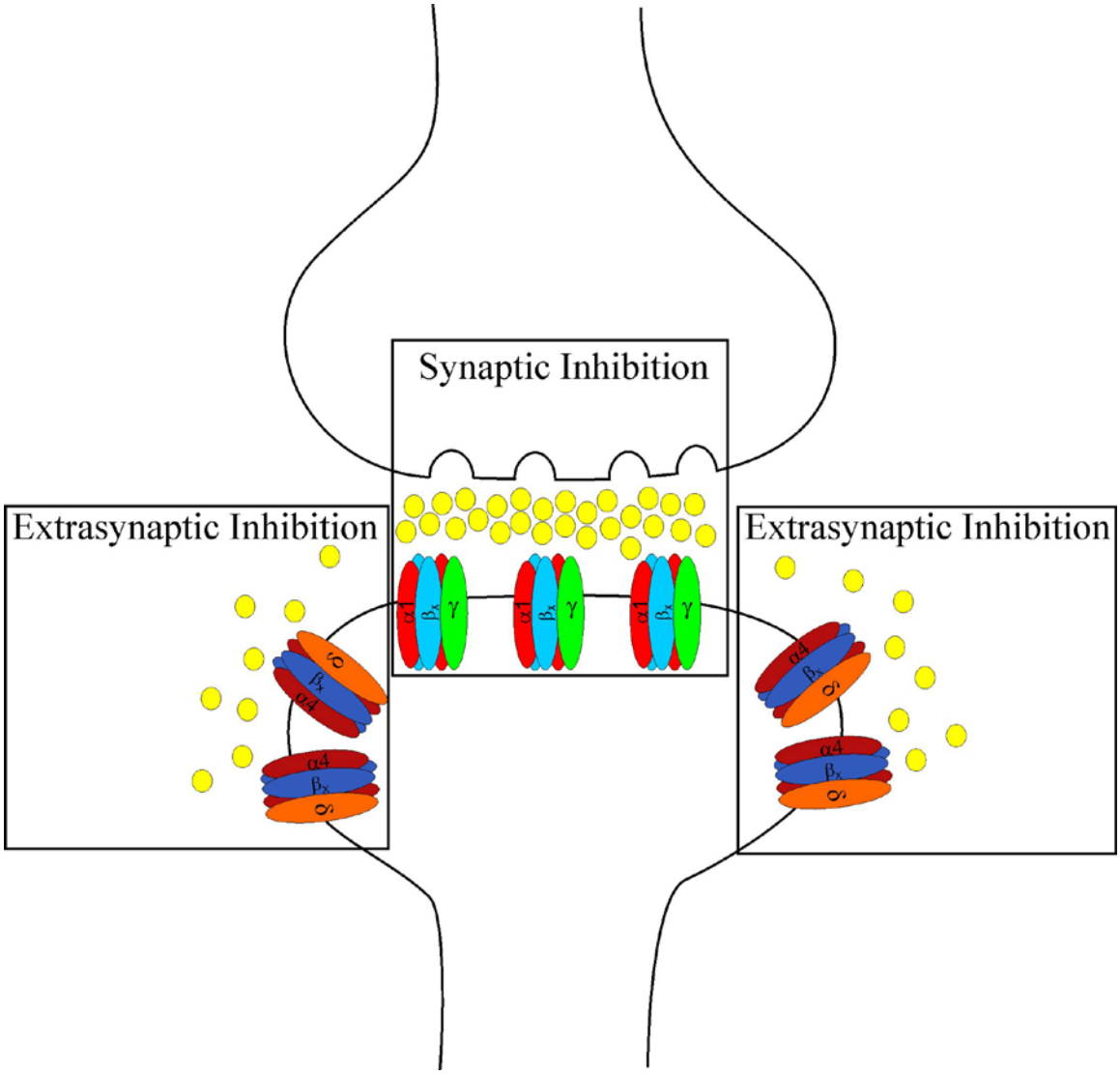

Figure 1.4. Representation of a GABAergic synapse. In the synaptic cleft region there is a high concentration of GABA (yellow circles) neurotransmission from the pre-synaptic terminal. $GABA_AR$'s comprised of $\alpha1\beta x\gamma$ subunits tend to be located in regions of the post-synaptic cleft. "Spill-over" represented by the GABA which leaves the synaptic cleft area is responsible for the tonic inhibition of neurons. Tonic inhibition due to this "spill-over" of GABA is generated by extrasynaptic $GABA_AR$'s generally comprised of $\alpha4\beta_x\delta$ subunit containing receptors in dentate granule cells.

GABAergic inhibition in dentate granule cells, as well as many other cell types, occurs through two different mechanisms using γ-aminobutyric acid type A receptors ($GABA_ARs$). These ligand-gated chloride channels are found at both the synaptic cleft of inhibitory synapses as well as in the extrasynaptic space on the dendrites and soma of neurons (Nusser et al., 1998;Mody, 2001;Farrant and Nusser, 2005;Glykys et al., 2008). At the synaptic cleft, $GABA_ARs$ are responsible for the phasic inhibition of dentate granule cells in response to neurotransmission of GABA from the pre-synaptic terminal (Wall and Usowicz, 1997). During the synaptic release of GABA not all of the GABA is bound to the post-synaptic $GABA_ARs$, some spills out of the synaptic cleft and some is taken up into the pre-synaptic neuron by GABA transporters or cleared by uptake into other cells. The "spill-over" of GABA into the extrasynaptic space is what activates tonic inhibition through $GABA_ARs$ and provides a steady state of inhibition for dentate granule cells (Rossi and Hamann, 1998). In dentate granule cells, phasic inhibition is a transient response relative to the tonic inhibition of dentate granule cells which provides a steady state of inhibition to these neurons (Mtchedlishvili and Kapur, 2006). $GABA_ARs$ which respond to synaptic GABA neurotransmission are formed by heterologous pentameric subunit combinations which contains 2 alpha 1, 2 beta, and a gamma subunit such as; $2\alpha_1 2\beta_x\gamma$, and tonic inhibition is generally contributed to $GABA_ARs$ with a subunit combination as such; 2 alpha 4, 2 beta and delta subunit, in this arrangement $2\alpha_4 2\beta_x\delta$ (Mody, 2001;Wei et al., 2003;Semyanov et al., 2004;Farrant and Nusser, 2005;Mtchedlishvili and Kapur, 2006;Glykys and Mody, 2007b;a). Changes to either the arrangement or location of these receptors could have significant consequences to inhibition of dentate granule cells.

In both TLE and PTE animal models, changes in both phasic and tonic inhibition of dentate granule cells have been reported. Most inhibitory signaling received by dentate granule cells is mediated by $GABA_A$Rs (Staley and Mody, 1992). Following pilocarpine induced status epilepticus, spontaneous inhibitory postsynaptic current (sIPSC) frequency of dentate granule cells is reduced and this is primarily attributed to the loss of hilar interneurons in this model (Buckmaster et al., 1994;Buckmaster and Dudek, 1997b;Buckmaster and Wen, 2011). Similarly, within the CCI model of PTE, an animal model which also results in hilar interneuron loss in the ipsilateral hemisphere (Hicks et al., 1993;Smith et al., 1995;Saatman et al., 2006), results in a reduction of sIPSC frequency in the ipsilateral dentate granule cells, but no change in contralateral dentate granule cells compared to control (Hunt et al., 2011;Boychuk et al., 2016).

Changes to $GABA_A$R subunit composition and function have been reported in both TLE and TBI animal models. In TLE animal models, changes in the $GABA_A$Rs subunit composition of dentate granule cells have been observed using mRNA expression and Western blot expression. In the hippocampus of pilocarpine-induced status epilepticus mice a reduction in α1 and δ subunit containing $GABA_A$Rs and an increase of α4 subunit containing $GABA_A$Rs following pilocarpine-induced status epilepticus has been reported (Brooks-Kayal et al., 1998;Peng et al., 2004;Zhang et al., 2007;Zhan and Nadler, 2009).

Use of zinc blockade and zolpidem to augment $GABA_A$Rs targets $GABA_A$Rs containing α1 subunits. Whole cell recordings from dentate granule cells after pilocarpine-induced status epilepticus using these techniques suggests reduction of α1

subunit-containing synaptic $GABA_A$Rs in these neurons (Brooks-Kayal et al., 1998). The results of these electrophysiology measures correlate to mRNA expression studies of α1 subunit-containing synaptic $GABA_A$Rs in these neurons as well (Brooks-Kayal et al., 1998;Zhang et al., 2007). Additionally, similar changes have been observed in dentate granule cells from resected tissue of human patients with intractable TLE, suggesting this mechanism could be important to the process of epileptogenesis or medical intractability of epilepsy (Brooks-Kayal et al., 1999). Injection of an adeno-assoicated virus containing the expression code for α1 subunit-containing $GABA_A$Rs before pilocarpine-induced status epilepticus in mice increased expression of α1 subunit containing $GABA_A$Rs in the dentate gyrus and reduced spontaneous seizure development by 61% (Raol et al., 2006). This report supports the role of α1 subunit containing $GABA_A$Rs in reduced synaptic inhibition of dentate granule cells in animal models of TLE (Kobayashi and Buckmaster, 2003;Shao and Dudek, 2005) and the potential of targeting synaptic inhibition of dentate granule cells for antiepileptic therapy.

In addition to reduced α1 subunit containing $GABA_A$Rs, increased expression of α4 subunit containing $GABA_A$Rs has been reported in animal models of TLE (Roberts et al., 2005). Some have suggested that this increase in α4 subunit containing $GABA_A$R's is also associated with a rearrangement of the subunit combination of $GABA_A$Rs (Lund et al., 2008). Additionally, there is a report of α4 subunit containing $GABA_A$Rs migrating from extrasynaptic locations to more synaptic or perisynaptic locations on dentate granule cell membranes of pilocarpine-induced status epilepticus mice (Zhang et al., 2007). The rearrangement of $GABA_A$R subunits or location could confer changes in kinetic and pharmacological properties of these receptors in disease states (Brooks-Kayal

et al., 2009). Although much work has been done using animal models of TLE, less is known about $GABA_AR$ changes in animal models of TBI or PTE.

Alterations in $GABA_AR$ expression and function in models of head injury have been less uniform compared to animal models of TLE, likely due to variation in head injury models used. Focusing on the α1 and α4 subunits in the fluid percussion injury model, it has been shown in the ipsilateral hemisphere of FPI injured rats that mRNA expression of α1 subunits is reduced in the hippocampus at 24 hours, 48 hours, and 1 week post-injury (Raible et al., 2012). Expression of α4 subunits in the ipsilateral hemisphere of FPI injured rats was increased 24 hours after injury (Raible et al., 2012), not different than controls at 48 hours post-inury, and reduced relative to controls 1 week post-injury (Raible et al., 2012). Additionally, other studies demonstrated that most expression changes in $GABA_ARs$ which occur within the first week after injury return to control levels in the months following injury (Pavlov et al., 2011;Drexel et al., 2015). These studies used a mean fluid pressure of 3.38 atm to induce injury. It is unclear what this return to baseline in $GABA_AR$ expression and function mean to the process of epileptogenesis in the FPI model, but it is important to remember that this model of TBI does not generally result in spontaneous seizures unless a severe (>3 atm pressure) injury is used (D'Ambrosio et al., 2004;D'Ambrosio et al., 2005;Kharatishvili et al., 2006;D'Ambrosio et al., 2009;Bolkvadze and Pitkanen, 2012). This reversion of $GABA_AR$ expression and function may be part of the explaination for why this brain injury model does not coincide with spontaneous seizure generation.

Alternatively, the controlled cortical impact (CCI) model of brain injury is a contusion injury model which is designed to have a focal non-penetrating brain injury

and results in seizure generation in 35-50% of the injured mice (Hunt et al., 2009;Statler et al., 2009;Guo et al., 2013;Kelly et al., 2015). Studies using this model of head injury have also noted varied results in regards to $GABA_AR$ expression and function (Mtchedlishvili et al., 2010;Raible et al., 2015;Boychuk et al., 2016). In two of these studies a greater injury severity was used (>1mm injury depth), which resulted in extensive damage to the ipsilateral hippocampus (Mtchedlishvili et al., 2010;Raible et al., 2015). In a previous study, a severe CCI injury was given to mice in which the ipsilateral hemisphere of the hippocampus was unsuitable for whole cell patch clamp recordings of ipsilateral dentate granule cells (Mtchedlishvili et al., 2010). The dentate granule cells in the contralateral hemisphere of CCI injured mice exhibited increased tonic $GABA_AR$ mediated inhibition. However, this study left a large knowledge gap for what changes $GABA_AR$ occur in the ipsilateral dentate granule cells of mice after CCI injury. Another study using a CCI injury model, in which the ipsilateral hippocampus remained structurally intact, was also done (Boychuk et al., 2016). In this study, ipsilateral dentate granule cells from CCI injured mice exhibited reduced 4,5,6,7-tetrahydroisoxazolo(5,4-c)pyridin-3-ol (THIP)-mediated current amplitude at both 1-2 and 8-13 weeks post-injury compared to sham control and contralateral dentate granule cells. This reduced THIP-mediated tonic inhibition in ipsilateral dentate granule cells was not correlated to altered resting tonic $GABA_AR$ mediated currents or mRNA expression of $GABA_AR$ subunits associated with THIP-mediated inhibitory currents. These results are different from FPI injury models in which $GABA_AR$ expression and function have been noted to be transient. Additionally, the underlying mechanism for the changes noted in $GABA_AR$ function of ipsilateral dentate granule cells after CCI does not appear to correlate to

expression changes. This leaves the possibility of changes such as post-transcriptional modification could be responsible for the observed reduction in THIP-mediated tonic inhibition of ipsilateral dentate granule cells after CCI injury.

1.4.7 Targeting GABAergic plasticity as antiepileptogenic therapy

Following TBI, changes in $GABA_AR$ function and expression have been observed. However it is unclear what underlying mechanisms are responsible for these changes and their relation to epilepsy. Due to the mRNA expression changes observed in the pilocarpine model of TLE, investigation into the underlying mechanisms of $GABA_AR$ changes in disease have focused on gene regulation. The cAMP response element binding protein (CREB) and inducible cAMP early repressor (ICER) proteins have been implicated as mediators of α1 subunit containing $GABA_AR$ expression (Hu et al., 2008;Lund et al., 2008). The activation of this cell signaling pathway promotes phosphorylation of janus kinase (Jak)/ signal transducer and activator of transcription (STAT). This is believed to cause reduction in α1 subunit transcription and increase α4 subunit transcription (Brooks-Kayal et al., 2009). For this reason targeting the Jak/STAT signaling pathway has been proposed as a mechanism for antiepileptogenic therapies. The use of a STAT3 inhibitor in the pilocarpine-induced status epilepticus model demonstrated potential for antiepileptogenic properties of inhibition of this cell signaling pathway (Grabenstatter et al., 2014). Currently in models of PTE it is only known that Jak/STAT3 activation after FPI and CCI injury is increased in the ipsilateral hemisphere of injured rodents, and use of a STAT3 inhibitor after CCI injury rescued the decrease in α1 subunit expression and vestibular motor function (Raible et al., 2012;Raible et al., 2015). This increased activation is correlated to modulation of GABA receptor subunits,

but no work has currently demonstrated potential antiepileptogenic of the STAT3 inhibitor use in these models of PTE.

1.4.8 Axonal sprouting

In cases of brain insult, many neuron populations in the hippocampus have been observed to sprout aberrant axons (Steward et al., 1973; 1974;Steward et al., 1976;Steward and Messenheimer, 1978;Nadler et al., 1980;Nadler et al., 1981;Staubli et al., 1984;Steward, 1992;Smith and Dudek, 1997; 2001; 2002;Hunt et al., 2009). This aberrant sprouting of surviving neurons can be either adaptive or maladaptive. One of the most prominent features associated with epilepsy development in the hippocampus of human resected tissue is the aberrant sprouting of mossy fibers. One common histological assessment of mossy fiber sprouting is the use of Timm staining to semi-quantitatively measure axonal sprouting of dentate granule cells. Timm stain is a derivative of silver staining techniques (Timm, 1958;Danscher et al., 1985) that selectively targets the mossy fibers of dentate granule cells due to the high levels of zinc in these axons (Crawford and Connor, 1972;Danscher et al., 1975;Hesse, 1979;Frederickson et al., 1981). A semi-quantitative score can be given to the degree of sprouting back into the dentate granule cell and inner molecular layers of the dentate gyrus (Buckmaster and Schwartzkroin, 1994;Buckmaster and Dudek, 1997b;a;Dudek and Spitz, 1997;Sutula et al., 1998;Buckmaster et al., 2002;Winokur et al., 2004;Hunt et al., 2009;Buckmaster, 2012;Guo et al., 2013). The aberrant axon sprouting of dentate granule cells causes excitatory synapses to form back on the dendrites of other dentate granule cells (Yamawaki et al., 2015). This sprouting of mossy fibers back into the inner molecular layer of the dentate gyrus onto dendrites of neighboring dentate granule cells likely

disrupts normal information flow and forms recurrent excitatory circuits in the hippocampus (Tauck and Nadler, 1985;Cronin et al., 1992). The use of Timm stain to assess the anatomical feature of aberrant sprouting of dentate granule cells does not address functional changes to the dentate gyrus. To assess the possibility of functional hyperexcitability in the hippocampus of these injured mice, electrophysiology techniques have been used.

Functional recurrent excitation in dentate granule cells has been observed in models of PTE (Hunt et al., 2009; 2010). For example, antidromic stimulation of the hilus, to activate a population response of dentate granule cells, has demonstrated an increased probability of dentate granule cells from the ipsilateral hemisphere of CCI-injured mice to fire secondary depolarizations compared to controls (Hunt et al., 2009). This recurrent excitation of ipsilateral dentate granule cells is also observed using whole cell patch clamp recording techniques when the extracellular environment is perturbed to "unmask" recurrent excitation (Hunt et al., 2010). This increase in excitation of ipsilateral dentate granule cells from CCI injured mice also coincides with a reduction in spontaneous inhibitory post-synaptic currents (sIPSCs) compared to controls (Hunt et al., 2011;Boychuk et al., 2016). Combined these results indicate a shift towards greater excitatory and less inhibitory signaling in mouse models of brain insult and this imbalance is similar to an established chemoconvulsant model of TLE in which mice have overt spontaneous seizures. However, the relationship of aberrant axonal sprouting of dentate granule cells and seizure development is not well understood since near removal of this axonal sprouting does not always prevent seizure expression in a mouse models of acquired epilepsy (Heng et al., 2013).This has led to controversy over the role

of mossy fiber sprouting in the process of epileptogenesis and the use of drugs to target this cell circuitry change.

Moreover, dentate granule cells also synapse onto inhibitory interneurons in the hilus and mossy fiber sprouting can change the connectivity of dentate granule cells with hilar interneurons. In models of TBI, surviving hilar inhibitory interneurons have been shown to fire more action potentials and receive more excitatory input (Halabisky et al., 2010;Hunt et al., 2011). This increase in excitation of surviving hilar inhibitory interneurons is believed to be a compensation for reduced inhibition in the ipsilateral hippocampus. However, increased excitatory drive from mossy fibers, or axon sprouting from other cell types, could lead to an increased probability of hilar interneurons entering a state of transient inactivation due to over-excitation (Hunt et al., 2011). Theoretically a prolonged inability to inhibit dentate granule cells would be detrimental to inhibition of recurrent activation of the hippocampus and potentially lead to seizure generation (Hunt et al., 2011).

Dentate granule cells are not the only neuron population of the hippocampus that has exhibited aberrant sprouting of axons. CA3 pyramidal neurons typically project to CA1 pyramidal neurons in the tri-synaptic circuit. However, on rare occasions these neurons will project back into the hilus onto GABAergic hilar interneurons and excitatory mossy cells (Scharfman, 1993;Scharfman, 1994;Scharfman, 2007). In animal models of TLE and PTE, CA3 pyramidal projections back into the hilus onto GABAergic hilar interneurons are increased compared to controls (Halabisky et al., 2010;Hunt et al., 2011;Zhang et al., 2012). In addition to this “backprojection” of CA3 pyramidal neurons, axon sprouting of CA1 pyramidal neurons and GABAergic interneurons in the CA1

region has also been reported in models of epilepsy (Perez et al., 1996;Smith and Dudek, 1997;Esclapez et al., 1999;Smith and Dudek, 2001; 2002;Peng et al., 2013). It remains unclear what extrinsic or intrinsic cell signaling regulates this form of axon sprouting in models of epilepsy. The role of these aberrant axon sprouting events to the progression of epileptogenesis is also not understood.

1.4.9 Targeting axon sprouting for antiepileptogenic therapy

Targeting of aberrant mossy fiber sprouting as a treatment for various epilepsy syndromes is the most studied target for epileptogenesis. Studies in kindling (Rashid et al., 1995;Van der Zee et al., 1995;Sutula et al., 1996), chemical convulsants (Longo and Mello, 1997;Muller-Schwarze et al., 1999;Pitkanen et al., 1999;Buckmaster et al., 2009;Zeng et al., 2009;Paradiso et al., 2011;Heng et al., 2013), and PTE (Guo et al., 2013) models of epilepsy have found positive or negative associations for reduction of mossy fiber sprouting and various drug treatments. Of the successful treatment options from animal studies, most have either not been successful in preventing epileptogenesis in humans or are have yet to enter/complete clinical trials. The lack of success from the therapeutic targets of these studies in humans, combined with a lack of direct correlation for mossy fiber sprouting and spontaneous seizure generation, has thrown into question the role this form of axon sprouting plays in the epileptogenic process. Other forms of axon sprouting, such as backprojections from CA3 pyramidal neurons or spouting of CA1 pyramidal cells and interneurons, are less understood in regard to their role in epileptogenesis. For this reason these forms of axon sprouting have not yet been targeted for antiepileptogenic therapies.

1.4.10 Other targets for antiepileptogenic therapy

Following TBI insult there is an upregulation of immune responses in the brain (Morganti-Kossmann et al., 2001;Lucas et al., 2006). These responses are mediated by many cell types; neurons, astrocytes, and glia. Additionally, a breakdown in the blood brain barrier after brain injury could contribute to peripheral immune signaling molecules or cells crossing into nervous tissue previously not activated by such signaling. Cytokines such as IL-1β, IL-6, tumor necrosis factor α, and cyclooxygenase-2 have all been shown to be upregulated in animal models of TBI and these pro-inflammatory factors also contribute to blood brain barrier breakdown. The correlation of these pro-inflammatory factors with potential epileptogenic processes has created a desire to test therapeutic strategies that inhibit upregulation of inflammatory signaling following TBI as an antiepileptogenic therapy. One of the preclinical trails done to assess an anti-inflammatory treatment was the use of Minozac, a suppressor of pro-inflammatory cytokine upregulation, in a closed head TBI model (Chrzaszcz et al., 2010). This study was performed in a model which has not been demonstrated to develop spontaneous seizures (weight drop closed head injury), and the measurements were made prior to spontaneous seizure generation in other PTE models (7 days post-injury). However, the administration of Minozac 3 or 6 hours after injury reduced susceptibility of mice to electrical stimulation induced seizures compared to sham treated mice. The use of this treatment strategy and testing of seizure susceptibility following treatment suggests potential of this drug, but it is currently unclear if the effects are simply anticonvulsant versus antiepileptogenic. Anticonvulsants reduce the number of spontaneous seizures, through broad effects on brain excitability, without addressing the underlying

mechanism(s) responsible for the development of spontaneous seizures. Antiepileptogenic effects, in contrast, target the exact mechanism(s) responsible for the expression of seizures. Thus, anticonvulsants are designed to reduce the symptoms of epilepsy whereas antiepileptogenic treatments are designed to reduce or cure the epilepsy itself.

Additionally, a recent study of TBI patients, of which ~16% developed PTE, was used to assess the correlation of IL-1β concentration in both the serum and central nervous system and genetic variations as biomarkers for PTE (Diamond et al., 2015). This study demonstrated that both a high ratio of central nervous system to serum ratio of IL-1β concentration and a single nucleotide polymorphism of the IL-1β gene correlated to development of PTE. One of the more interesting points of this study was that all TBI patients demonstrated high levels of IL-1β in the central nervous system, but patients which developed PTE showed lower serum levels of IL-1β, contributing to the overall effect of the higher ratio in these patients. These data would suggest that transport of IL-1β into the brain could be a mechanism to target for antiepileptogenic therapies. Combined, these studies demonstrate promise for intervention of inflammatory processes following TBI as a therapeutic for PTE, but little is currently understood on which inflammatory processes are critical for epileptogenesis. Therefore a better understanding of these mechanisms is necessary. The following demonstrates our knowledge of mTOR signaling in models of epilepsy and gaps in our understanding of the mechanisms of action associated with mTOR.

1.5 Targeting mTOR for antiepileptogenic therapy

Although the exact causes remain unknown, the alterations in the hippocampus discussed above are thought to occur through a multitude of extra- and intracellular signals activated within the first few hours to days following the initial insult. The exact activation period for these different signaling molecules varies, but generally there is a large peak of activity in the first hours to days after injury with a decay over the following days and weeks after the initial injury. Targeting of these cell signaling pathways for therapeutic strategies has become a hotbed of interest in the development of antiepileptic therapies. Cell signaling pathways which demonstrate increased activity in the initial days and weeks following brain injury and have roles in mechanisms associated with epileptogenesis or other models of epilepsy are of particular interest in the study of PTE. Potential extracellular signals include stress and growth hormones and inflammatory cytokines permeating the blood brain barrier (Robertson et al., 1984;McClain et al., 1986;McClain et al., 1987;Young et al., 1988;Chiolero et al., 1989;Goodman et al., 1990;Hadfield et al., 1992). One particularly intriguing intracellular cell signaling pathway which has roles in cell death, growth, and proliferation is mTOR.

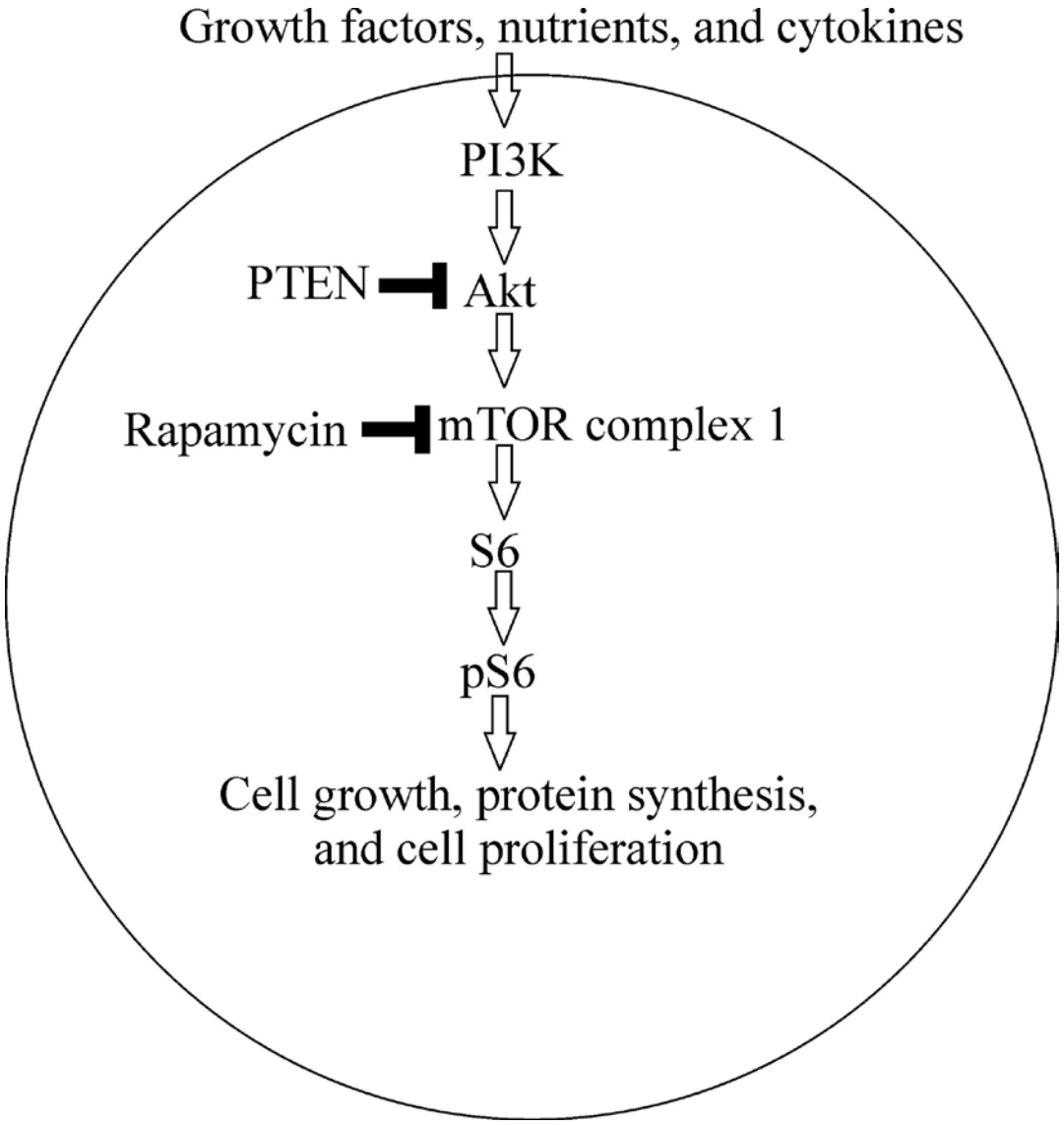

Figure 1.5. mTOR signaling pathway schematic. This illustration demonstrates some of the primary upstream activators of mTOR signaling such as growth factors, nutrients and cytokines, which result in downstream activities of cell growth, protein synthesis, and cell proliferation. Two of the endogenous inhibitors of mTOR activity are PTEN and rapamycin and are also depicted.

mTOR is a serine/threonine kinase involved in many cellular activities associated with nutrient recognition, cell growth/ proliferation, and cell death (Nave et al., 1999). Generally growth hormones or other nutrition factors activate external membrane bound receptors, which then signal downstream through mTOR to activate protein synthesis for cellular responses associated with cell growth/proliferation and cell death. Although the

brain only comprises ~2% of the total body mass, it is responsible for 20% of energy expenditure in humans (Sokoloff et al., 1955;Sokoloff, 1999;Raichle and Gusnard, 2002). Therefore, cell signaling pathways associated with nutrition or energy expenditure are extremely important in normal brain function. Additionally, after insults to the brain these signals are often thought to play a large role in the remodeling process. In both animal models of TLE and TBI, mTOR activity, measured by phosphorylated S6 (pS6) expression, increases following the initial insult (Buckmaster et al., 2009;Zeng et al., 2009;Guo et al., 2013). However, the time period for this elevated activity appears to be model specific. For example, the pilocarpine model of TLE demonstrates increased mTOR activity over the course of 10 weeks (Huang et al., 2010), while the controlled cortical impact model of TBI has an increase in mTOR activity for only 4 weeks in the ipsilateral hemisphere following brain injury (Guo et al., 2013). These two experimental models share similar pathology related cell circuitry changes including; axonal sprouting, cell death, and increased cellular proliferation (Lowenstein et al., 1992;Hicks et al., 1993;Smith et al., 1995;Buckmaster et al., 2002;Winokur et al., 2004;Saatman et al., 2006;Hunt et al., 2009; 2010; 2011;Hunt et al., 2012;Guo et al., 2013). The development of these cell circuitry changes has been associated with an increase in mTOR activation. However, the exact contribution of mTOR activation to these cell circuit changes in disease models and the potential seizure development is unknown or controversial.

The use of an inhibitor of mTOR signaling, rapamycin has been studied in models of both TLE and TBI to assess the contribution of mTOR activity to some of the cell circuit changes associated with these disease states (Buckmaster et al., 2009;Zeng et al., 2009;Buckmaster and Wen, 2011;Guo et al., 2013;Heng et al., 2013). However, the

previous studies on rapamycin's epileptogenic effects have been primarily limited to histological analysis of anatomical axon sprouting and correlation with seizure frequency (Zeng et al., 2008;Zeng et al., 2009;Guo et al., 2013;Heng et al., 2013). A direct correlation between mossy fiber sprouting and spontaneous seizure development is not well established, and has therefore become an issue of controversy over the years (Buckmaster and Dudek, 1997b;Buckmaster et al., 2009;Buckmaster, 2012;Heng et al., 2013). In addition, the removal of rapamycin treatment in both TLE and PTE animal models resulted in the reemergence of aberrant mossy fiber sprouting and increased seizure frequency (Buckmaster et al., 2009;Guo et al., 2013). Even at high doses of rapamycin treatment (10 mg/kg) in the pilocarpine induced status epilepticus model, mice given rapamycin treatment after pilocarpine exhibited Timm staining similar to controls on average, but seizure frequency was no different (Heng et al., 2013). These data could be interpreted in a manner that mTOR inhibition does not prevent the development of epilepsy, but rather pauses some of the cascade of events leading to epilepsy following injury. This information would also suggest that mTOR activation in models of TLE and PTE is not only associated with the aberrant sprouting of mossy fibers from dentate granule cells, but could also be associated with many other processes involved in epileptogenesis. Due to the lack of investigation into the effects of mTOR inhibition on mechanisms, other than mossy fiber sprouting, that are associated with epileptogenesis, we currently have an incomplete understanding of how mTOR activity contributes to epileptogenesis. For this reason, the focus of this dissertation was to determine possible mechanisms of action for rapamycin treatment on cell circuitry changes, other than

mossy fiber sprouting of dentate granule cells, associated with epileptogenesis in a model of PTE.

The focus of previous research on the effects of mTOR inhibition on aberrant axon sprouting and associated seizure expression presents an opportunity to investigate other mechanisms associated with epileptogenesis that could be affected by mTOR inhibition. mTOR activity has been demonstrated to be involved in cell death through both apoptotic and necrotic signaling in the hippocampus (Corradetti and Guan, 2006;Carloni et al., 2008;Guo et al., 2013;Tanaka et al., 2013). Two strategies previously used to measure cell death in TLE and PTE models are 1) histological stains to measure overall cell death in the dentate granule cell layer and hilus and 2) a transgenic mouse model to identify and count eGFP-positive hilar inhibitory neurons. Using rapamycin has resulted in mixed reports depending on area measured, model used, and staining technique (Guo et al., 2013;Tanaka et al., 2013). The use of Cresyl violet stain, a stain which tags ribosomal RNAs (Alvarez-Buylla et al., 1990), and Fluoro-Jade B, an anionic fluorescein derivative used to stain neurons undergoing degeneration (Schmued and Hopkins, 2000), has demonstrated extensive cell loss in the ipsilateral hippocampus after CCI injury (Hicks et al., 1993;Smith et al., 1995;Anderson et al., 2005;Saatman et al., 2006). However, these stains do not differentiate this cell loss into subtypes of neurons which could be more susceptible to injury versus other subtypes which may not be susceptible to injury. Since the hippocampus is comprised of many different cell types such as: dentate granule cells, hilar inhibitory interneurons, molecular layer perforant path-associated inhibitory interneurons, excitatory mossy cells, CA3 pyramidal neurons,

and CA1 pyramidal neurons, cellular subtype distinctions may prove important in our understanding of which neuron populations are most affected by injury.

The development of transgenic mice has made it possible to begin selectively examining some of these neuronal subtypes. In particular, FVB-Tg(GadGFP)4570Swn/J (i.e. GIN) mice, which express enhanced green fluorescent protein (eGFP) in somatostatin-positive neurons, have allowed the selective study of a subtype of inhibitory interneurons in the hilus during normal physiology and in disease states (Oliva et al., 2000). To date, only one study has investigated the effect of rapamycin treatment on these hilar interneurons in a model of epilepsy (Buckmaster and Wen, 2011). Rapamycin treatment in mice given pilocarpine induced status epilepticus did not alter cell loss of eGFP-positive hilar interneurons. However, rapamycin treatment did reduce soma size and the axon sprouting of surviving eGFP-positive hilar interneurons relative to vehicle treated status epilepticus mice (Buckmaster and Wen, 2011). Aside from these histological assessments, no electrophysiological assessments of rapamycin's effect on these eGFP-positive neurons in TLE mice have been made. This gap in knowledge presented an opportunity to investigate the effects of rapamycin treatment on inhibitory circuitry after CCI injury.

After both pilocarpine induced status epilepticus and the CCI model of PTE, surviving hilar eGFP-positive neurons exhibited increased sEPSCs and action potential firing (Halabisky et al., 2010;Hunt et al., 2011). Using UV light activation, caged glutamate was released in areas of dentate granule cells and CA3 pyramids, and ipsilateral eGFP-positive hilar inhibitory interneurons demonstrated increased responsiveness to uncaging of glutamate in both dentate granule cells and CA3 pyramid

regions compared to controls (Hunt et al., 2011). These studies demonstrate axon sprouting from both dentate granule cells and CA3 pyramidal neurons onto surviving hilar inhibitory interneurons in animal models of TLE and PTE. Due to the reduction of mossy fiber sprouting in several animal models of epilepsy treated with rapamycin, it would be predicted that rapamycin could also affect the excitatory sprouting onto surviving eGFP-positive hilar interneurons in the ipsilateral hemisphere. However, this potential effect of rapamycin has yet to be tested.

mTOR activation can occur through a diverse range of extracellular signals including growth factors, cell stress, cytokines, amino acids, and mitogens. One of the most well-characterized upstream activation pathways of mTOR signaling is the insulin pathway (Foster and Fingar, 2010;Sengupta et al., 2010;Magnuson et al., 2012). The activation of the insulin pathway has also been associated with neurogenesis in the hippocampus after TBI. Insulin signaling itself has a wide range of effects on neurons including energy homeostasis, reproductive endocrinology, and neuronal survival (Plum et al., 2005). Using transgenic mice that conditionally express astrocyte-specific human insulin-like growth factor 1, a study demonstrated that after CCI injury these transgenic mice exhibited increased neuronal differentiation in the ipsilateral hemisphere compared to wild-type littermates 10 days post-injury (Carlson et al., 2014). Interestingly, activation of mTOR signaling, using a mouse model in which phosphatase and tensin homolog (PTEN) is knocked out of dentate granule cells, results in increased neurogenesis, aberrant cell migration, and spontaneous seizures (Sunnen et al., 2011;Hester and Danzer, 2013;LaSarge et al., 2015). This data would suggest that mTOR activation could play a role in neurogenesis after TBI, but this has yet to be tested.

The contribution of mTOR activation to aberrant excitatory axon sprouting of dentate granule cells has been studied at length (Buckmaster et al., 2009;Zeng et al., 2009;Guo et al., 2013;Heng et al., 2013). However, changes to inhibitory circuitry of the dentate gyrus have been observed after CCI injury (Hunt et al., 2011;Boychuk et al., 2016), but no experiments have tested the possibility of mTOR signaling contributing to these function changes. mTOR blockade in a mouse model of pilocarpine induced status epilepticus reduced hilar interneuron axon sprouting and soma size (Buckmaster and Wen, 2011). Additionally, phosphorylation of Akt altered translocation of $GABA_AR$'s to the cell membrane of cultured neurons (Wang et al., 2003). This data would suggest a potential role of mTOR activity in GABAergic inhibition of dentate granule cells.

Considering our general lack of knowledge on the effects of mTOR inhibition in TLE and PTE models outside of dentate granule cell axon sprouting, it is important to examine other aspects of mTOR modulation in the hippocampal circuitry. Previous studies have already demonstrated many effects of CCI injury associated with epileptogenesis in this model including: enhanced neurogenesis, reduced synaptic inhibition of ipsilateral dentate granule cells, reduced THIP induced tonic $GABA_AR$ mediated currents in ipsilateral dentate granule, enhanced excitatory drive of surviving ipsilateral eGFP-positive hilar interneurons, and increased axon sprouting of ipsilateral CA3 pyramidal neurons onto eGFP-positive hilar interneurons. This all establishes a foundation to investigate the effects of rapamycin treatment after CCI injury on a variety of cell circuitry changes associated with epileptogenesis.

1.6 Study aims and significance

This study will focus on the role of mTOR signaling in epileptogenesis in the CCI model of PTE. In order to avoid some of the confounds associated with reemergence of phenotypes associated with seizures and epilepsy following cessation of mTOR inhibition, the use of rapamycin as an mTOR inhibitor will be given daily throughout the entirety of the experiment in all studies. Although synaptic reorganization of dentate granule cells in models of TLE and PTE has been a focus of previous work, it is not the only mechanism by which epilepsy and seizures could develop. A broader scope of investigation into different mechanisms of mTOR activity following CCI injury will help dissect areas of interest or therapeutic targets for future studies, as well as increase our knowledge of how mTOR signaling is involved in remodeling of the hippocampus following brain injury.

The specific aims of this project are as follows:

1. Does mTOR inhibition following CCI injury modify injury-induced cell death or neurogenesis in the dentate gyrus? Cell death is one of the most common features of TBI and seizures, however it remains controversial what role mTOR signaling plays in the regulation of this process after CCI injury. Increased neurogenesis has been exhibited in models of TLE, and could be part of epileptogenic process in PTE. Using doublecortin (DCX) to label immature neurons, neurogenesis was measured to assess injury-induced effect on neurogenesis and the effect of mTOR inhibition on this injury-induced change.

2. Does mTOR inhibition after CCI injury reduce functional recurrent excitation in dentate granule cells and seizure expression? Electrophysiology in both models of

TLE and PTE indicate increased recurrent excitation of dentate granule cells and mTOR inhibition has been noted to histologically reduce indices of this recurrent excitation. However no studies have assessed the functional implications of mTOR inhibition in the synaptic reorganization of dentate granule cells. sEPSC frequency of dentate granule cells, as well as extracellular population responses of dentate granule cells to hilar stimulation, were measured to assess the effect of rapamycin treatment after CCI injury on recurrent excitatory in the ipsilateral hemisphere of CCI injured mice.

3. Does mTOR inhibition after CCI injury modulate phasic or tonic inhibition of dentate granule cells? Synaptic inhibition of dentate granule cells in models of TLE and PTE is reduced. Tonic inhibition of dentate granule cells also largely contributes to inhibition of dentate granule cells, but reports of altered tonic inhibition of dentate granule cells has varied across animal models used. It is unknown if mTOR plays a role in these mechanisms of phasic and tonic inhibition. Therefore, using whole cell patch-clamp electrophysiology measures of sIPSC frequency and inducible tonic $GABA_A$ receptor mediated currents were made to assess the role of mTOR in the inhibition of dentate granule cells following CCI injury.

4. Does mTOR inhibition reduce excitatory synaptic plasticity from dentate granule cells and CA3 pyramidal neurons onto a subset of surviving hilar inhibitory neurons? Mouse models of both TLE and PTE exhibit increased excitatory responses in eGFP-positive hilar interneurons, which are extensively lost following insult, to stimulation of both dentate granule cells and CA3 pyramidal neurons. This suggests that dentate granule cell sprouting is not the only form of axon sprouting associated with the epileptogenic process. Although the role of mTOR in axon sprouting of dentate granule

cells has been explored rigorously using histology and electrophysiology techniques, no one has investigated if rapamycin is preferential to axon sprouting of one cell type or a general suppressant of axon sprouting. Using GIN mice, eGFP-positive neurons in the hilus will be selectively investigated. Whole cell and on cell recording of eGFP-positive hilar inhibitory interneurons will be used to measure change in excitatory synaptic input onto surviving eGFP-positive hilar interneurons. Additionally, using whole cell patch clamp recordings of these eGFP hilar interneurons, photoactivation of caged glutamate will be used to measure excitatory connections from both dentate granule cell and CA3 pyramidal neuron populations. This experiment will be the first to assess the effect of rapamycin treatment on axon sprouting from CA3 pyramidal neurons after CCI injury.

Chapter 2: Materials and Methods

Animals: Six to eight week old (25-32 g) male CD-1 (Harlan, Indianapolis, IN) or male FVB-Tg(GadGFP)4570Swn/J (GIN; Jackson Laboratory; (Oliva et al., 2000) mice were housed in a 14 hr light/10 hr dark cycle. Mice were housed for a minimum of 7 days prior to experimentation in the University of Kentucky vivarium and food and water was provided *ad libitum*. All procedures were approved by the University of Kentucky Animal Care and Use Committee and adhered to NIH guidelines for the care and use of animals. Experiments were performed on mice 3 days to 13 weeks post-injury. Power analysis was performed to estimate sample sizes required to detect a significant effect for outcome measures assess in the following studies.

Traumatic brain injury: Mice were subjected to severe unilateral, cortical contusion injury by CCI, as described previously (Scheff et al., 1997;Hunt et al., 2009; 2010; 2011;Hunt et al., 2012). Briefly, mice were anesthetized by 2% isoflurane inhalation and placed in a stereotaxic frame. The skull was exposed by midline incision, and a ~5 mm craniotomy was made lateral to the sagittal suture and centered between bregma and lambda. The skull cap was removed, taking care to avoid damage to the exposed underlying dura. The contusion device consisted of a computer-controlled, pneumatically driven impactor fitted with a beveled stainless-steel tip 3 mm in diameter (Precision Systems and Instrumentation, Fairfax, VA). Brain injury was delivered using this device to compress the cortex to a depth of 1.0 mm at a velocity of 3.5 m/s and 500 ms duration. This brain injury model consistently produced a focal cortical lesion. Although there is no direct damage to the hippocampus from the injury, hippocampal evulsion usually occurs

(Hunt et al., 2009;Hunt et al., 2012). Sham-injured mice received anesthesia and only a craniotomy before closure of the incision. A qualitative postoperative health assessment was performed daily for 4 days after CCI and periodically thereafter.

Rapamycin injection: Rapamycin (LC Laboratories, Woburn, MA) was dissolved in 100% ethanol (20 mg/ml), stored at -20^{o}C, and diluted in a vehicle solution containing 5% Tween 80, 5% PEG 400, and 4% ethanol (all from Fisher Scientific, Pittsburgh, PA) dissolved in distilled, deionized water immediately before intraperitoneal (i.p.) injection (Guo et al., 2013;Heng et al., 2013). Rapamycin (3 mg/kg or 10 mg/kg) or vehicle was injected intraperitoneal (i.p.) after mice regained consciousness following CCI injury (20-30 min) and the treatment was continued once daily until the day of experimentation. Hippocampal homogenates from mice 24 hr. after injury indicated an increase in pS6 expression levels in the ipsilateral hemisphere of CCI-injured mice with vehicle treatment; rapamycin treatment reduced pS6 to sham levels at this post-injury time point (unpublished data), similar to previous reports (Zeng et al., 2008;Buckmaster et al., 2009;Guo et al., 2013).

Seizure observations: As described previously (Hunt et al., 2009), mice were monitored for behavioral seizures by observation for 6 hrs per week beginning at 6 weeks post-injury and ending 10 weeks post-injury. Using a modified Racine scale (Racine, 1972) only behavioral seizures at or above a grade 2 (i.e., prolonged freezing and wet dog shakes) and lasting longer than 10 seconds were counted as behavioral seizures.

Timm staining: After the recording experiment concluded, slices were placed in 0.1 M sodium phosphate buffer containing 0.37% sodium sulfide (pH 7.4) for ~30 minutes

followed by 4% paraformaldehyde in 0.15M sodium phosphate buffer (pH=7.4) overnight. Slices were then equilibrated in a 30% sucrose solution in phosphate buffered saline (0.1M; PBS) overnight, embedded in Optimal Cutting Temperature (OCT) compound (Fisher Scientific), sectioned at 30 μm on a cryostat, rinsed in PBS, mounted on charged slides (Superfrost Plus; Fisher Scientific), and dried on a slide warmer. Sections were subsequently treated as in previous protocols, using Timm stain to reveal mossy fibers and Nissl counterstain to reveal cell bodies (Tauck and Nadler, 1985;Shibley and Smith, 2002;Winokur et al., 2004;Hunt et al., 2009;Bhaskaran and Smith, 2010;Hunt et al., 2010; 2011;Hunt et al., 2012). To semi-qualitatively assess mossy fiber sprouting after CCI, sections at equivalent positions relative to bregma ipsilateral and contralateral to injury were examined and assigned Timm scores ranging from 0-3, with a score of 0 corresponding to little to no granular staining, 1 indicating moderate Timm staining through the granule cell layer, but not into the inner molecular layer, 2 indicating continuous staining through the granule cell layer with discontinuous puncta in the inner molecular layer, and 3 indicting a continuous band of staining in the inner molecular layer. The scorer was blinded to treatment. Using a modified scoring scale (Hunt et al., 2009; 2010), regions of the dentate gyrus with Timm scores >1 were considered to exhibit mossy fiber sprouting (Tauck and Nadler, 1985;Patrylo and Dudek, 1998;Shibley and Smith, 2002;Hunt et al., 2009; 2010; 2011;Hunt et al., 2012). To obtain the Timm score for each animal, each 350 μm slice used for recording was analyzed using two 30 μm sections, ~180 μm apart mounted onto slides. Each blade of the dentate gyrus was assessed independently and the average score of the 2 blades was given for

each slice. The scores from each slice were then averaged per hemisphere per animal to obtain the Timm score for each animal.

Immunohistochemistry: Mice were perfused transcardially with a 0.15M sodium phosphate buffer followed by 4% paraformaldehyde fixative solution (0.15M sodium phosphate buffer) 14 days post-injury. The brain was removed and placed in fixative overnight and then transferred to a 30% sucrose solution in PBS until the tissue equilibrated. Brains were covered in OCT compound and sectioned serially at on a cryostat (-22 ^{o}C) at 20 μm. Sections (every 6th section in series) were rinsed in Tris-buffered saline (TBS; pH=7.4) briefly before being mounted onto slides and incubated in a solution containing Triton X-100 (0.3%) and normal goat serum (10%) in TBS for 30 min at room temperature. Sections were then incubated overnight at 4^{o}C with a rabbit primary antibody against doublecortin (DCX; 1:5000; Abcam; Cambridge, MA) in blocking solution (2% normal goat serum; 0.15% Triton X-100; TBS). Sections were rinsed 3 times for 5 minutes in blocking solution and then incubated for 1 hr at room temperature in a goat anti-rabbit secondary antibody (IgG) conjugated to Alexa Flour 488 (IgG; 1:1000; Molecular Probes; Grand Island, NY) in the same blocking solution. Sections were then rinsed 3 times for 5 minutes with TBS. Slides were covered with Vectashield mounting medium with DAPI (Vector Labs; Burlingame, CA) to image immunofluorescence.

Dentate granule cell layer area: In order to measure changes in area of the dentate granule cell layer after CCI mice were perfused transcardially with a 0.15M sodium phosphate buffer followed by 4% paraformaldehyde fixative solution (0.15M sodium phosphate buffer) 14 days post-injury. The brain was removed, placed in fixative

overnight, and then transferred to a 30% sucrose solution in PBS until the tissue equilibrated. Brains were covered in OCT compound and sectioned serially at on a cryostat (-22^{o}C) at 30 μm. Sections were stained with cresyl violet (i.e., every 6th section in series). Sections were imaged using a SPOT RT camera (Diagnostic Instruments; Sterling Heights, MI) mounted on an upright microscope (BX-40; Olympus) and dentate granule cell area measurements were made using ImageJ software. Images were taken at 4x and 10x magnification to capture the entire dentate gyrus. After scaling the ImageJ software, the cresyl violet-stained dentate granule cell layer was traced freehand and the area measured. The area measurements were assessed from -1.22 to -3.52 posterior to bregma. Each animal received an averaged area measurement from this region of hippocampus which was then averaged per experimental group.

Fluoro-Jade B (FJB) staining: Mice were perfused transcardially with a 0.15M sodium phosphate buffer followed by 4% paraformaldehyde fixative solution (0.15M sodium phosphate buffer) 3 days post-injury. The brain was removed, placed in fixative overnight, and then transferred to a 30% sucrose solution in PBS until the tissue equilibrated. Brains were covered in OCT compound and sectioned serially at on a cryostat (-22^{o}C) at 30 μm. FJB protocols used were similar to those reported previously (Hall et al., 2008). In brief, tissue sections were mounted on slides, and treated with a solution of 1% NaOH in 80% ethanol for 5 min followed by 70% ethanol (2 min) and distilled water (2 min). Sections were then incubated in a 0.06% permanganate solution for 10 min on a rotating stage, rinsed in distilled water (3 min) and incubated in a 0.0004% solution of FJB (Histo-Chem Inc., Jefferson, AR; 10 min). They were then

rinsed in distilled water and air dried before being placed on a 50^{o}C slide warmer for 30 min. They were then placed in xylene for 20 min and coverslipped in permount.

Slice preparation: Slices used for electrophysiological studies were obtained from mice 8-13 weeks post-CCI injury. Mice were deeply anesthetized by isoflurane inhalation to effect (i.e. lack of tail pinch response) and decapitated while anesthetized. The brain was removed and placed in ice-cold (2-4^{o}C) oxygenated artificial cerebrospinal fluid (ACSF) containing, in mM: 124 NaCl, 3 KCl, 1.3 $CaCl_2$, 26 $NaHCO_3$, 1.3 $MgCl_2$, 11 glucose and 1.4 NaH_2PO_4 equilibrated with 95% O_2-5% CO_2 (pH 7.2-7.4). Brains were blocked and glued to a sectioning stage, and 350 μm-thick slices were cut in the coronal or horizontal plane in cold, oxygenated ACSF using a vibrating microtome (Vibratome Series 1000; Technical Products International, St. Louis, MO). The hippocampus was isolated from surrounding tissue, making sure to completely remove the entorhinal cortex. Slices were transferred to a chamber containing oxygenated ACSF at 32-34^{o}C, where they were equilibrated for at least one hour prior to recording. Slices of the septal and temporal hippocampus from the hemispheres ipsilateral and contralateral to CCI injury were used in these experiments and compared to comparable slices from sham-injured mice (i.e., craniotomy, but no impact injury).

Extracellular field potential recordings: Field potential recordings were obtained from the granule cell layer of the dentate gyrus in horizontal slices. Slices were placed into a submersion type recording chamber (RC21-BW, Warner Instruments, Hamden, CT) on an upright, fixed stage microscope (Olympus BX50WI, Center Valley, PA) and continuously perfused with oxygenated, nominally Mg^{2+} free ACSF containing 30 μM bicuculline to block $GABA_A$ receptors, and unmask recurrent excitation (Winokur et al.,

2004;Hunt et al., 2009). Extracellular recording electrodes were filled with 1 M NaCl and placed near the apex of the dentate granule cell layer. A concentric bipolar electrode made of platinum-iridium wire (125 μm, FHC Inc., Bowdoinham, ME) was used to apply a single stimulus to the mossy fiber pathway at 0.1 Hz. Stimulus intensity was adjusted to evoke a population response of ~50% maximum amplitude after a single stimulus. Electrical signals were recorded using an Axopatch 200B amplifier (Axon Instruments, Sunnyvale, CA), low pass filtered at 2-5 kHz, digitized at 20 kHz using a 1322A Digidata (Axon Instruments), and analyzed on a PC computer using pClamp 10.2 (Clampfit, Molecular Devices, Sunnyvale, CA). The number of population spikes following antidromic stimulation of mossy fibers in the hilus was measured as described previously (Hunt et al., 2009).

Whole cell recordings: Coronal hippocampal slices containing the dorsal third of the dentate gyrus were transferred to a recording chamber on an upright, fixed-stage microscope equipped with infrared, differential interference contrast optics (i.e., IR-DIC; Olympus BX50WI), where they were perfused with continuously warmed (32-34^{o}C) ACSF. Recordings were performed from dentate granule cells, which were identified using DIC imaging. Recording pipettes were pulled from borosilicate glass (1.65 mm outer diameter, 0.45 mm inner diameter; King Precision Glass, Claremont, CA) with a P-87 puller (Sutter Instrument, Novato, CA). The intracellular solution contained (in mM): 130 K^+- or 140 Cs^+-gluconate, 1 NaCl, 5 EGTA, 10 HEPES, 1 $MgCl_2$, 1 $CaCl_2$, 3 KOH or CsOH, and 2 ATP, with an osmolarity range of 275-283 mOsm/kgH_2O. Open tip series resistance was 2-5 MΩ. Recordings were obtained using an Axon 200B or 700B amplifier (Molecular Devices), low-pass filtered at 5-6 kHz, digitized at 20 kHz with a

1332A Digidata or Digidata 1550A (Molecular Devices), and acquired using pClamp 10.2 or 10.5 programs (Clampfit, Molecular Devices). Cells were voltage-clamped at -70mV or 0mV for 5-10 min to allow equilibration of pipette and intercellular solutions prior to data collection, after which time whole-cell patch-clamp recordings of spontaneous excitatory postsynaptic currents (sEPSCs) or spontaneous inhibitory postsynaptic currents (sIPSCs) were obtained. All sEPSCs and sIPSCs were assessed over a 2-3 min period to assess frequency; amplitude was measured only from unitary events. Although the investigator was not blinded to experimental group for electrophysiological experiments, the investigator was blinded to experimental group for all offline data analyses.

Pharmacology: The following agents were added to the ACSF for some experiments: bicuculline methiodide (30 μM; Tocris Biosciences), kynurenic acid (1mM; Sigma-Aldrich), 4,5,6,7-tetrahydroisoxazolo[5,4-c]pyridine-3-ol hydrochloride (THIP; gaboxadol; 3 μM; Sigma-Aldrich), 4-Methoxy-7-nitroindolinyl-caged-L-glutamate (i.e. MNI-caged glutamate; 250μM; Tocris, Minneapolis, MN), and tetrodotoxin (TTX; 1μM, Tocris Biosciences).

Glutamate photostimulation: Slices were perfused with MNI-caged glutamate (250μM; Tocris, Minneapolis, MN) added to recirculating ACSF. Brief pulses of fluorescent light (30ms exposure; UV filter; Chroma Technology, Bellow Falls, VT) were directed into the slice through the 40X microscope objective (Bhaskaran and Smith, 2010;Hunt et al., 2010; 2011) with aperture and filter at lowest levels, which reduced the diameter of light stimulus to 250 μm. The objective was initially positioned to uncage glutamate directly

over the recorded neuron, which consistently resulted in a large inward current and APs. No difference in current amplitude or AP firing evoked by direct stimulation of the recorded cell was detected between groups. The effective radius of stimulation (~60μm) was determined by manually moving the focal point of the stimulus in three different directions away from the recorded neuron until a direct inward current after stimulation was no longer observed. The objective was then moved to the DG or CA3 and photostimulation was applied focally to stereotyped sites along the DGC layer (tips of upper and lower blades, apex, and a midpoint on each blade between tip and apex) and in the proximal CA3 region. A series of 5 stimuli were applied per stimulation site at 0.1 Hz. For analysis, evoked excitatory post-synaptic currents (eEPSCs) were compared in the period 200 ms prior to and after the uncaging event to determine evoked response (#eEPSCs after stim - #eEPSCs pre-stim).

Data and statistical analysis: For histological data on cell counts, area measurement, and aberrant axon sprouting, data is presented as mean ±SEM (where n's=animal numbers). For cell density measures of FJB and DCX-positive neurons groups were compared using a One-way ANOVA followed by Tukey's *post hoc* test or Two-way ANOVA followed by Bonferroni's *post hoc* test for the normally distributed parametric data. To assess aberrant axonal sprouting measured by Timm scores a Kruskal-Wallis ANOVA with Dunn's *post hoc* comparisons was performed, due to this outcome measure being semi-quantitative nonparametric data. Data analysis was performed using ImageJ and Graphpad (La Jolla, CA).

Electrophysiology measurements included sEPSC frequency, sEPSC amplitude, antidromic stimulation responses, sIPSC frequency, resting and THIP-induced tonic

GABAAR currents, whole cell capacitance, and evoked responses to glutamate photoactivation. For electrophysiology measurements data analysis was performed using pClamp 10.2 and 10.5 software (Molecular Devices), MiniAnalysis 6.0.3 (Synaptosoft; Decatur, GA) and Graphpad (La Jolla, CA) software programs. To measure sIPSC or sEPSC frequency, a 3 minute sample of the baseline recording was used. Only events with three times the amplitude of root mean squared baseline noise were included. Events characterized by a typical fast rise phase and exponential decay were automatically detected and then manually verified in MiniAnalysis. Event frequency, mean amplitude, whole cell capacitance, and kinetics were averaged across neurons (i.e. n= neurons) and groups were compared using a One Way ANOVA followed by Tukey's *post hoc* tests for these normally distributed parametric data. Data are expressed as mean ±SEM. Antidromic stimulation data are expressed as percentage of slices which responded to the stimulation with multiple depolarization population spikes. These data were compared using a Chi-square test because these are nonparametric nominal data. Resting or THIP-induced tonic current measures were made by subtracting averaged holding current measures from unitary events during baseline or THIP application from bicuculline holding current measures and normalized to whole cell capacitance. Data are expressed as mean ±SEM and groups were compared using a One Way ANOVA followed by Tukey's *post hoc* tests for these normally distributed parametric data. For photostimulation data analysis, eEPSCs were compared in the period 200 ms prior to and after the uncaging event to determine evoked response (#eEPSCs after stim - #eEPSCs pre-stim). A series of 5 stimuli were applied per stimulation site at 0.1 Hz. The average response of the 5 stimuli was recorded per site. The mean glutamate photostimulation

evoked response for all sites of each group is reported as well as ratio of responding and non-responding sites. This data was compared using Kruskal-Wallis ANOVA with Dunn's *post hoc* tests because this was nonparametric data.

Any variation to these methods is described in an additional methods section for the chapter in which they were used.

Chapter 3: Effects of rapamycin treatment on neurogenesis and synaptic reorganization in the dentate gyrus after controlled cortical impact injury in mice

This chapter was published in Frontiers in Systems Neuroscience. Nov. 2015; 9 (163). Jeffery A. Boychuk and Bret N. Smith are additional authors for this paper, and this chapter is similar to the published manuscript. Some additions/modifications to the text and figures have been made for clarity of information.

3.1 Introduction

Traumatic brain injury (TBI) can result in post-traumatic epilepsy (PTE) in a significant proportion of moderate to severe TBI patients, and PTE accounts for about 20% of symptomatic epilepsies (Caveness et al., 1979;Annegers et al., 1998;Englander et al., 2003). PTE most commonly manifests as neocortical or temporal lobe epilepsy (Diaz-Arrastia et al., 2000;Hudak et al., 2004). Preventative therapies for PTE have been largely ineffective or have had varying outcomes depending on the type of epilepsy, leaving ~30% of PTE patients intractable to medical therapies (Temkin et al., 1998;Temkin et al., 2001;Temkin, 2009). One treatment proposed to prevent PTE in mice is the use of the mammalian target of rapamycin (mTOR) inhibitor rapamycin after injury (Guo et al., 2013). Rapamycin has shown promise in reducing aberrant axonal sprouting and some forms of epileptogenesis, but its effectiveness in preventing seizures in models of acquired epilepsy has been inconsistent (Zeng et al., 2008;Buckmaster and Wen, 2011;Guo et al., 2013;Heng et al., 2013). Studies of rapamycin effects in chemical convulsant models of TLE indicated that rapamycin reduced or eliminated mossy fiber sprouting, but did not prevent spontaneous seizures (Buckmaster and Wen, 2011;Heng et al., 2013). Rapamycin suppressed the development of PTE in mice after controlled

cortical impact (CCI) injury, but mossy fiber sprouting recurred after cessation of treatment (Guo et al., 2013). Although mossy fiber sprouting is a hallmark of TLE in animal models and in patients, its causative association with epilepsy development is still controversial and functional outcomes of rapamycin treatment on synaptic reorganization in models of acquired epilepsy are not well described.

Expanding our understanding of how rapamycin treatment exerts its disease-modifying effects in a model of PTE may identify key antiepileptogenic components of mTOR inhibition and guide future treatments and therapeutics for PTE. The mechanism(s) by which mTOR inhibition may alter epileptogenesis, however, are not fully described. Some of the known biochemical and structural cellular effects of increased mTOR signaling include increased protein synthesis, cell growth, and cell proliferation, which may contribute to several outcomes associated with both TBI and TLE, including mossy fiber sprouting, recurrent excitation of dentate granule cells, and enhanced neurogenesis in the dentate gyrus (Buckmaster and Dudek, 1997b;Parent and Lowenstein, 1997;Winokur et al., 2004;Parent et al., 2006). Selective genetic upregulation of mTOR activity in newborn granule cells leads to an epilepsy phenotype (Hester and Danzer, 2013), and increased adult neurogenesis has been hypothesized to contribute substantially to epileptogenesis (Parent et al., 2006;Kron et al., 2010). In this study, we investigated cellular, electrophysiological, and disease modifying effects of rapamycin treatment after CCI in mice, a model of PTE (Hunt et al., 2009; 2010; 2011;Hunt et al., 2012;Guo et al., 2013). We tested the hypothesis that continual rapamycin treatment after CCI injury reduces post-injury neurogenesis, mossy fiber

sprouting, and synaptic reorganization in the dentate gyrus, which may correlate with reduced seizure expression.

3.2 Methods

Cell counts: FJB labeling was performed on sections from mice 3 days post-injury. Numbers of FJB-labeled neurons were counted between -1.22 to -3.52 mm from bregma in the upper and lower blade of the dentate granule cell layer and the hilus at 20x and 40x magnification (Olympus, BX40) by an investigator blinded to animal treatment. For figures, representative images were taken at 4x and 10x magnification to display the whole dentate gyrus. FJB labeling was normalized to the area of the dentate gyrus and hilus obtained from sections adjacent to those used for FJB labeling. These adjacent sections were Nissl stained and area measurement included the dentate granule cell layer and the hilus inside the region outlined by a line around the outer edge of the granule cell layer and connecting the tips of the dentate granule cell layer with the most proximal point of the CA3 pyramidal cell layer using ImageJ software. For each animal, cell density was calculated per section and then averaged across the entire hippocampus to obtain an overall measure of cell density. Additionally, cell density was measured as a function of distance from bregma. For these measurements tissue sections were placed in anatomical order using a mouse brain atlas (Paxinos and Franklin, 2001) and cell density was averaged for each animal at each anatomical location.

DCX-immunolabeled sections were obtained from mice perfused 14 days after injury. Numbers of DCX-immunolabeled dentate granule cells were counted between -1.22 to -3.52 mm from bregma in the upper and lower blade of the dentate granule cell

layer at 20x and 40x magnification (Olympus, BX40) by an investigator blinded to animal treatment. For figures, representative images were taken at 4x and 10x magnification to display the whole dentate gyrus. DCX cell counts were normalized to the dentate granule cell area measured from DAPI counterstain of immunolabeled sections. Area measurement included only included the dentate granule cell layer and was outlined by tracing in ImageJ. Cell density for DCX-immunolabeling was measured the same as described for FJB-labeled neurons, both across the hippocampus measured and subdivided into anatomical locations.

Methods used in Chapter 3 also include: traumatic brain injury, rapamycin injection, seizure observations, Timm staining, immunohistochemistry, dentate granule cell layer area, FJB staining, slice preparation, extracellular field recordings, and whole cell recordings described in Chapter 2 of this dissertation.

3.3 Results

We compared cellular and behavioral outcomes (i.e., FJB staining, DGC area, DCX staining, mossy fiber sprouting, field potential responses, sEPSC frequency, and seizures) in the dentate gyrus of mice from sham-injured, CCI-injured with vehicle treatment, and CCI-injured with rapamycin treatment (3 or 10 mg/kg). For cellular outcomes, each hemisphere was assessed independently for all groups. Initial comparisons between hemisphere from sham-injured mice and the hemisphere contralateral to CCI injury in vehicle- and rapamycin-treated mice indicated there were no differences in the cellular outcomes for these groups. Data from sham and

contralateral hemisphere were compared using a One-way ANOVA for normally distributed parametric data, or Kruskal Wallis/Chi-square statistic for non-parametric data, and significance was set at $p < 0.05$. No significant differences were found for any measure between sham-injured mice and those made in the hemisphere contralateral to CCI injury ($p>0.05$). For each analysis of cellular outcome, these groups were therefore combined as a single control group for clarity of presentation. Table 3.1 compares results of measurements from both hemispheres after sham surgery with results from the hemisphere contralateral to CCI injury in mice treated with vehicle or rapamycin.

Table 3.1. Measures from sham operated mice (both hemispheres) and the hemisphere contralateral to injury after CCI in mice treated with vehicle or rapamycin.

Group	FJB + cell density (FJB-positive cells/mm^2)	DGC area (mm^2)	DCX + cell density (DCX-positive cells/mm^2)	Timm score	Recurrent excitation (% slices with secondary depolarization)	sEPSC frequency (Hz)
Sham (contralateral)	N/A	0.130 ± 0.012 (n = 7)	774.50 ± 96.37 (n = 6)	0.285 ± 0.02	0% (0/5 slices)	N/A
Sham (ipsilateral)	N/A	0.130 ± 0.012 (n = 7)	637.42 ± 44.42 (n = 6)	0.248 ± 0.047	20% (1/5 slices)	N/A
CCI + vehicle (contralateral)	7.07 ± 1.20 (n = 7)	0.133 ± 0.013 (n = 8)	957.00 ± 133.99 (n = 6)	0.260 ± 0.034	25% (2/8 slices)	0.83 ± 0.11 (n = 14)
CCI + Rapa (3 mg/kg; contralateral)	8.33 ± 1.30 (n = 7)	0.130 ± 0.013 (n = 6)	742.77 ± 142.46 (n = 5)	0.333 ± 0.108	20% (2/10 slices)	0.5 ± 0.10 (n = 9)
CCI + Rapa (10 mg/kg; contralateral)	7.19 ± 1.32 (n = 6)	0.126 ± 0.014 (n = 7)	760.86 ± 131.20 (n = 6)	0.437 ± 0.091	25% (2/8 slices)	0.81 ± 0.26 (n = 12)

One-way ANOVA with Tukey's post hoc analysis, or Kruskal Wallis/Chi-square statistic where appropriate, were used to obtain the p-value; $p > 0.05$ for all analyses.

3.3.1 Behavioral seizure monitoring

Subsets of mice were monitored for behavioral seizures after severe (1.0 mm depth) unilateral CCI injury from 6-10 weeks post-injury (6 hr/week) to qualitatively assess spontaneous seizure development. Consistent with previous reports, four of 10 mice (40%) that received CCI injury and vehicle treatment displayed spontaneous seizures during this period post-injury (Hunt et al., 2009; 2010;Guo et al., 2013). All were S2 seizures with tail stiffness and freezing for more than 30 seconds. One of 12

mice (8%) in the low-dose (3mg/kg) rapamycin-treated group and one of 11 mice (9%) in the high-dose (10 mg/kg) rapamycin-treated group were observed to have spontaneous seizures (all category S2). Although numerically lower in the rapamycin treatment groups, and a trend toward reduced seizures was apparent, the prevalence of observed seizures in CCI injured mice with no treatment and CCI injured mice with rapamycin treatment was not significantly different using a Chi-square test of probability (3mg/kg, p=0.078; 10mg/kg, p=0.097). These data indicate that mTOR activity may influence seizure development after CCI in some cases, but mTOR inhibition is not sufficient to prevent epileptogenesis after CCI injury in all mice.

3.3.2 Fluoro-Jade B (FJB) labeling

Regional cell loss (i.e., dentate gyrus, hilus, and CA3 pyramids) in the hippocampus is a common feature after TBI (Lowenstein et al., 1992;Hicks et al., 1993;Smith et al., 1995). The role of mTOR in neuronal death and survival after TBI has been controversial (Guo et al., 2013;Tanaka et al., 2013). This is likely due to the complex role mTOR plays in the balance of autophagy and apoptosis after injury. Based on previous reports, FJB staining in the ipsilateral hemisphere peaks following CCI injury in the first 3 days after injury (Anderson et al., 2005). We therefore measured FJB staining at 72 hrs post-CCI injury to evaluate this peak FJB staining. Representative images of FJB stained sections from CCI-injured mice treated with vehicle, low-dose rapamycin (3mg/kg), and high-dose rapamycin (10mg/kg) in hemispheres ipsilateral to the injury are shown in Figure 3.1A. The granule cell layer and hilus of mice with CCI

injury + vehicle (309.1 ±37.8 FJB-positive cells/mm^2; n=7), CCI + low-dose rapamycin (256.6 ±27.3 FJB-positive cells/mm^2; n=6), and CCI + high-dose rapamycin (238.6 ±27.0 FJB-positive cells/mm^2; n=7) treatment displayed significantly more FJB-labeled cells ipsilateral to injury than contralateral controls (7.38 ±0.73 FJB-positive cells/mm^2; n=20; One-way ANOVA; $F(3,37)= 66.58$, $p<0.0001$; Tukey's, $p<0.0001$ control vs CCI ipsi, $p<0.0001$ control vs CCI+Rapa(3) ipsi, $p<0.0001$ control vs Rapa(10) ipsi; Fig. 3.1B). There was no difference in the density of FJB-labeled cells between the ipsilateral hemispheres of vehicle- or rapamycin-treated mice after CCI injury ($p>0.05$).

Previously, rapamycin treatment was reported to reduce FJB staining in one region of the dentate gyrus (Guo et al., 2013), so we investigated FJB staining throughout the septo-temporal dentate gyrus and hilus at 180 μm intervals. Using a Two-Way ANOVA we found an interaction effect of FJB labeling between the groups measured at these anatomical locations (Two-way ANOVA; $F(18,224)=7.715$, $p<0.0001$). We therefore investigated the differences between the treatment groups at these anatomical locations, particularly noting reduction of FJB labeling within the rapamycin treated groups as previously described (Guo et al., 2013). We found only 2 intervals in which FJB staining in CCI-injured mice treated with high dose rapamycin was reduced in the ipsilateral hemisphere relative to CCI + vehicle (Bonferroni, p=0.0451 CCI+Rapa(10) ipsi vs CCI ipsi at -2.64 to -2.82, p=0.0026 CCI+Rapa(10) ipsi vs CCI ipsi at -3.00 to -3.18; Figure 3.1C). These locations were between -2.62 to -3.18 mm from bregma, which is ~1 mm posterior to injury epicenter (Fig 3.1C). There was no significant reduction in FJB staining at any other location along the hippocampal axis after CCI injury in

rapamycin-treated mice and FJB labeling was significantly increased relative to controls at all septo-temporal locations.

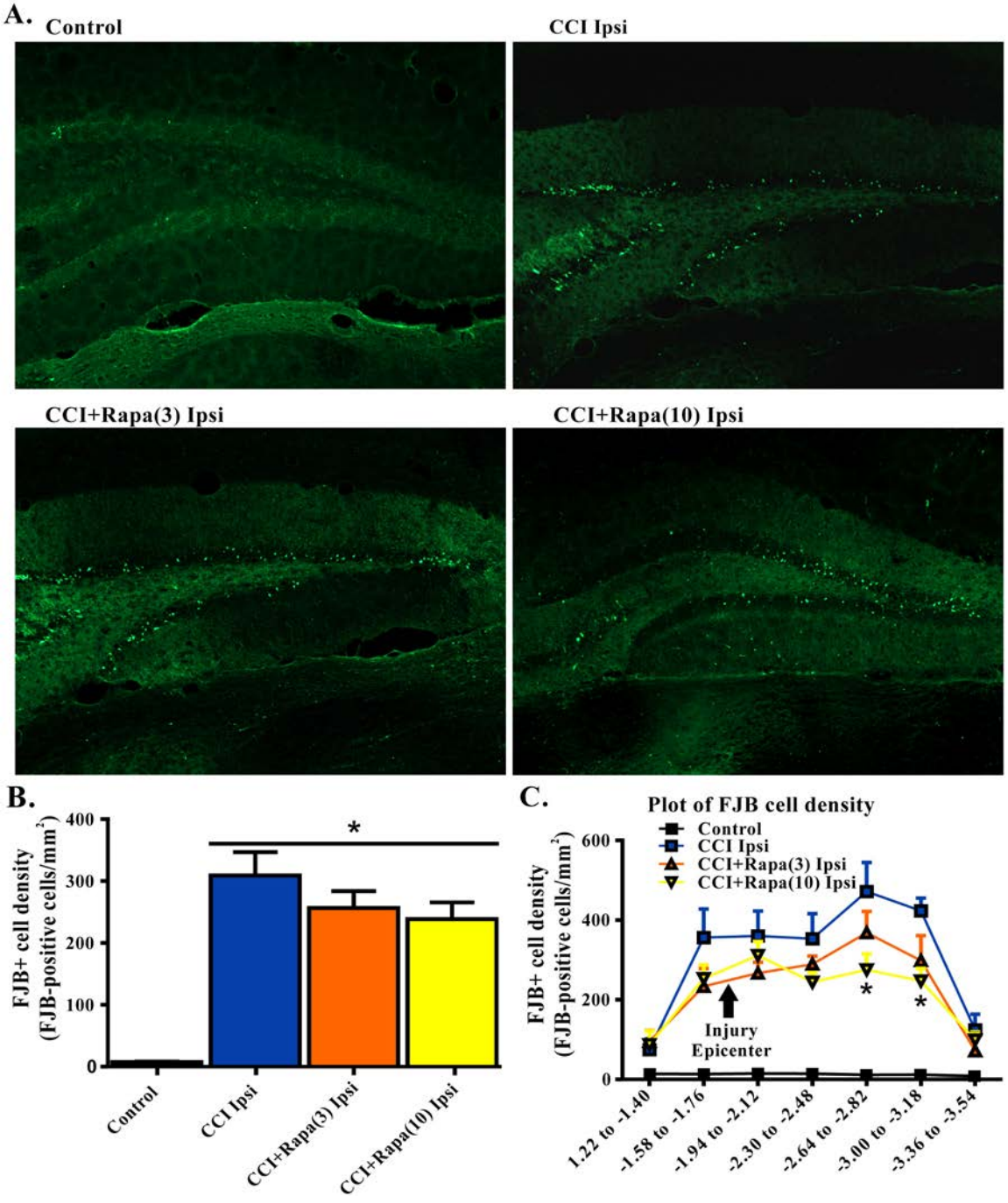

Figure 3.1. Fluoro-Jade B labeling in dentate gyrus 3 days after control treatment, CCI or CCI with daily rapamycin administration. A. Representative images of Fluoro-Jade B (FJB) labeling from four different groups: control, ipsilateral to CCI injury + vehicle (CCI Ipsi), ipsilateral to CCI injury + rapamycin at 3 mg/kg (CCI+Rapa(3)

Ipsi), and ipsilateral to CCI injury + rapamycin at 10 mg/kg (CCI+Rapa(10) Ipsi). **B.** Mean FJB labeling in control, CCI Ipsi, CCI+Rapa(3) Ipsi, and CCI+Rapa(10) Ipsi groups. FJB-positive cell density (cells/mm^2) was averaged across coronal slices from -1.22 to -3.52 mm from bregma. All CCI ipsilateral hemispheres exhibited increased FJB-positive cell density relative to controls. No significant difference was observed after CCI injury between vehicle- and rapamycin-treated mice. **C.** FJB-positive cells/mm^2 as a function of distance from bregma along the septo-temporal axis of hippocampus. The CCI+Rapa(10) group exhibited reduced FJB-positive cell density only in a limited region of posterior hippocampus relative to CCI + vehicle treatment. Error bars indicate SEM; asterisk (*) indicates $p < 0.05$.

3.3.3 Dentate granule cell layer area

Both cell death and cell proliferation are common features in the dentate granule cell layer following injuries such as TBI and seizures (Parent et al., 1997;Rola et al., 2006;Carlson et al., 2014). After TBI in rodents, a reduction in dentate granule cell count or area has been observed early (48 hr.) after injury (Smith et al., 1995). This reduction persists for up to 7 days (Witgen et al., 2005) and is alleviated by 2 weeks post-injury (Grady et al., 2003), suggesting cell proliferation compensates for early cell loss after injury. To test the effect of rapamycin on dentate granule cell layer thickening at a time point corresponding to its restoration after CCI injury, dentate granule cell layer area was measured 14 days after injury in Nissl stained sections from control (0.125 ±0.006 mm^2; n=35; Fig. 3.2B), CCI with vehicle (0.110 ±0.009 mm^2; n=8; Fig 3.2B), CCI with low-dose rapamycin treatment (0.094 ±0.010 mm^2; n=6; Fig. 3.2B), and CCI with high-dose rapamycin treatment (0.093 ±0.005 mm^2; n=7; Fig. 3.2B). Representative images of Nissl stained sections are shown in Figure 3.2A. The overall One-way ANOVA indicated a significant change in dentate granule cell area among the experimental groups (One-way ANOVA; $F(3,41)=6.476$, $p=0.0003$; Fig. 3.2B) Rapamycin treatment resulted in a significant reduction of DGC layer area ipsilateral to the injury relative to control

(Tukey's, p=0.0053 control vs CCI+Rapa(3) ipsi, p=0.0007 control vs CCI+Rapa(10) ipsi; Fig. 3.2B). There was a trend toward decreased granule cell layer area after CCI, but a significant change was not detected (Tukey's, p=0.0846).

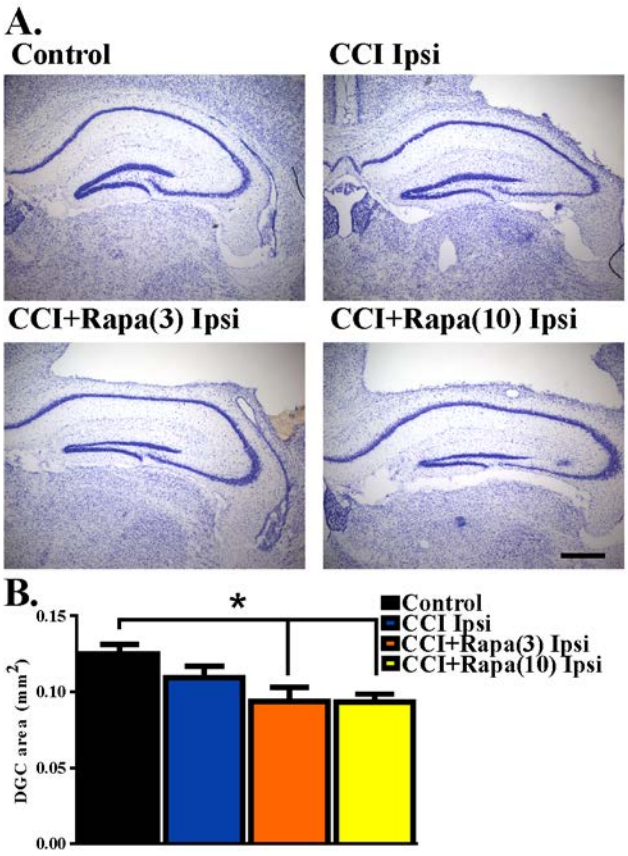

Figure 3.2. Dentate granule cell area 14 days after injury in mice from control, CCI-injured, and CCI-injured with rapamycin treatment. A. Representative images of Nissl stained sections ipsilateral to injury from the four different treatment groups: sham-operated control, CCI injury + vehicle (CCI Ipsi), CCI injury + 3 mg/kg rapamycin (CCI+Rapa(3) Ipsi), and CCI injury + 10 mg/kg rapamycin (CCI+Rapa(10) Ipsi). Hippocampal sections were from similar anterior-posterior coordinates. **B.** Mean dentate granule cell area from Nissl stained sections in control, CCI Ipsi, CCI+Rapa(3) Ipsi, and CCI+Rapa(10) Ipsi groups. Scale bar indicates 0.5 mm. Error bars indicate SEM; asterisk (*) indicates $p < 0.05$.

3.3.4 Doublecortin (DCX) immunolabeling

Shortly after CCI injury there is an initial decrease in DCX expression ipsilateral to injury, but from days 7 to 14 after injury an increase in DCX expression ipsilateral to the injury has been reported (Dash et al., 2001;Rola et al., 2006;Barha et al., 2011). This proliferation of newborn dentate granule cells after injury or status epilepticus has been proposed to contribute substantially to epileptogenesis (Parent et al., 2006;Hester and Danzer, 2013;LaSarge et al., 2015). Therefore, DCX expression was examined 14 days after injury in control mice (n=29), vehicle-treated CCI-injured mice (n=6), CCI-injured mice with low-dose rapamycin treatment (n=5), and CCI-injured mice with high-dose rapamycin treatment (n=6). Figure 3.3A shows representative images of DCX staining from the dentate gyrus ipsilateral to the injury (or sham surgery) in these groups. The overall One-way ANOVA indicated a significant change in DCX immunolabeling among the experimental groups (One Way ANOVA; $F(3,39)=4.838$, $p=0.0059$)In the ipsilateral hemisphere, a significant increase in DCX expression was observed in vehicle-treated CCI-injured mice relative to controls (Control: 730.04 ±51.71 DCX-positive cells/mm^2; CCI: 1154.15 ±114.00 DCX-positive cells/mm^2; Tukey's; $p=0.0081$; Fig. 3.3B). The relative increase in DCX expression after CCI was observed up to ~1.5 mm temporal to the injury epicenter (Fig. 3.3C). Rapamycin treatment after CCI injury significantly reduced DCX expression to levels similar to control (rapamycin 3mg/kg: 653.94 ±85.99 DCX-positive cells/mm^2, $p=0.6098$ control vs CCI+Rapa(3) ipsi, $p=0.0081$ CCI ipsi vs CCI+Rapa(3) ipsi; rapamycin 10mg/kg: 728.51 ±117.2 DCX-positive cells/mm^2, $p=0.8848$ control vs CCI+Rapa(10) ipsi, $p=0.0267$ CCI ipsi vs CCI+Rapa(10) ipsi; Fig.

3.3B). These results are consistent with an inhibitory effect of rapamycin treatment on post-injury neurogenesis.

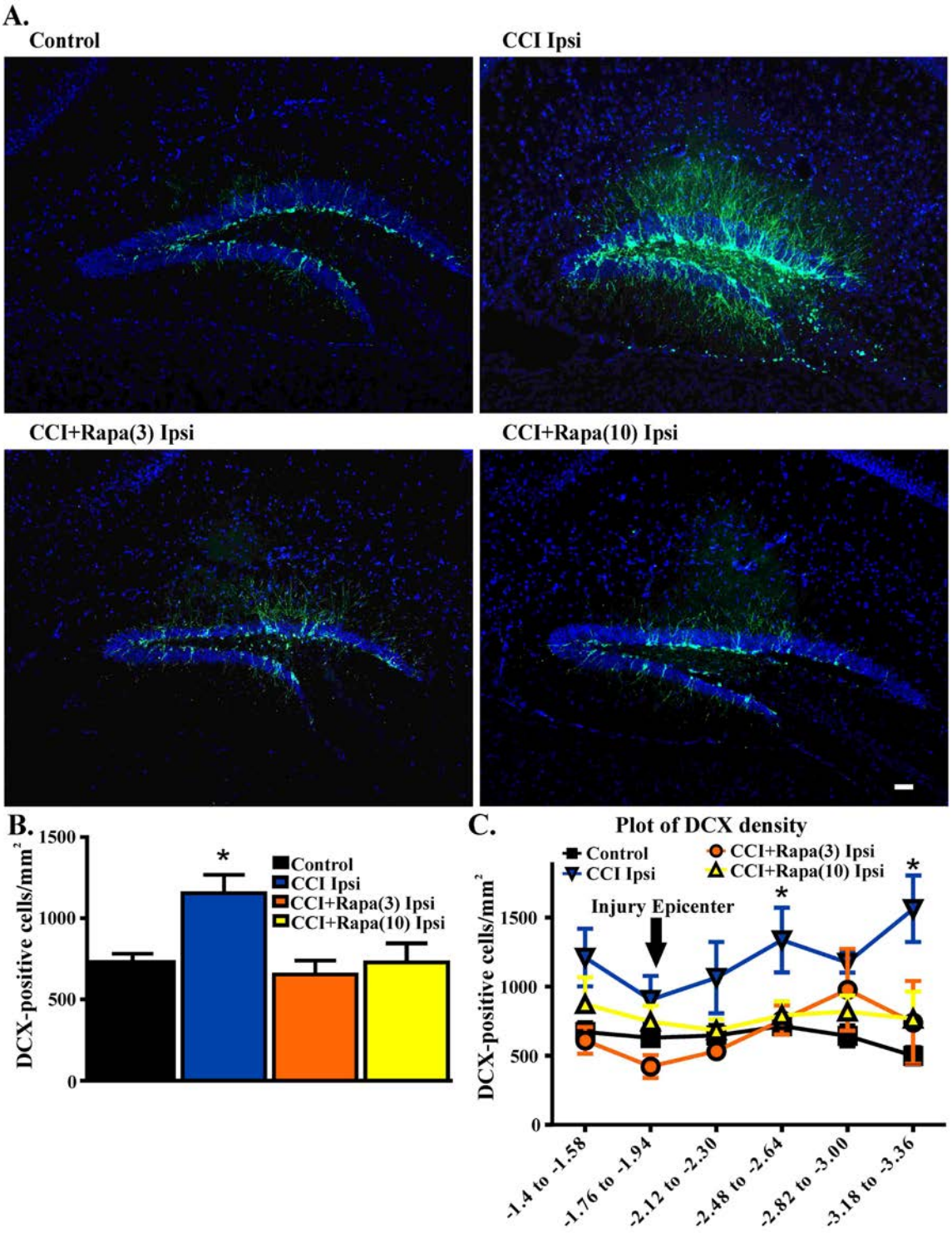

Figure 3.3. Doublecortin (DCX) immunolabeling in dentate gyrus 14 days after injury in mice from control, CCI-injured, and CCI-injured with rapamycin groups. **A.** Representative images of DCX expression from four treatment groups: control, CCI Ipsi, CCI+Rapa(3) Ipsi, and CCI+Rapa(10) Ipsi. **B.** Mean DCX expression in control, CCI Ipsi, CCI+Rapa(3) Ipsi, and CCI+Rapa(10) Ipsi groups. Ipsilateral CCI exhibited greater DCX-positive cell density compared to controls. The injury-induced increase in DCX-positive cell density in CCI ipsi mice was not observed in either CCI+Rapa treatment group. **C.** DCX-positive cells/mm^2 as a function of distance from bregma along septo-temporal axis of hippocampus. Scale bar indicates 0.1 mm. Error bars indicate SEM; asterisk (*) indicates $p < 0.05$.

3.3.5 Timm staining

Several weeks after CCI, there is an increase in Timm staining in the inner molecular layer of the dentate gyrus ipsilateral to the injury relative to the contralateral hemisphere or in sham-treated mice (Hunt et al., 2009; 2010; 2011;Hunt et al., 2012;Guo et al., 2013). Rapamycin treatment for 4 weeks post-injury reduced Timm staining five weeks after CCI (Guo et al., 2013). However, as with studies done in the pilocarpine-induced status epilepticus model of TLE (Buckmaster et al., 2009), mossy fiber sprouting recurred after cessation of treatment. To assess the effects of continuous rapamycin treatment on mossy fiber sprouting after injury, Timm staining was examined in control mice and in CCI-injured mice treated daily for 8-13 weeks with rapamycin or vehicle. Slices used for extracellular field potential recordings, as well as mice perfused for histology, were used for Timm staining measurements. There was no significant difference between the contralateral hemispheres of any of the groups (all exhibited Timm scores <1; Table 3.1). Figure 3.4A shows representative images of Timm stained sections ipsilateral to the injury from control, CCI+vehicle, CCI+rapamycin (3mg/kg), and CCI+rapamycin (10mg/kg) treated mice. The overall Kruskal-Wallis test indicated a

difference in Timm scores among the experimental groups (Kruskal Wallis stat=41.41, $p<0.0001$). In vehicle-treated mice, Timm scores in hemispheres ipsilateral to CCI injury were increased relative to control hemispheres (control: 0.364 ±0.05, n=31; vehicle+CCI: 2.035 ±0.300, n=12; Dunn's, $p<0.0001$; Fig. 3.4B). In low-dose rapamycin-treated mice, Timm scores were reduced (1.275 ±0.315, n=12; Fig 3.4B) ipsilateral to the injury relative to vehicle-treated mice after CCI injury (Dunn's, $p=0.025$), but remained greater than controls (Dunn's, $p<0.0001$). Mossy fiber sprouting was not different from controls in the high-dose rapamycin treatment group (0.55 ±0.09, n=11; Dunn's, $p=0.145$ versus control, $p<0.0001$ versus CCI ipsi; Fig. 3.4B). Although the average mossy fiber sprouting score was reduced in mice that received rapamycin treatment, localized areas of mossy fiber sprouting into the inner molecular layer were always observed in the dentate gyrus of mice that expressed spontaneous behavioral seizures. These data indicated that continual rapamycin treatment reduced mossy fiber sprouting after CCI injury and this reduction was maintained during treatment for up to 12 weeks.

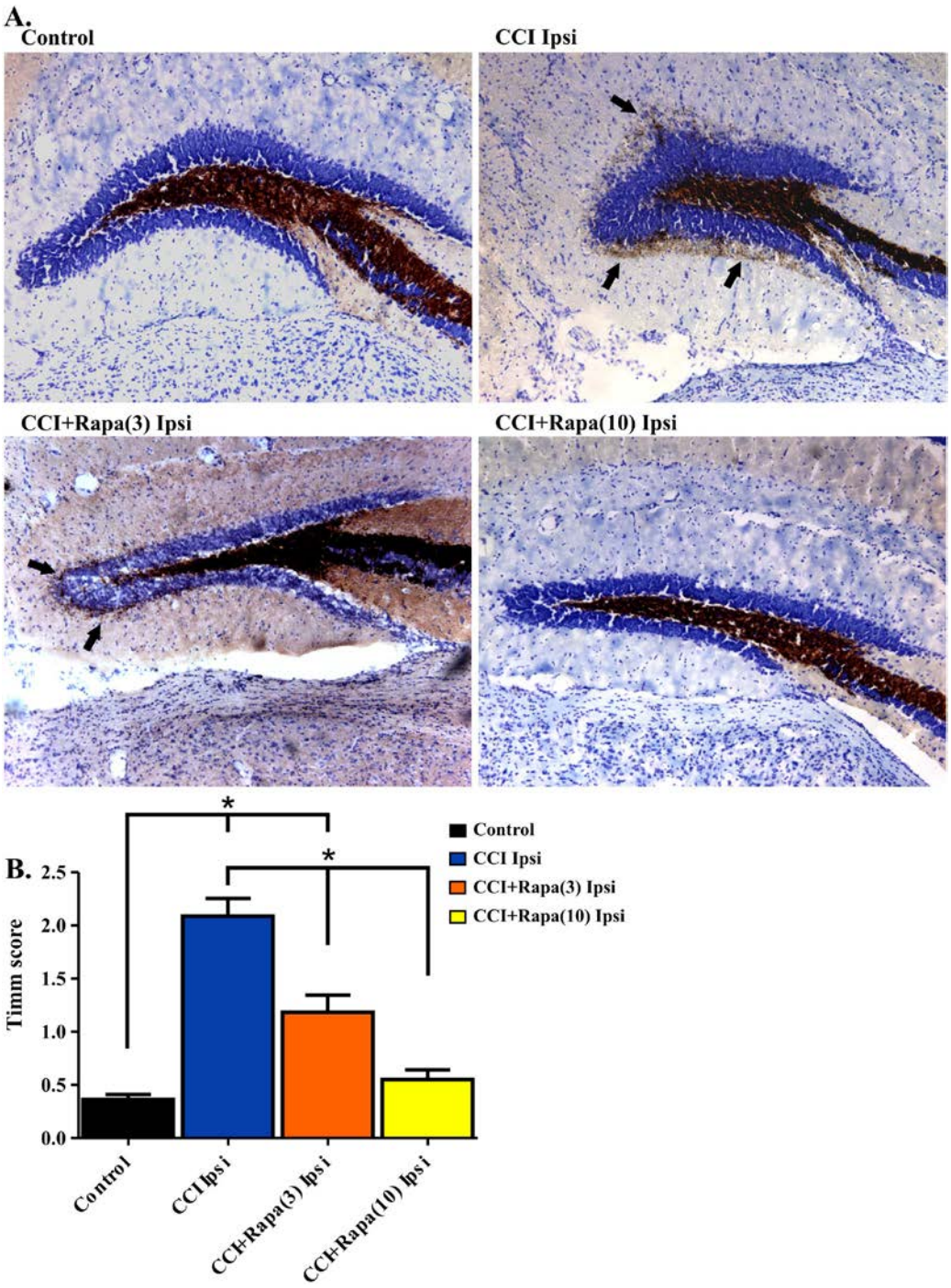

Figure 3.4. Timm staining in the dentate gyrus 8-13 weeks post-injury from sham-operated control, CCI injured, and CCI-injured with rapamycin treatment groups. **A.** Representative images of Timm staining from the four different groups: control, CCI Ipsi, CCI+Rapa(3) Ipsi, and CCI+Rapa(10) Ipsi. **B.** Mean Timm scores in control, CCI Ipsi, CCI+Rapa(3) Ipsi, and CCI+Rapa(10) Ipsi groups. The injured hemisphere of both CCI Ipsi and CCI+Rapa(3) Ipsi groups exhibited higher Timm scores relative to the control group. Mice receiving rapamycin treatment (10 mg/kg) after CCI had Timm scores similar to controls. Error bars indicate SEM; asterisk (*) indicates $p < 0.05$.

3.3.6 Network excitability in dentate gyrus

Increased network excitability (Hunt et al., 2009) and synaptic connectivity between granule cells (Hunt et al., 2010) emerge in the dentate gyrus several weeks after CCI injury. Antidromically-evoked field potentials following electrical stimulation of the hilus were examined in slices perfused with Mg^{2+} free ACSF with bicuculline (30 μM) 8-13 weeks after injury. Data are expressed as percent of slices with SEM as multiple slices were obtained from individual animals. In these recordings, a single antidromic population spike was elicited after hilar stimulation in most slices (29/36) from five control animals (Table 3.1; Fig. 3.5A). In contrast, a secondary after discharge was observed in most slices (11/14 slices from 9 mice) from the ipsilateral hemisphere of vehicle-treated CCI-injured mice (Fig. 3.5A), similar to previous findings in this model (Hunt et al., 2009); Chi-square statistic= 15.295; $p<0.0001$; Fig. 3.5B). Low-dose rapamycin treatment reduced, but did not normalize the percentage of slices with secondary depolarization in ipsilateral hemisphere (5/9 slices from 8 mice; Chi square statistic= 1.3707; $p=0.241$ versus CCI ipsilateral; Fig 3.5B). In mice treated with high-dose rapamycin, the percentage of slices ipsilateral to the injury that responded with a secondary depolarization (2/10 slices from 10 mice) was significantly lower than for vehicle-treated CCI-injured mice (Chi-square statistic= 8.0607; $p=0.0045$; Fig. 3.5B), and was similar to controls ($p=0.9687$). Notably, 86% of slices from CCI-injured, rapamycin-treated mice that displayed increased network excitability also exhibited localized mossy fiber sprouting near the recording site upon *post hoc* examination. Overall, rapamycin treatment after CCI significantly reduced dentate granule cell network excitability

following hilar antidromic stimulation, but excitability was maintained in slices with mossy fiber sprouting.

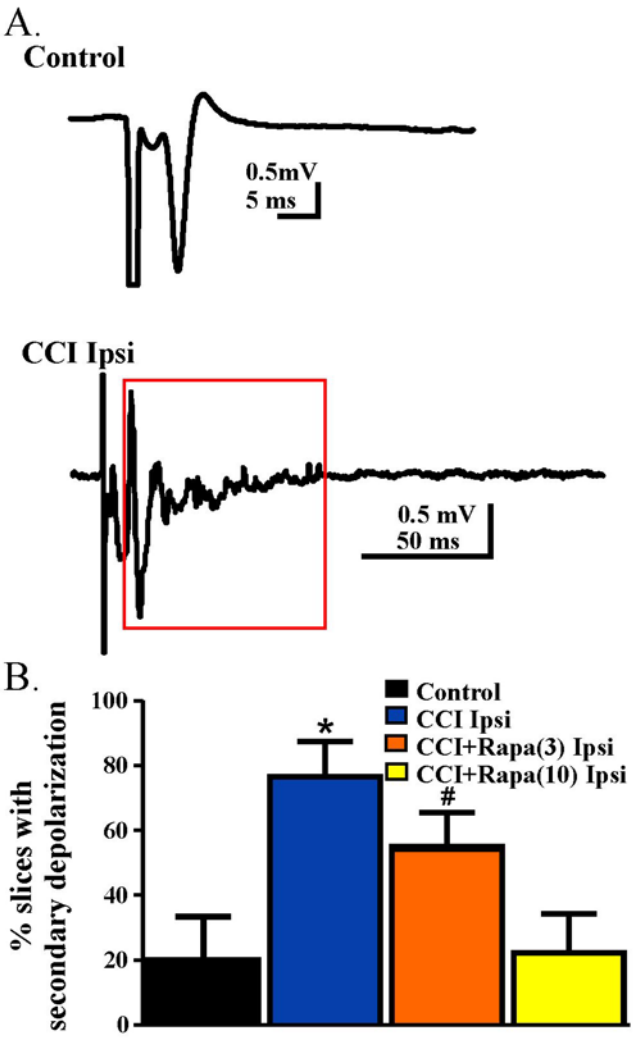

Figure 3.5. Network excitability of dentate granule cells after antidromic electrical stimulation 8-13 weeks post-injury. A. Representative traces of field potential responses to antidromic hilar stimulation in control and CCI-injured mice. A secondary depolarization was often observed in slices ipsilateral to CCI injury (red box indicates area of secondary depolarization). **B.** Percentage of slices ipsilateral to injury that displayed secondary depolarization from control, CCI Ipsi, CCI+Rapa(3) Ipsi, and CCI+Rapa(10) Ipsi treatment groups. Error bars represent SEM; * indicates $p < 0.05$ for CCI Ipsi relative to control or CCI+Rapa(10). # indicates $p < 0.05$ for CCI+Rapa(3) Ipsi versus control.

3.3.7 sEPSCs in DGCs

Spontaneous EPSCs (sEPSCs) were recorded from dentate granule cells in slices from vehicle- and rapamycin-treated mice 8-13 weeks after CCI. Slices were perfused with nominally Mg^{2+}-free ACSF containing 30 μM bicuculline and cells were voltage-clamped at -70mV (Fig. 3.6A). The overall One-way ANOVA indicated differences in sEPSC frequency between experimental groups (One Way ANOVA; $F(3,56)= 5.336$, $p=0.0026$). sEPSC frequency was greater in DGCs ipsilateral to CCI injury with vehicle treatment relative to controls (control: 0.72 ±0.08 Hz; n=29; CCI: 1.51 ±0.38 Hz, n=14; Tukey's, $p=0.0081$; Fig. 3.6B). The increase in sEPSC frequency after CCI injury was reduced in rapamycin-treated mice (CCI+rapamycin 3 mg/kg: 1.16 ±0.18 Hz; n=11; $p=0.187$ vs CCI+vehicle; CCI+rapamycin 10mg/kg: 0.67 ±0.30 Hz; n=12; Tukey's, $p=0.0267$ vs CCI+vehicle). Relative to controls, however, sEPSC frequency in dentate granule cells from rapamycin-treated (3 mg/kg) mice remained significantly elevated (Tukey's, $p=0.0154$), with no difference between controls and rapamycin treated (10 mg/kg) mice (Tukey's, $p=0.847$). No differences in sEPSC amplitude were found among any of the experimental groups (Control: 12.04 ±0.49 pA; CCI+vehicle: 11.12 ±1.09 pA; CCI+rapamycin 3 mg/kg: 12.06 ±0.78 pA; CCI+rapamycin 10 mg/kg: 10.84 ±1.54 pA; One Way ANOVA, $p= 0.6894$; Fig. 3.6B). Increased sEPSC frequency was observed ipsilateral to the injury after CCI. Low-dose rapamycin treatment reduced, but did not eliminate this increase, whereas sEPSC frequency was similar to controls in mice treated with 10 mg/kg rapamycin daily.

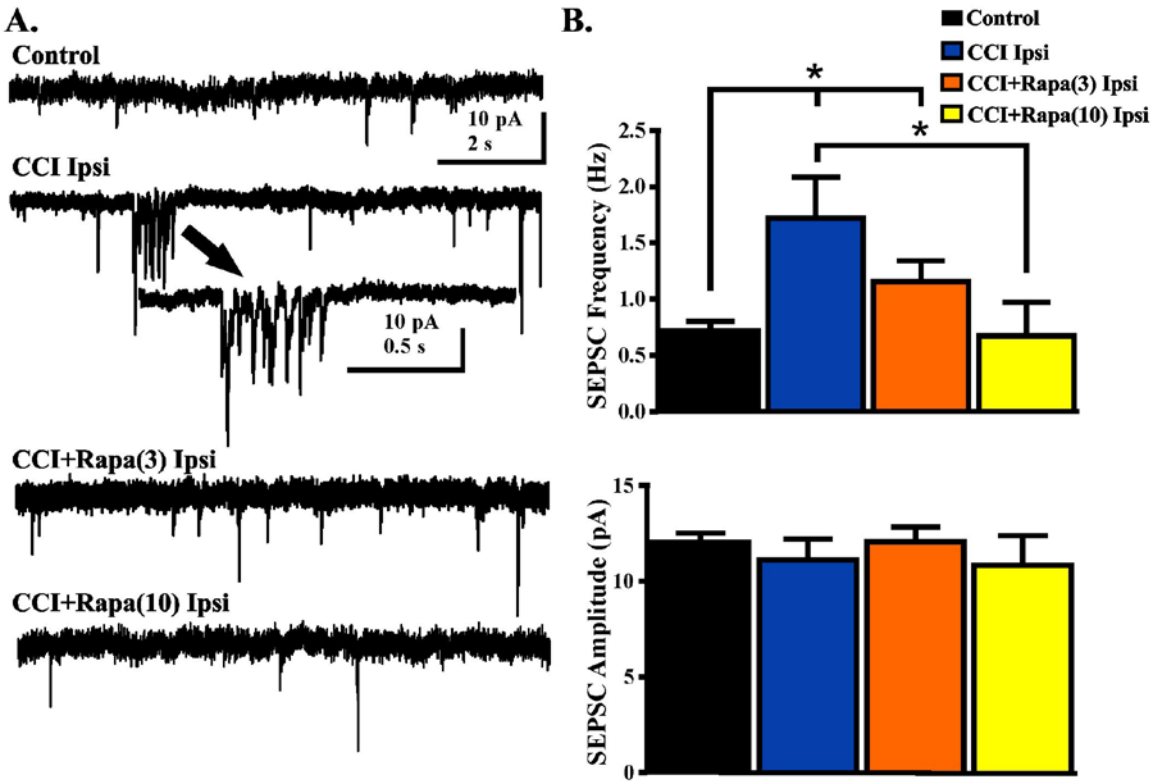

Figure 3.6. Spontaneous EPSCs (sEPSCs) in dentate granule cells 8-13 weeks post-injury. A. Representative traces of sEPSCs in dentate granule cells ipsilateral to injury from four treatment groups: sham and contralateral control, CCI injury + vehicle (CCI Ipsi), CCI injury + 3 mg/kg rapamycin (CCI+Rapa(3) Ipsi), and CCI injury + 10 mg/kg rapamycin (CCI+Rapa(10) Ipsi). All recordings were performed in the presence of nominally Mg^{2+}-free ACSF containing 30 μM bicuculline. Arrow indicates expanded example of a burst of sEPSCs in a dentate granule cell from the vehicle-treated CCI group. **B.** Mean sEPSC frequency and amplitude in the same treatment groups. Error bars indicate SEM; asterisk (*) indicates $p < 0.05$.

3.4 Discussion

Multiple outcome measures associated with epileptogenesis after CCI have been established in the dentate gyrus, allowing for mechanistic investigation of cellular events subsequent to TBI. Within a few weeks after CCI trauma in mice, sprouting of dentate granule cell axons to proximal granule cell dendrites in the inner molecular layer of the dentate gyrus (i.e., mossy fiber sprouting) occurs, synaptic reorganization of dentate

granule cells is observed near the injury site, and mice develop spontaneous seizures after several weeks (Hunt et al., 2009; 2010;Guo et al., 2013). This study focused on the role of mTOR signaling in PTE development using the CCI model of TBI. Previous studies on the effects of rapamycin treatment in acquired epilepsy models have focused mainly on the anatomical phenotype of mossy fiber sprouting and the functional correlation with seizure frequency (Buckmaster and Lew, 2011;Guo et al., 2013). However, increased mossy fiber sprouting and seizure frequency were noted after cessation of rapamycin treatment, suggesting epileptogenic mechanisms that trigger mTOR activity and subsequent neurogenesis or other cellular activity post-injury may be sustained, although the activity itself is suppressed during rapamycin treatment. To avoid confounds associated with reemergence of mTOR activity-related phenotypes after cessation of rapamycin treatment, we continued rapamycin treatment daily throughout the duration of our experiments. Here, we report that rapamycin treatment after CCI injury inhibits the progression of epileptogenesis after focal brain injury in a manner that involves effects on several cellular outcomes associated with development of spontaneous seizures after TBI, including post-injury neurogenesis, mossy fiber sprouting, and synaptic reorganization in the dentate gyrus ipsilateral to the injury. No differences were observed contralateral to injury, implying rapamycin alone had little effect compared to uninjured controls. Both doses of daily rapamycin treatment (3 and 10 mg/kg) were effective in reducing the proportion of mice that developed spontaneous seizures, consistent with effects of an intermediate dose (6 mg/kg) administered for four weeks after CCI injury (Guo et al., 2013). Both rapamycin doses also significantly reduced post-injury neurogenesis in the granule cell layer. Other outcomes, including mossy fiber sprouting and elevated

synaptic excitation were reduced, but not abolished by the lower rapamycin dose, but were abrogated by the high-dose regimen. Granule cell layer area and FJB staining measurements indicated that neither rapamycin dose significantly reduced overall neuronal death after CCI, but cell death was reduced by the high dose regimen at a specific site along the septo-temporal hippocampal axis. The lack of effect on cell death is consistent with the re-emergence of spontaneous seizures after cessation of rapamycin treatment in previous reports and suggests that important components of the underlying injury that triggers the eventual development of epilepsy are not abrogated by mTOR inhibition, even though several other cellular correlates of epileptogenesis are suppressed during high-dose rapamycin treatment.

3.4.1 Newborn neurons

The continual adult generation of selective neuron populations, including within the subgranular zone (SGZ) of the hippocampus (Altman and Das, 1965b;Eriksson et al., 1998), remains one of the least well understood types of experience-dependent brain plasticity. Adult neurogenesis has been proposed to either decrease (Gould and Tanapat, 1997;Rola et al., 2006) or increase after TBI (Liu et al., 1998;Parent et al., 1998;Dash et al., 2001;Arvidsson et al., 2002;Chirumamilla et al., 2002), and markers of adult neurogenesis are diminished if rapamycin is administered pre-SE (Zeng et al., 2009), suggesting effects of rapamycin on proliferation and/or survival of newborn neurons. Two weeks post-injury, we identified an increase in DCX-positive cell density in the dentate gyrus ipsilateral to the injury, consistent with previous reports linking seizures with increased adult neurogenesis (Parent et al., 1997;Parent et al., 1998;Parent et al., 2006).

Both rapamycin doses used in this study suppressed post-injury neurogenesis in association with diminished seizure prevalence, consistent with the hypothesis that mTOR inhibition is associated with decreased adult neurogenesis. Little is known about the role immature dentate granule cells play in the functional connectivity of the hippocampal circuit after brain injury, but several studies have linked seizure-associated synaptic reorganization to abnormal connectivity of newborn neurons. The hypothesis that newborn dentate granule cells contribute selectively to synaptic reorganization and epileptogenesis has been proposed (Kron et al., 2010). Genetic enhancement of the PI3K→AKT→mTOR pathway by deletion of PTEN (i.e., transgenic phosphatase and tensin homolog), specifically in neural progenitors, is sufficient to increase adult neurogenesis (Amiri et al., 2012) and cause development of spontaneous seizures (Pun et al., 2012;Hester and Danzer, 2013;LaSarge et al., 2015). Further, mTOR inhibition with rapamycin attenuates development of seizures in PTEN knockout mice (Sunnen et al., 2011), implicating the mTOR-mediated modulation of adult neurogenesis in the development of acquired epilepsy. Interestingly, and perhaps paradoxically, increased mTOR activation has been proposed as a means of diminishing injury and improving cognitive recovery after TBI in patients (Don et al., 2012), whereas use of rapamycin to suppress mTOR activity post-TBI has been proposed to prevent or suppress epileptogenesis (Guo et al., 2013). A better understanding of the contribution of newly-born neurons to adult brain function in healthy and disease states appears necessary in order to optimally utilize mTOR modulation after TBI for cognitive recovery and prevention of PTE.

3.4.2 Mossy fiber sprouting

Synaptic reorganization in the dentate gyrus after CCI injury was also reduced by rapamycin treatment. The relationship between modulation of post-injury synaptic reorganization and reducing the prevalence of spontaneous seizures in rapamycin treated mice is unclear, since the treatment did not completely eliminate either seizures or mossy fiber sprouting. This was most apparent at the low dose of rapamycin, where both mossy fiber sprouting and seizure prevalence were reduced but not eliminated. It is possible that even limited synaptic reorganization is sufficient for seizure expression (Hunt et al., 2010;Pun et al., 2012). The general failure of many studies to quantitatively link post-injury mossy fiber sprouting with spontaneous seizures, along with recent studies showing that seizures develop in the absence of robust mossy fiber sprouting in the pilocarpine-induced status epilepticus model of epilepsy after rapamycin treatment, have led to the suggestion that mossy fiber sprouting and spontaneous seizures are not causally linked. However, even when quantitatively reduced in rapamycin treated mice, some degree of mossy fiber sprouting was observed in all mice that displayed spontaneous seizures here. While no proven causal relationship exists to date, the qualitative presence of post-injury mossy fiber sprouting suggests it cannot be excluded as a cellular correlate of epileptogenesis. Alternatively, mossy fiber sprouting and synaptic reorganization may represent a secondary change associated with epileptogenesis, since rapamycin prevented significant mossy fiber sprouting, but not spontaneous seizures, in rapamycin treated mice after pilocarpine-induced status epilepticus (Heng et al., 2013). It is also possible that the synaptically reorganized dentate gyrus reflects a relatively mature stage of epileptogenic circuit formation, whereas other factors that occur in earlier stages of

epileptogenesis, including cell loss and adult neurogenesis, contribute to the eventual change in connectivity. The cellular triggers of epileptogenesis remain poorly defined. However, the association of rapamycin treatment with a reduction in seizure prevalence and cellular markers of PTE is consistent with the hypothesis that activation of the mTOR pathway plays a role in development of PTE.

Mice receiving severe unilateral CCI injury begin to develop PTE after a latent period of ~6-10 weeks post-injury (Hunt et al., 2009;Guo et al., 2013). The percentage of mice reported to develop spontaneous behavioral or electrographically measured seizures varies from 36 to 50% (Hunt et al., 2009;Guo et al., 2013). Here 40% of mice receiving CCI without drug treatment developed spontaneous behavioral seizures, similar to previous reports. Rapamycin treatment (6 mg/kg) for 4 weeks after injury reduced seizure prevalence, with 13% of mice expressing electrographically identified seizures (Guo et al., 2013). The proportion of mice exhibiting spontaneous behavioral seizures observed here was similarly reduced in mice that received either low- or high-dose rapamycin treatment in the present study to 8 and 9%, respectively, representing a trend toward reduced seizure prevalence. Notably, our behavioral seizure measurements probably underestimate the total number of seizures in all groups, due to periodic observation. Rapamycin treatment therefore tended to reduce, but did not eliminate, development of generalized spontaneous seizures after CCI.

3.4.3 Network excitability

Electrophysiological indices of network excitability are increased in the dentate gyrus after CCI, including evoked network responses and sEPSC frequency in dentate

granule cells. Commensurate with diminished mossy fiber sprouting, synaptic excitability was suppressed in rapamycin treated CCI-injured mice, and was comparable to controls with the high dose regimen, although increased network excitability was observed in slices where mossy fiber sprouting was present. Others have reported effects of mTOR inhibition on mossy fiber sprouting, but assessment of synaptic or network activity has not been reported previously. Increased electrophysiological responses are hallmarks of synaptic reorganization in excitatory circuitry of the dentate gyrus and are correlated with mossy fiber sprouting and development of spontaneous seizures in this and other epilepsy models (Dudek and Spitz, 1997;Patrylo and Dudek, 1998;Lynch and Sutula, 2000;Winokur et al., 2004;Hunt et al., 2009; 2010; 2011;Hunt et al., 2012). Axon plasticity after injury or seizures is a feature of many neuron types, and these neurons could also contribute to increased sEPSC frequency in dentate granule cells. Although a causative link between synaptic reorganization and epilepsy remains controversial, these results are consistent with reduced functional synaptic reorganization after CCI injury in rapamycin-treated mice.

3.4.4 Cell death

Another hallmark of CCI injury is selective cell loss, particularly in the hilus and dentate gyrus (Hicks et al., 1993;Graham et al., 2000;Maxwell et al., 2003;Anderson et al., 2005). The use of FJB as a marker to infer cell degeneration and necrotic cell death indicates peak cell loss within the first 3 days after CCI injury, with a gradual reduction in neuronal degeneration over time (Anderson et al., 2005;Ansari et al., 2008;Hall et al., 2008). Rapamycin was shown previously to reduce FJB staining in dentate gyrus, CA3, and CA1 regions of the hippocampus three days post-injury at a site ~1 mm posterior to

epicenter (Guo et al., 2013). Here, we assessed the full septo-temporal axis of the hippocampus and found that neither low- nor high-dose rapamycin treatment attenuated FJB staining in the dentate gyrus and hilus. Although FJB labeling remained significantly greater than in controls, 10 mg/kg rapamycin treatment did attenuate FJB staining relative to vehicle treatment after CCI in the ipsilateral hemisphere in the same area (i.e. ~ 1 mm from injury epicenter) as previously reported (Guo et al., 2013). This region corresponds to the area of greatest cell death in this brain injury model. Together, these results suggest the possibility that rapamycin may moderately suppress post-injury neuronal death regionally, even if cell death overall in the dentate gyrus and hilus is unaffected by the treatment.

3.4.5 Conclusions

The findings of this study are consistent with the hypothesis that mTOR inhibition reduces synaptic reorganization among granule cells and inhibits post-traumatic epileptogenesis after CCI. Continuous rapamycin treatment reduced the percentage of mice expressing spontaneous seizures, inhibited measures of synaptic reorganization in the granule cell layer, and abrogated the increase in neurogenesis following CCI injury. Notably, even the highest dose of rapamycin failed to completely prevent PTE or specific cellular changes associated with epileptogenesis, including post-injury cell death, in a substantial number of injured mice. These findings suggest that mTOR inhibition alters disease progression, but does not prevent the initiation of epileptogenesis. The relationship between adult neurogenesis, excitatory synaptogenesis, and seizure susceptibility remains uncertain in the CCI and other models of acquired epilepsy, but we hypothesize that the inhibition of post-injury neurogenesis is a significant feature of the

antiepileptogenic effects of rapamycin treatment following CCI injury. Effects of hormones and growth factors that cross the blood brain barrier after injury have been attributed to an increase in neurogenesis mediated by mTOR activity, and several studies have targeted this mechanism as a therapeutic option to restore cognitive function post-injury (Lu et al., 2005;Sun et al., 2009;Xiong et al., 2012;Carlson et al., 2014). However, the present results imply that potential benefits of increased mTOR signaling might be mitigated by the potentially detrimental epileptogenic effects over time. This study highlights the need for further work to be done in understanding how newly born dentate granule cells integrate and function in the injured hippocampus and how this integration is related to both functional recovery after TBI and the potentially increased risk of seizure susceptibility. Understanding mTOR's role in these processes may help define the critical features of epileptogenesis and recovery from TBI.

Chapter 4: Differential effects of rapamycin treatment on GABAergic inhibition in mouse dentate granule cells after focal controlled cortical impact

4.1 Introduction

In cases of moderate to severe TBI, the incidence of spontaneous seizure development is ~10 to 30 times higher than those of non-injured patients (Temkin et al., 1998;Temkin et al., 2001;Temkin, 2009). The development of spontaneous seizures after a latent, non-symptomatic post-injury period is referred to as post-traumatic epilepsy (PTE) and often manifests as temporal lobe epilepsy (TLE) (Caveness et al., 1979;Annegers et al., 1998;Diaz-Arrastia et al., 2000;Englander et al., 2003;Hudak et al., 2004). One of the primary origins for seizure generation in patients with TLE is the hippocampus, which is also often affected by TBI (Newcomb et al., 1997;Hall et al., 2005;Saatman et al., 2006;Hall et al., 2008). After focal TBI in mice, both excitation and inhibition of dentate granule cells (DGCs) is altered in conjunction with PTE development (Hunt et al., 2009; 2010; 2011). Sprouting of DGC axons into the granule cell and inner molecular layer of the dentate gyrus (i.e. mossy fiber sprouting) leads to recurrent excitation of DGCs and disrupts the normal information processing of the hippocampus. Synaptic inhibition of DGCs is also altered after TBI, and $GABA_A$ receptors ($GABA_AR$'s) undergo functional changes in models of TBI and epilepsy(Mtchedlishvili et al., 2010;Hunt et al., 2011;Raible et al., 2012;Raible et al., 2015;Boychuk et al., 2016).

One prominent cell signaling pathway associated with both TBI and epileptogenesis is the mammalian target of rapamycin (mTOR). Some of the common

biochemical and cellular structure alterations associated with increased mTOR activation after TBI are increased protein synthesis and phosphorylation, axon sprouting, cell migration, and neurogenesis (Buckmaster and Wen, 2011;Guo et al., 2013;Heng et al., 2013;Hester and Danzer, 2013;Butler et al., 2015;LaSarge et al., 2015). Previous studies of mTOR activation in both TBI and epilepsy models have predominately focused on the excitatory circuitry of the hippocampus and, in particular, axonal plasticity of DGCs (Buckmaster and Schwartzkroin, 1994;Wuarin and Dudek, 1996;Winokur et al., 2004;Zeng et al., 2008;Hunt et al., 2009; 2010;Buckmaster and Wen, 2011;Hunt et al., 2012;Guo et al., 2013;Heng et al., 2013;Hester and Danzer, 2013;Butler et al., 2015;LaSarge et al., 2015). The effect of mTOR inhibition in TBI and TLE models on neuron loss is controversial (Buckmaster and Wen, 2011;Guo et al., 2013;Butler et al., 2015), but rapamycin treatment suppresses TLE-related morphological changes in hilar inhibitory interneurons (Buckmaster and Wen, 2011). Hilar interneuron loss likely contributes to altered GABAergic circuitry function and receptor responsiveness after TBI (Mtchedlishvili et al., 2010;Hunt et al., 2011;Boychuk et al., 2016), but effects of mTOR modulation on inhibitory signaling in the dentate gryus after focal brain injury have not been adequately described. We hypothesized that chronic rapamycin treatment following CCI injury leads to reduced TBI-induced changes in synaptic and non-synaptic inhibition of DGCs in the ipsilateral hemisphere.

4.2 Methods

eGFP-positive Hilar Cell Density Measurements: 72 hours after injury, GIN mice were anesthetized by isoflurane inhalation to effect (lack of tail pinch response) and perfused transcardially with 4% paraformaldehyde in 0.1 M sodium phosphate buffer (pH=7.4)

while anesthetized. Brains were then removed and placed in fixative overnight, equilibrated in 30% sucrose for 48 hours, and sectioned at 30 μm on a cryostat (-22^{o}C). 1-in-6 serial section series (180 μm between mounted sections) containing the hippocampus were mounted in Vectashield with DAPI counterstain (Vector Labs) and images were taken on a Zeiss 5 Live confocal microscope (Zeiss; Oberkochen, Germany). Hilar area was measured using ImageJ software to trace along the inner surface of the upper and lower blades of the dentate gyrus and in a line from the tip of each blade of the dentate gyrus to the proximal most point of CA3 pyramidal cell layer. Cell counts from each section were divided by this hilar area measure to give enhanced green fluorescent protein (eGFP) cell density measures for each section. On average, 15 serial sections were taken from each animal and cell density measurements were then averaged for each animal, divided into dorsal, medial, and ventral thirds of hippocampus (i.e. 5 sections per region). Each area covered ~900 μm. The investigator was blinded to animal treatment for all cell counts.

Whole cell recordings: Cells were voltage-clamped at 0 mV for 5-10 min to allow equilibration of pipette and intracellular solutions prior to data collection, after which time whole-cell patch-clamp recordings of spontaneous inhibitory postsynaptic currents (sIPSCs) were obtained. An initial 5 minute baseline recording period was followed by the addition of 4,5,6,7-tetrahydroisoxazolo[5,4-c]pyridine-3-ol hydrochloride (THIP; gaboxadol; 3 μM; Sigma-Aldrich) to the ACSF, a super-agonist of $GABA_AR$'s containing δ subunits. At the concentration used here (3 μM), THIP selectively targets δ subunit-containing, putatively extrasynaptic $GABA_ARs$ that contribute to the tonic GABA current (Ebert et al., 1994;Brown et al., 2002). THIP was applied for 10 minutes

and followed by addition of bicuculline methiodide (30 μM; Tocris Bioscience) to the ACSF for 8 minutes to eliminate postsynaptic inhibitory currents and measure resting tonic current. Recordings exhibiting >25 MΩ (mean= 13.53 ±0.62 MΩ, n=88) series resistance or in which series resistance changed by >20% were discarded.

Data and statistical analysis: Only events with three times the amplitude of root mean squared (RMS) baseline noise were included (RMS= 1.59 ±0.05, n=88). Events characterized by a typical fast rise phase and exponential decay were automatically detected and then manually verified in MiniAnalysis. Tonic current amplitude was detected by subtracting mean steady-state holding current values during baseline or during THIP application from mean steady-state holding current values in the presence of bicuculline methiodide, a competitive antagonist of $GABA_AR$'s. Tonic current amplitude values were normalized to whole cell capacitance (Glykys and Mody, 2007b).

Methods used in Chapter 4 of this dissertation also include: traumatic brain injury, rapamycin injection, slice preparation, and data analysis, as described previously in Chapter 2.

4.3 Results

4.3.1 eGFP-positive hilar interneuron counts

After brain injury, a significant percentage of hilar GABA neurons are depleted (Lowenstein et al., 1992;Toth et al., 1997;Santhakumar et al., 2000). Cell loss following CCI injury peaks within the first three days after insult (Anderson et al., 2005). Therefore, we measured eGFP-positive cell density at 72 hours post-injury to determine the effect of rapamycin on hilar inhibitory interneuron survival after CCI. Cell density

measurements were made in mice from groups of sham operated controls (n=7 mice), CCI injured with vehicle treatment (n=7 mice), and CCI injured with 3 mg/kg rapamycin treatment (n=10 mice). Figure 4.1A shows representative images of eGFP-positive hilar interneurons with DAPI counterstain in the dorsal, medial, and ventral thirds of the hippocampus from sham injured mice and in the hippocampus ipsilateral to CCI injury with vehicle or rapamycin treatment. In the dorsal and medial sections of the hippocampus, there was an interaction effect between group and hemisphere using a Two-way ANOVA (Dorsal; Two-way ANOVA; $F(5,40)=20.12$; $p=0.0033$: Medial; Two-way ANOVA; $F(5,40)=10.57$; $p=0.0005$). CCI injured mice with vehicle or rapamycin treatment exhibited lower eGFP-positive hilar cell density compared to sham-injured controls and hemispheres contralateral to injury in the dorsal (Bonferroni, $p<0.0001$ Sham contra vs CCI ipsi, $p<0.0001$ Sham ipsi vs CCI ipsi, $p<0.0001$ CCI contra vs CCI ipsi, $p<0.0001$ CCI+Rapa contra vs CCI ipsi, $p<0.0001$ Sham contra vs CCI+Rapa ipsi, $p<0.0001$ Sham ipsi vs CCI+Rapa ipsi, $p=0.0003$ CCI contra vs CCI+Rapa ipsi, $p<0.0001$ CCI+Rapa contra vs CCI+Rapa ipsi; Figure 4.1B) and medial (Bonferroni, $p=0.0025$ Sham contra vs CCI ipsi, $p=0.0409$ Sham ipsi vs CCI ipsi, $p=0.0019$ CCI contra vs CCI ipsi, $p=0.0003$ CCI+Rapa contra vs CCI ipsi, $p=0.0004$ Sham contra vs CCI+Rapa ipsi, $p=0.0159$ Sham ipsi vs CCI+Rapa ipsi, $p=0.0003$ CCI contra vs CCI+Rapa ipsi, $p<0.0001$ CCI+Rapa contra vs CCI+Rapa ipsi; Figure 4.1B) portions of the hippocampus (Table 4.1). In the ventral portions of hippocampus there was no significant difference among experimental groups, hemispheres, or the interaction of these variables (Two-way ANOVA; $F(5,40)=0.217$,$p>0.05$; Table 4.1; Figure 4.1B). Rapamycin treatment did not alter hilar interneuron survival after focal brain injury in the

dorsal or medial portions of the hippocampus compared to vehicle treated mice after CCI injury (Bonferroni, $p>0.05$). These data indicate that rapamycin does not affect the loss of eGFP-positive hilar interneurons ipsilateral to CCI injury. Power analysis was performed to estimate sample sizes required to detect a significant effect between vehicle and rapamycin treated mice after CCI injury. The results of this analysis indicated that sample sizes of 44 mice for dorsal and 1563 mice for medial hippocampus would be required in order to reach significance. A previous study which did observe reduced FJB labeling with rapamycin, indicative of neuroprotection, used 6 mice per group which is lower than group sizes in this study (Guo et al., 2013).

Tabel 4.1. Hilar inhibitory interneuron cell counts

Experimental group	Dorsal (cells/mm^2)	Medial (cells/mm^2)	Ventral (cells/mm^2)
Sham contra	17.43 ±2.47 n=7	27.77 ±5.34	39.89 ±7.16
Sham ipsi	15.92 ±1.26 n=7	24.21 ±7.53	42.23 ±7.89
CCI contra	12.34 ±3.37 n=7	22.66 ±3.72	34.15 ±5.37
CCI ipsi	3.16 ±0.67 * n=7	6.61 ±1.63 *	29.28 ±7.14
CCI+Rapa contra	13.02 ±3.41 n=10	28.62 ±5.71	35.89 ±5.72
CCI+Rapa ipsi	5.13 ±0.85 * n=10	7.24 ±2.32 *	36.65 ±3.16

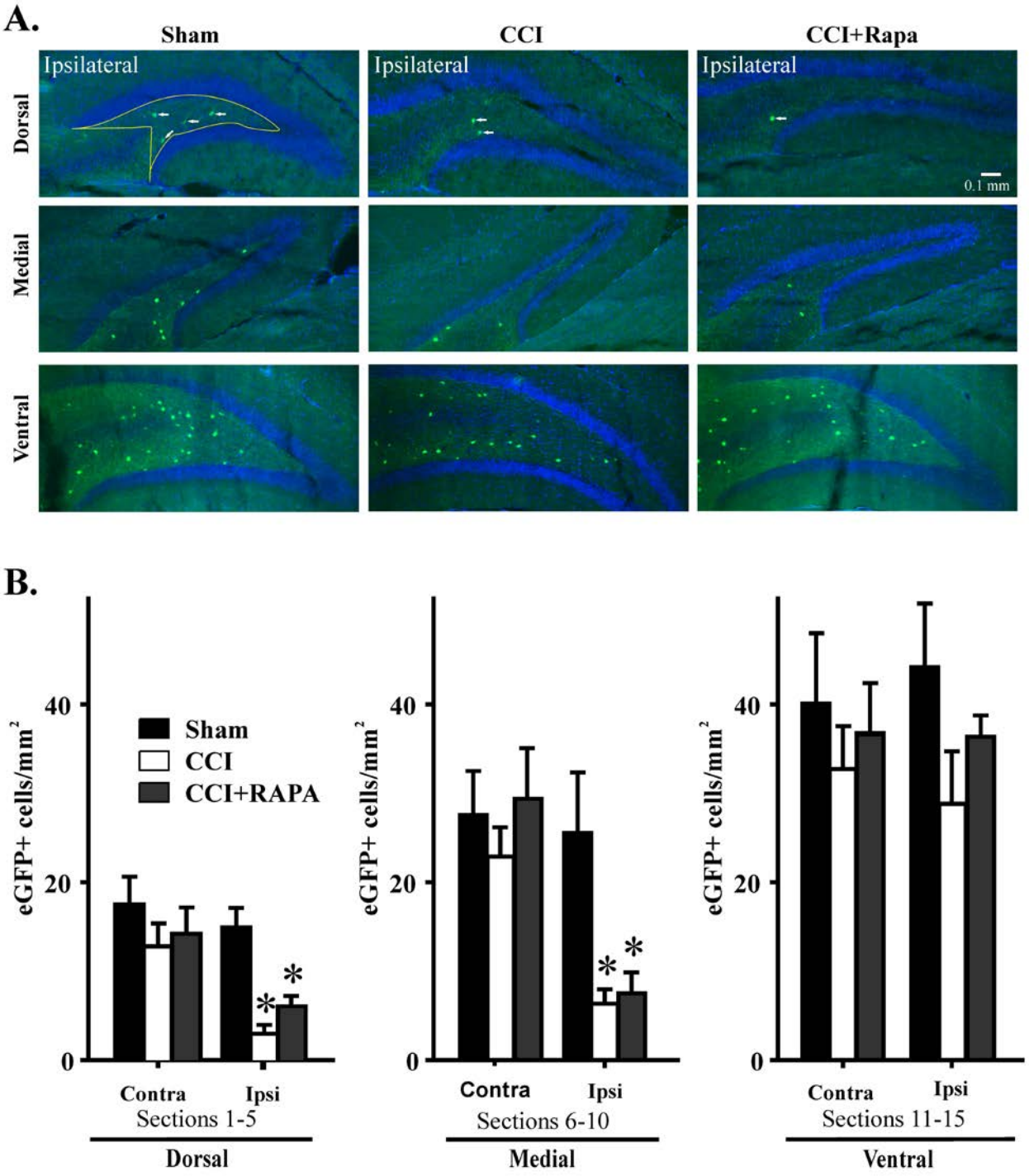

Figure 4.1. eGFP-positive cell density 72 hours post-CCI injury. A. Representative images of eGFP-positive cell distribution in the hilus 72 hours post-injury in three different groups: ipsilateral to sham injury (Sham), ipsilateral to CCI injury + vehicle (CCI Ipsi), and ipsilateral to CCI injury + rapamycin at 3 mg/kg (CCI+Rapa Ipsi) in the dorsal, medial, and ventral thirds of hippocampus. **B.** Representative histograms of mean eGFP-positive cell density 72 hours post-injury in ipsilateral to sham injury, CCI injury with vehicle treatment, and CCI injury with rapamycin treatment in the dorsal, medial

and ventral thirds of hippocampus. In the dorsal and medial thirds, sections ipsilateral to CCI injury exhibited decreased eGFP-positive cell density compared to sham and contralateral hemispheres. Rapamycin treatment did not alter the reduction in eGFP-positive cell density. No difference was observed between any experimental group in the ventral third of hippocampus. Error bars indicate SEM; asterisk (*) indicates $p < 0.05$ versus sham.

4.3.2 sIPSC frequency in DGCs

Although it has been shown that rapamycin reduces axon sprouting of eGFP-positive hilar inhibitory interneurons after pilocarpine treatment in GIN mice (Buckmaster and Wen, 2011), it is not known if this is accompanied by altered inhibition of DGCs. sIPSC frequency was measured in DGCs from sham-injured mice, CCI-injured mice with vehicle treatment, and CCI-injured mice with rapamycin treatment at 1-2 (sham= 5 mice, CCI+vehicle= 7 mice, CCI+Rapa= 8 mice; Figure 4.2A) or 8-13 weeks after injury (sham= 6 mice, CCI+vehicle= 8 mice, CCI+Rapa= 7 mice; Figure 4.2C). At 1-2 weeks post-injury, there was no difference in sIPSC frequency among groups in DGCs contralateral to injury (Sham contra: 2.43 ±0.22 Hz, n=5 cells, CCI contra: 2.41 ±0.23 Hz, n=9 cells, CCI+Rapa contra: 2.29 ±0.27 Hz, n=12 cells; $F(2,24)=0.1112$, $p=0.8953$; One-way ANOVA; Figure 4.2B). The overall ANOVA of the sIPSC frequency from ipsilateral DGCs did indicate an effect among experimental groups (One-way ANOVA; $F(2,27)=4.112$, $p=0.0184$). DGCs from the ipsilateral hemisphere of CCI injured mice with either vehicle or rapamycin treatment exhibited reduced sIPSC frequency relative to DGCs from the ipsilateral hemisphere of sham injured mice (Sham ipsi: 2.61 ±0.22 Hz, n=6 cells, CCI ipsi: 1.44 ±0.09 Hz, n=9 cells, CCI+Rapa ipsi: 1.39 ±0.26 Hz, n=13 cells; Tukey's, $p<0.0001$ Sham ipsi vs CCI ipsi, $p=0.0053$ Sham ipsi vs

CCI+Rapa ipsi; Figure 4.2B), but there was no difference between ipsilateral DGCs from vehicle- and rapamycin-treated mice after CCI injury (Tukey's, p=0.8775). Rapamycin treatment therefore did not alter the reduction in sIPSC frequency detected in DGCs ipsilateral to CCI injury.

As at the earlier time point post-injury, there was no difference in sIPSC frequency among groups in the contralateral hemisphere 8-13 weeks after injury (Sham: 2.24 ±0.14 Hz, n=5 cells, CCI contra: 2.13 ±0.25 Hz, n=8 cells, CCI+Rapa contra: 1.71 ±0.38 Hz, n=8 cells; $F(2,19)=0.7659$, $p=0.4803$; One-way ANOVA; Figure 4.2D). However, the overall ANOVA of the sIPSC frequency from ipsilateral DGCs did indicate an effect among experimental groups (One-way ANOVA; $F(2,17)=20.38$, $p<0.0001$). In CCI-injured mice, DGCs from the ipsilateral hemisphere of vehicle and rapamycin treatment groups exhibited reduced sIPSC frequency compared to DGCs from sham-treated controls 8-13 weeks post-injury, which was similar to the earlier time point (Sham ipsi: 2.10 CCI ±0.10 Hz, n=5 cells, CCI ipsi: 1.35 ±0.11 Hz, n=7 cells, CCI+Rapa ipsi: 0.83 ±0.15 Hz, n=8 cells; Tukey's, p=0.0003 Sham ipsi vs CCI ipsi, p<0.0001 Sham ipsi vs CCI+Rapa ipsi; Figure 4.2D). Unlike at 1-2 weeks post-injury, there was a significant reduction in sIPSC frequency 8-13 weeks after injury in DGCs from the ipsilateral hemisphere of rapamycin treated mice compared to the vehicle-treated CCI-injured mice (p=0.017). These data indicate that reduced synaptic inhibition in the ipsilateral hemisphere observed 1-2 weeks after CCI was not altered by rapamycin treatment. However, continued rapamycin treatment for 8-13 weeks further reduced synaptic inhibition of DGCs ipsilateral to CCI injury.

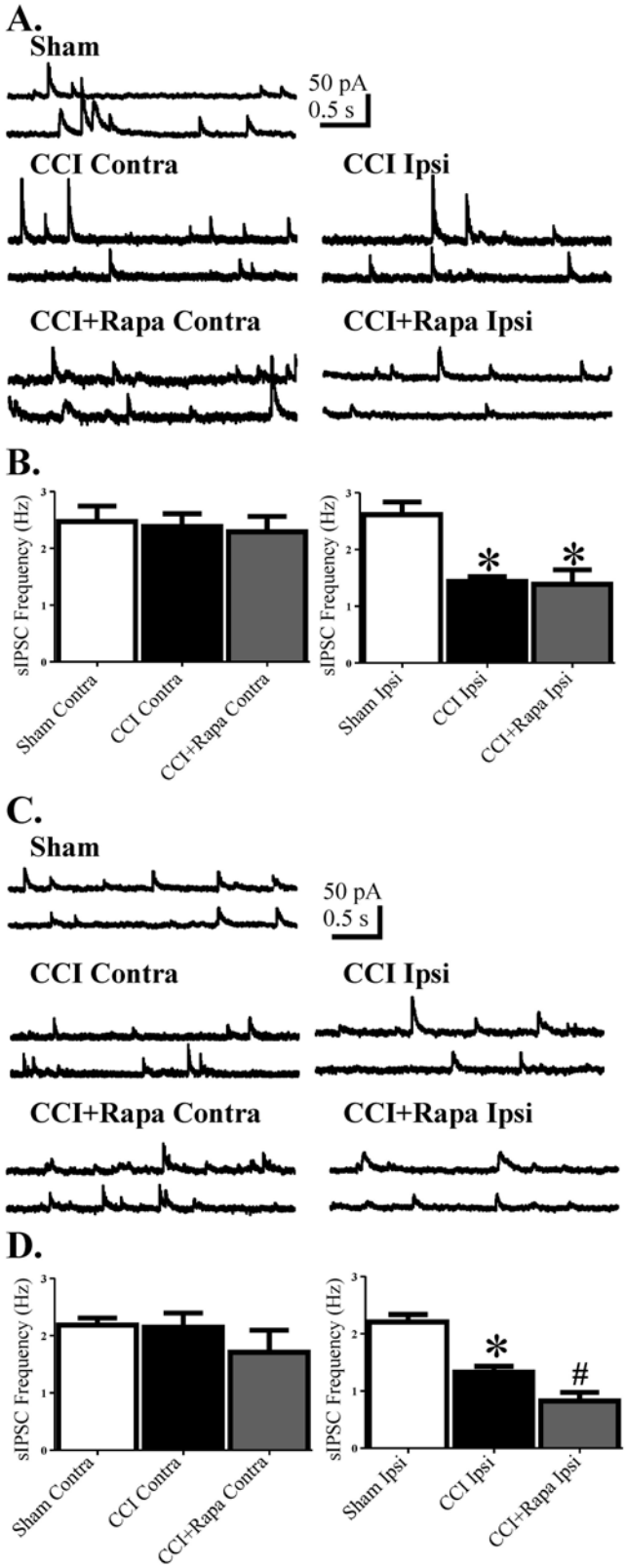

Figure 4.2. sIPSCs in dentate granule cells (DGCs) at 1-2 and 8-13 weeks post-injury. A. Representative traces showing sIPSCs in DGCs 1-2 weeks post-injury in five

different groups: sham-operated control, contralateral to CCI injury + vehicle (CCI Contra), ipsilateral to CCI injury + vehicle (CCI Ipsi), contralateral to CCI injury + rapamycin at 3 mg/kg (CCI+Rapa Contra), and ipsilateral to CCI injury + rapamycin at 3 mg/kg (CCI+Rapa Ipsi). **B.** Representative histograms of mean sIPSC frequency 1-2 weeks post-injury. DGCs in the ipsilateral hemispheres exhibited decreased sIPSC frequency after CCI relative to sham injury. No significant difference was observed contralateral to injury. **C.** Representative traces showing sIPSCs in DGCs 8-13 weeks post-injury in the same groups. **D.** Representative histograms of mean sIPSC frequency 8-13 weeks post-injury. Decreased sIPSC frequency was observed ipsilateral to CCI injury, regardless of treatment. Additionally, CCI+Rapa Ipsi exhibited reduced sIPSC frequency relative to CCI Ipsi. No significant difference was observed in cells from contralateral hemispheres after CCI injury. Error bars indicate SEM; asterisk (*) indicates $p < 0.05$ relative to sham; (#) indicates $p < 0.05$ relative to both sham and CCI Ipsi.

4.3.3 Tonic $GABA_AR$ currents 1-2 week post-injury

THIP-induced tonic $GABA_AR$-mediated currents in DGCs are altered in rodent models of TBI and TLE (Mtchedlishvili et al., 2010;Pavlov et al., 2011;Gupta et al., 2012;Boychuk et al., 2016). In mice, resting tonic $GABA_AR$ current is not altered after CCI, but the THIP- or neurosteroid-induced tonic $GABA_AR$ current amplitude is reduced in the ipsilateral hemisphere after CCI, and this reduction is sustained for at least 3 months (Boychuk et al., 2016). Although synaptic GABAergic transmission was not altered by rapamycin treatment 1-2 weeks after injury, it is not known what effect rapamycin has on resting or THIP-induced tonic $GABA_AR$ mediated currents. Therefore, both resting and THIP-induced $GABA_AR$ mediated tonic currents were measured 1-2 weeks post injury in sham and vehicle- or rapamycin-treated mice after CCI.

Figure 4.3A shows representative traces of whole-cell recordings of DGCs from sham-injured mice, and contralateral and ipsilateral DGCs from CCI-injured mice with vehicle or rapamycin treatment. Rapamycin treatment after CCI did not alter resting tonic

$GABA_AR$-mediated currents in DGCs from either the contralateral (Table 4.2; p=0.6772; F(2,21)=0.3979; One-way ANOVA) or ipsilateral hemisphere (Table 4.2; p=0.5458; F(2,22)=0.6242; One-way ANOVA; Figure 4.3A, B). Additionally, there was no change in THIP-induced tonic GABA current response of DGCs in the contralateral hemisphere of any treatment group (sham contra: 2.98 ±0.57 pA/mF, n=5 cells, CCI+vehicle contra: 3.11 ±0.50 pA/mF, n=9 cells, CCI+Rapa contra: 3.09 ±0.44 pA/mF, n=8 cells; p=0.9862; F(2,21)=0.01388; One-way ANOVA; Figure 4.3C). There was an overall change in THIP-induced tonic currents in the ipsilateral DGCs among experimental groups (One-way ANOVA; F(2,26)=3.560; p=0.0443). Similar to our previous report (Boychuk et al., 2016), CCI injury resulted in a reduction in the response to THIP in DGCs ipsilateral to injury relative to DGCs ipsilateral to sham-injured controls (sham ipsi: 3.08 ±0.42 pA/mF, n=6 cells, CCI+vehicle ipsi: 1.81 ±0.30 pA/mF, n=9 cells; Tukey's, p=0.0261 sham ipsi vs CCI+vehicle ipsi; Figure 4.3C). Rapamycin treatment prevented the reduction of THIP-induced tonic $GABA_AR$ current amplitude in ipsilateral DGCs 1-2 weeks after injury (CCI+Rapa ipsi: 3.22 ±0.56 pA/mF, n=10 cells, p=0.8402 relative to sham, p=0.0321 relative to CCI+vehicle ipsi; Figure 4.3C). These data indicated that rapamycin treatment did not alter resting tonic $GABA_AR$ currents following CCI injury, but eliminated the reduction in THIP-induced $GABA_AR$ current amplitude measured in DGCs ipsilateral to CCI injury.

Table 4.2. Resting tonic GABA currents in DGCs

Animal Group	1-2 weeks post injury resting tonic current (pA/mF)	8-13 weeks post-injury resting tonic current (pA/mF)
Sham Contra	0.64 ±0.17, n=5	0.76 ±0.35, n=5
Sham Ipsi	0.84 ±0.13, n=6	0.79 ±0.34, n=5
CCI Contra	0.84 ±0.13, n=9	0.89 ±0.14, n=8
CCI Ipsi	0.72 ±0.15, n=9	0.74 ±0.13, n=7
CCI+Rapa Contra	0.82 ±0.22, n=8	0.94 ±0.29, n=8
CCI+Rapa Ipsi	0.92 ±0.14, n=10	0.85 ±0.16, n=8

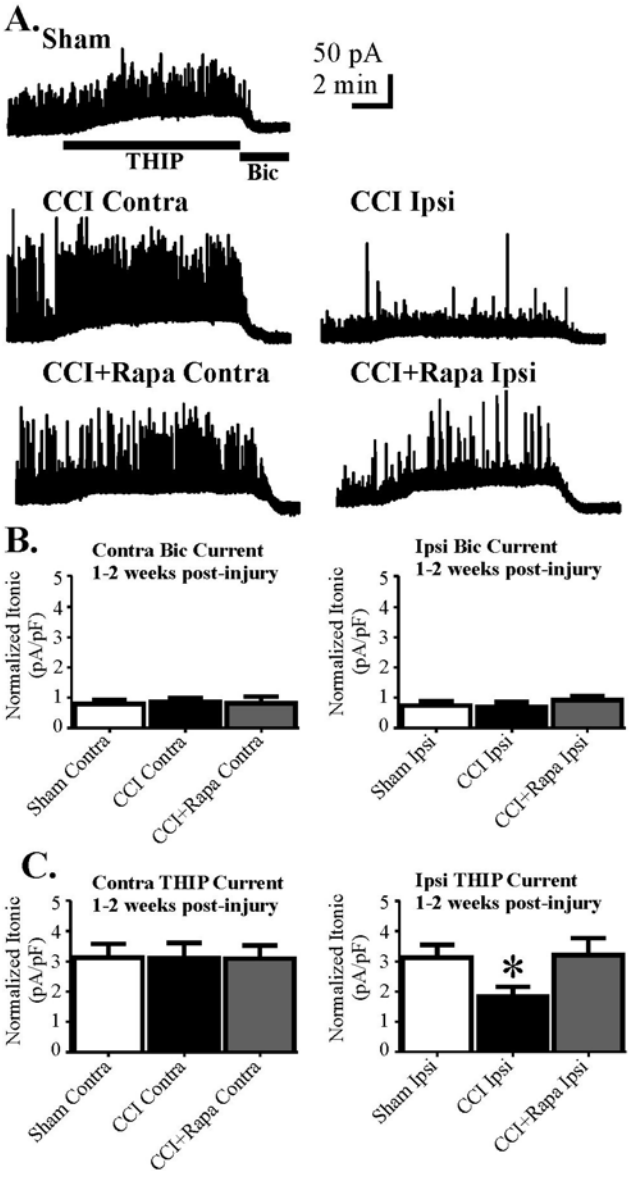

Figure 4.3. Bicuculline- and THIP-sensitive tonic currents in DGCs 1-2 weeks post-injury. A. Representative traces from DGCs 1-2 weeks post-injury in five experimental groups: sham-injured control (Sham), contralateral to CCI injury + vehicle (CCI Contra), ipsilateral to CCI injury + vehicle (CCI Ipsi), contralateral to CCI injury + rapamycin at 3 mg/kg (CCI+Rapa Contra), and ipsilateral to CCI injury + rapamycin at 3 mg/kg (CCI+Rapa Ipsi). Cells were voltage-clamped at 0 mV; bars under the Sham trace indicate times of THIP and bicuculline application during recordings. **B.** Mean bicuculline-sensitive tonic current density 1-2 weeks post-injury in each experimental group. No significant difference was observed for bicuculline sensitive resting currents after injury between any experimental group. **C.** Mean THIP-sensitive tonic current density in DGCs 1-2 weeks post-injury. Error bars indicate SEM; asterisk (*) indicates $p < 0.05$ relative to sham.

4.3.4 Tonic $GABA_AR$ currents 8-13 weeks post-injury

Based on reduced synaptic GABAergic transmission to ipsilateral DGCs 8-13 weeks after injury and attenuated THIP-induced tonic $GABA_AR$ currents 1-2 weeks after CCI injury, we tested the effect of chronic rapamycin treatment 8-13 weeks after CCI on resting and THIP-induced $GABA_AR$-mediated tonic currents. Figure 4.4A shows representative traces of whole-cell recordings of DGCs from sham, and contralateral and ipsilateral to CCI injury with vehicle or rapamycin treatment. There was no difference in THIP-induced tonic current amplitude in DGCs from the contralateral hemisphere of any treatment group (sham contra: 3.43 ±0.33 pA/mF, n=5 cells, CCI contra: 3.79 ±0.39 pA/mF, n=8 cells, CCI+Rapa contra: 3.34 ±0.38pA/mF, n=8 cells; p=0.6191; F(2,22)=0.4912; One-way ANOVA; Figure 4.4C). Similar to a previous report (Boychuk et al., 2016), and similar to currents measured 1-2 weeks post-injury, there was an overall effect on THIP-induced tonic currents in the ipsilateral DGCs (One-way ANOVA; F(2,21)=10.69; p=0.0008). DGCs from the ipsilateral hemisphere of CCI injured mice exhibited reduced THIP-induced tonic currents compared to DGCs from the ipsilateral hemisphere of sham-operated controls (sham ipsi: 3.83 ±0.37 pA/mF, n=5 cells, CCI ipsi: 1.69 ±0.23 pA/mF, n=7 cells: Tukey's, p=0.0009 Sham ipsi vs CCI ipsi; Figure 4.4C). Chronic rapamycin treatment for 8-13 weeks after CCI attenuated the reduction in THIP-induced tonic currents in the ipsilateral hemisphere (CCI+Rapa ipsi: 2.84 ±0.26 pA/mF, n=8 cells; p=0.0982 relative to sham, p=0.0064 relative to CCI+vehicle ipsi). There was no difference in resting $GABA_AR$-mediated tonic current in DGCs from any treatment group contralateral (Table 4.2; p=0.9103; F(2,22)=0.09441; One-way ANOVA; Figure 4.4B), or ipsilateral to the injury (Table 4.2; p=0.9244; F(2,21)=0.07894; One-way

ANOVA; Figure 4.4B). Although resting tonic current was unaltered after CCI or by rapamycin treatment post-injury, THIP-induced tonic current amplitude was reduced ipsilateral to CCI injury. Rapamycin treatment attenuated this reduction and restored tonic inhibition to values similar to controls. This occurred despite diminished synaptic inhibition in rapamycin treated mice.

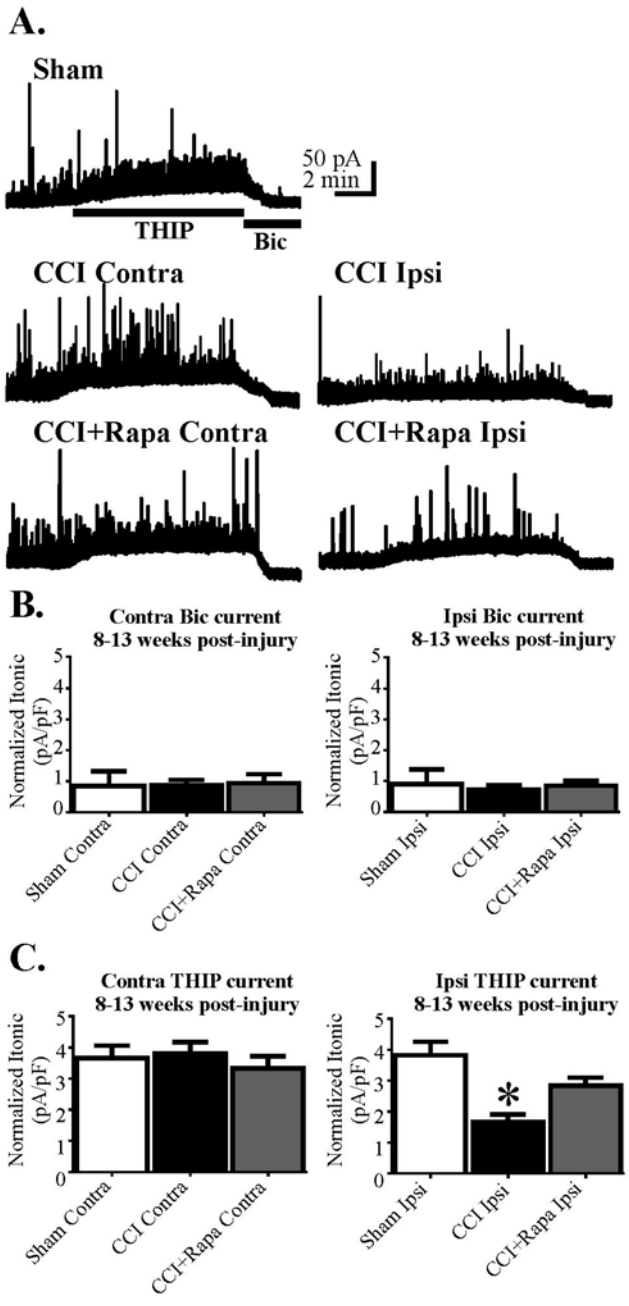

Figure 4.4. Bicuculline- and THIP-sensitive tonic currents in DGCs 8-13 weeks post-injury: A. Representative traces from DGCs 8-13 weeks post-injury in five different experimental groups. Cells were voltage-clamped at 0 mV and bars under Sham trace indicate THIP and bicuculline application during recordings. **B.** Mean bicuculline-sensitive current density 8-13 weeks post-injury. **C.** Mean THIP-sensitive current density DGCs 8-13 weeks post-injury. Error bars indicate SEM; asterisk (*) indicates $p<0.05$ relative to Sham.

4.4 Discussion

Little is known about the effects of rapamycin treatment on GABAergic signaling in the dentate gyrus after CCI or in models of epilepsy. Most previous work on the role of mTOR modulation in epilepsy and in models of TBI has focused on plasticity of excitatory circuitry, including mossy fiber sprouting and synaptic reorganization of glutamatergic circuits in the dentate gyrus (Buckmaster et al., 2009;Zeng et al., 2009;Guo et al., 2013;Heng et al., 2013;Butler et al., 2015). Although effects of rapamycin treatment on hilar inhibitory neuron morphology have been reported (Buckmaster and Wen, 2011), mTOR's role in regulating inhibitory synaptic reorganization or $GABA_AR$'s mediating tonic GABA currents in DGCs has not been previously studied. However, axon sprouting in surviving inhibitory hilar interneurons could be a mechanism to compensate for the loss of GABAergic neurons and their connections to DGCs after pilocarpine-induced status epilepticus or TBI. Alternatively, aberrant axon sprouting could be a generalized response of injured neurons. Here, chronic rapamycin treatment did not prevent hilar inhibitory neuron cell loss after CCI, and suppressed sIPSC frequency to a greater extent than CCI alone by 8-13 weeks post-injury. This is consistent with reduced axon sprouting in eGFP hilar interneurons after rapamycin treatment in mice with acquired TLE (Buckmaster and Wen, 2011), and could be predicted to further

diminish synaptic inhibition of DGCs. Reduced synaptic inhibition after rapamycin treatment post-CCI would be inconsistent with an antiepileptogenic effect of the treatment. This feature would actually be predicted to increase seizure susceptibility by further aggravating the imbalance of excitation and inhibition of DGCs in the ipsilateral hemisphere. Additionally, chronic mTOR inhibition in patients with cancer can lead to the eventual upregulation of ERK/MAPK/Akt pathways in the cancerous tumors (O'Reilly et al., 2006;Tabernero et al., 2008), which can upregulate mTOR complex 2 and compensate for the rapamycin-induced suppression of mTOR complex 1. Analogous compensation may be a consideration in chronic rapamycin treatment for patients with epilepsy.

Synaptic inhibition of DGCs is only one form of inhibitory control, and small changes in tonic $GABA_AR$ mediated currents may have a large impact on inhibitory control of DGCs (Mody and Pearce, 2004;Coulter and Carlson, 2007). Unlike effects on synaptic inhibition, rapamycin attenuated the reduction in THIP-sensitivity seen in DGCs ipsilateral to injury at both early and chronic phases post-injury. Present and previously reported results indicate that, while resting tonic current is unaltered by injury or rapamycin treatment, the reduction in THIP sensitivity of ipsilateral DGCs from CCI injured mice was responsive to mTOR inhibition. A previous study concluded that receptor trafficking was affected after CCI to account for the diminished THIP-sensitivity in DGCs ipsilateral to injury (Boychuk et al., 2016). This normalized response suggests a role for mTOR in receptor trafficking, likely targeting the available, unbound receptors in the ipsilateral hemisphere following CCI injury. This could also indicate a change in either the $GABA_AR$ subtypes responding to different stimuli, a reorganization of the

pentameric archetypal structure of the $GABA_AR$'s, such as the substitution of different α subunits or δ/γ subunits in disease states, or a change in receptor distribution within the membrane.

The hilar inhibitory interneuron loss observed here is consistent with previous work showing that CCI injury results in loss of hilar neurons (Lowenstein et al., 1992;Hicks et al., 1993). Following CCI, higher doses of rapamycin treatment resulted in a reduction in Fluoro-Jade B staining in a limited area of the hippocampus ~1mm posterior to injury epicenter (Guo et al., 2013;Butler et al., 2015), although cell loss was still significant relative to uninjured-controls. The loss of eGFP-positive interneurons after CCI in this study was observed only in the dorsal and middle hippocampal regions along the septo-temporal axis after CCI injury, with no measurable cell loss occurring in the ventral third of the hippocampus. Rapamycin had no effect on this inhibitory hilar interneuron loss, consistent with previous conclusions (Butler et al., 2015). Furthermore, a lack of rapamycin treatment effect on cell loss in the dorsal and middle regions of hippocampus after CCI suggests effects on synaptic or tonic inhibition in DGCs ipsilateral to injury are not likely to be related to prevention of eGFP-positive interneuron loss, though it does not rule out effects on other interneuron phenotypes.

Although rapamycin treatment had little effect on the reduction in sIPSC frequency ipsilateral to CCI injury 1-2 weeks after injury, continued administration of rapamycin for 8-13 weeks post-injury further reduced sIPSC frequency in ipsilateral DGCs relative to vehicle treatment. This result is consistent with reduced axon sprouting of hilar interneurons in pilocarpine treated mice that received rapamycin (Buckmaster and Wen, 2011), and suggests the reduced axon sprouting after rapamycin treatment may

also contribute to reduced sIPSC frequency in DGCs ipsilateral to CCI. Similarly, in models of both TLE and TBI surviving hilar inhibitory interneurons have been shown to receive increased excitatory input and exhibit increased action potential activity (Halabisky et al., 2010;Hunt et al., 2011). This increase in excitatory synaptic drive is due to axon plasticity of both DGCs (i.e. mossy fiber sprouting) and CA3 pyramidal neurons (i.e. CA3 backprojections). Rapamycin treatment in models of both TLE and TBI reduces mossy fiber sprouting, and could also lead to reduced excitatory drive to this interneuron population, contributing to reduced recurrent synaptic inhibition of DGCs (Buckmaster et al., 2009;Zeng et al., 2009;Buckmaster and Lew, 2011;Guo et al., 2013;Heng et al., 2013;Butler et al., 2015). Effects of rapamycin treatment on synaptic inhibition may reflect a role of mTOR in functional morphological changes underlying synaptic reorganization after focal brain injury.

The processes underlying altered $GABA_AR$ function continue to be inadequately understood, especially in models of epilepsy and TBI. The precise mechanisms by which cellular changes in $GABA_AR$-mediated responses occur remain unknown and alterations of both $GABA_AR$ location and organization are not consistently reported across various models of epilepsy and TBI. This variation may reflect differing sampling techniques, brain area selection, and the various mechanisms by which these animal models achieve epileptogenesis. One of the more interesting differences in modulation of $GABA_AR$'s between the models of TBI used to study PTE is the reversion of changes in $GABA_AR$'s after a latent period in the fluid percussion injury model (Pavlov et al., 2011), which is not seen in the CCI model. This difference may reflect the different mechanisms which underscore the increased susceptibility of epileptogenesis in mice receiving CCI injury

vs. fluid percussion injury. Although some work in cell culture has linked the Akt→mTOR pathway to altered $GABA_AR$ phosphorylation and surface expression (Wang et al., 2003), our understanding of how this translates to normal function and in models of disease is insufficient.

mTOR's role in cortical excitation after TBI and in severe forms of epilepsy has been investigated rigorously, but the role it plays in regulating inhibition is less clear. This study suggests inhibition of mTOR activity following CCI injury could promote maintenance of normal responses to THIP-induced $GABA_AR$ activity, but that long term rapamycin treatment may also lead to reduced synaptic inhibition of DGCs. Effects of mTOR inhibition on epileptogenesis do not seem to outlast treatment (Buckmaster et al., 2009;Guo et al., 2013), possibly due to persistent effects of injury-induced interneuron loss or effects of rapamycin on potentially compensatory axon sprouting and synaptic reorganization of inhibitory circuits. This detriment could contribute to the eventual development of an epileptogenic circuit and recurrence of seizure susceptibility after treatment removal. Prolonged rapamycin treatment could therefore exacerbate the imbalance of excitation and inhibition in the dentate gyrus after TBI, and could potentially lead to the re-activation of cell signaling pathways involving the mTOR complex 2. These potential pitfalls and the mechanisms by which mTOR contributes to $GABA_AR$ modulation require further investigation, which would not only be informative but critical to our understanding of the complex nature of how changes in inhibitory synaptic organization and the $GABA_AR$ system relate to the development of PTE. In conclusion, rapamycin treatment after CCI injury has restorative effects on the THIP-induced tonic $GABA_AR$ currents, but chronic treatment demonstrates possible deleterious

effects on synaptic inhibition and does not alter resting tonic $GABA_AR$ currents. This combined with a lack of neuroprotection for eGFP-positive hilar inhibitory interneurons suggests that rapamycin treatment does not restore or prevent all inhibitory alterations in the dentate gyrus after CCI injury.

Chapter 5: Rapamycin treatment reduces recurrent excitation of eGFP+ hilar interneurons from dentate granule cells, but not CA3 backprojections after controlled cortical impact injury

5.1 Introduction

The reactive plasticity of dentate granule cells (DGCs), CA3 pyramids, and hilar inhibitory neurons has been associated with seizure and epilepsy generation following severe brain trauma (Scharfman, 2007;Hunt et al., 2009; 2010; 2011;Hunt et al., 2012;Guo et al., 2013). Although the synaptic reorganization of excitatory inputs among DGCs in the form of mossy fiber sprouting may contribute to the formation of an epileptogenic circuit, the nature of their contribution is controversial. Increased mossy fiber innervation of hilar inhibitory interneurons is also a component of this synaptic plasticity (Halabisky et al., 2010;Hunt et al., 2011). Increased excitation of inhibitory neurons could counter the loss of inhibitory neurons (Lowenstein et al., 1992;Hicks et al., 1993), and could thus restore inhibitory regulation in the dentate gyrus following brain injury. For this reason, loss of these interneurons has been theorized to be detrimental to the excitatory and inhibitory balance of the dentate gyrus, and could lead to increased susceptibility to burst-like firing in the dentate gyrus and seizure susceptibility. Many inhibitory interneuron subtypes are vulnerable to injury, and somatostatin interneurons in the hilus of the dentate gyrus are particularly susceptible to cell death after injury (Lowenstein et al., 1992;Hicks et al., 1993). This class of interneuron is of particular interest due to the unique location of its axonal projections, which form synapses directly on the dendrites of DGCs across from excitatory entorhinal cortex projections (Buckmaster et al., 1994;Buckmaster and Schwartzkroin, 1995).

The role of the mammalian target of rapamycin (mTOR) activity in excitatory and inhibitory axon sprouting has been demonstrated in the pilocarpine model of temporal lobe epilepsy (TLE) and in the controlled cortical impact model (CCI) of posttraumatic epilepsy (PTE) (Hunt et al., 2009; 2010;Buckmaster and Wen, 2011;Hunt et al., 2011;Hunt et al., 2012;Guo et al., 2013;Yamawaki et al., 2015). After CCI, reorganization of DGC and CA3 pyramidal neuron inputs to surviving hilar inhibitory interneurons has been identified (Hunt et al., 2011), and mirrors findings of the pilocarpine model of TLE and undercut cortex model of epilepsy (Halabisky et al., 2010;Jin et al., 2011). The role of mTOR signaling in reactive plasticity after CCI has been studied in the excitatory circuitry of DGCs (Guo et al., 2013;Butler et al., 2015). Rapamycin treatment after CCI or pilocarpine-induced status epilepticus reduces mossy fiber sprouting and neurogenesis post-injury though treatment also reduces morphological changes in hilar interneurons after pilocarpine-induced status epilepticus (Buckmaster et al., 2009;Buckmaster and Wen, 2011;Guo et al., 2013;Butler et al., 2015). However, little is known of mTOR's role in functional reorganization of inhibitory circuitry and associated reactive plasticity with inhibition of the dentate gyrus after TBI. In this study we used a transgenic mouse line in which the somatostatinergic hilar inhibitory interneurons express eGFP (Oliva et al., 2000), to study effects of rapamycin treatment on reorganization of excitatory synaptic input to hilar inhibitory interneurons after CCI injury. We tested the hypothesis that continuous rapamycin treatment following CCI injury would reduce excitatory drive onto surviving ipsilateral eGFP-positive hilar neurons arising from both DGCs and CA3 pyramids.

5.2 Methods

On-cell recordings: After an equilibration period of at least one hour, slices were transferred to a recording chamber on an upright, fixed-stage microscope equipped with infrared, differential interference contrast, and epifluorescence optics (Olympus BX50WI), and continuously perfused with warmed (32^{o}C- 34^{o}C) oxygenated ACSF. Recordings were performed from hilar eGFP-positive labeled interneurons, identified by epiflorescence illumination. Recording pipettes were pulled from boroscilliate glass (1.65 mm outer diameter, 0.45 mm inner diameter; King's Precision Glass) with a P-87 puller (Sutter Instrument). The intracellular solution contained 130 K^{+}-gluconate, 1 NaCl, 5 EGTA, 10 HEPES, 1 $MgCl_2$, 1 $CaCl_2$, 3 KOH, and 2 ATP. Open tip series resistance was 2-5 MΩ. Recordings were obtained using an Axon Axopatch 200B or Axon Multiclamp 700B amplifier (Molecular Devices), low-pass filtered at 2-5 kHz, digitized at 20 kHz with a Digidata 1322A or Digidata 1550A (Molecular Devices), and acquired using pClamp 10.2 and 10.5 programs (Clampfit, Molecular Devices). On-cell recordings of spontaneous AP firing were obtained with no holding command.

The methods used in Chapter 5 of this dissertation also include: traumatic brain injury, rapamycin injection, slice preparation, whole cell recording, and glutamate photostimulation, as described previously in Chapter 2.

5.3 Results

5.3.1 Action potential frequency of surviving eGFP-postive hilar interneurons

After CCI, surviving eGFP-positive hilar interneurons ipsilateral to the injury display increased spontaneous action potential firing rate and sEPSC frequency (Hunt et

al., 2011). The effect of rapamycin treatment on activity and synaptic input to eGFP-positive hilar interneurons after CCI is not known. Spontaneous action potential firing rate was recorded in eGFP-positive hilar interneurons in slices from sham (n=6 cells, 5 mice), slices from CCI-injured mice (contralateral, n=10, ipsilateral, n=12, 10 mice), and analogous slices from CCI-injured mice that were treated daily for 8-12 weeks with rapamycin (contralateral, n=8; ipsilateral, n=9, 11 mice). Representative traces of spontaneous action potential firing in eGFP-positive neurons from control (i.e. sham and contralateral hemisphere), ipsilateral to CCI injury with vehicle treatment, and ipsilateral to CCI injury with rapamycin treatment groups are shown in Figure 5.1A. There was no significant difference between cells from contralateral and ipsilateral hemispheres in sham-treated mice for any measurements made; therefore results from sham-treated mice were combined into one group. Using a One-way ANOVA, we detected changes in firing rates of eGFP-positive neurons among experimental groups (One-way ANOVA; $F(4,43)=21.38, p<0.0001$). There was also no significant difference between cells in slices from sham versus the contralateral hemisphere of CCI groups (Tukey's, $p>0.05$). In eGFP-positive hilar interneurons ipsilateral to CCI injury increased firing rates relative to eGFP-positive neurons from the contralateral hippocampus or from sham-injured mice (Sham= 4.22 ± 1.16 Hz, CCI contra= 3.93 ±0.76 Hz , CCI ipsi= 11.79 ±0.94 Hz; Tukey's, $p=0.0002$ Sham vs CCI ipsi, $p<0.0001$ CCI contra vs CCI ipsi; Fig 5.1B). In ipsilateral eGFP-positive neurons from rapamycin treated mice, firing rate was reduced relative to vehicle treated mice, but remained significantly elevated compared to eGFP-positive neurons from sham injured or cells contralateral to CCI injury (CCI+Rapa contra= 4.43 ±0.64 Hz, CCI+Rapa ipsi= 8.86 ±0.49 Hz; Tukey's, $p<0.0001$ Sham vs

CCI+Rapa ipsi, p=0.0002 CCI contra vs CCI+Rapa ipsi, p=0.0003 CCI+Rapa contra vs CCI+Rapa ipsi, p=0.014 CCI ipsi vs CCI+Rapa ipsi; Fig 5.1B).

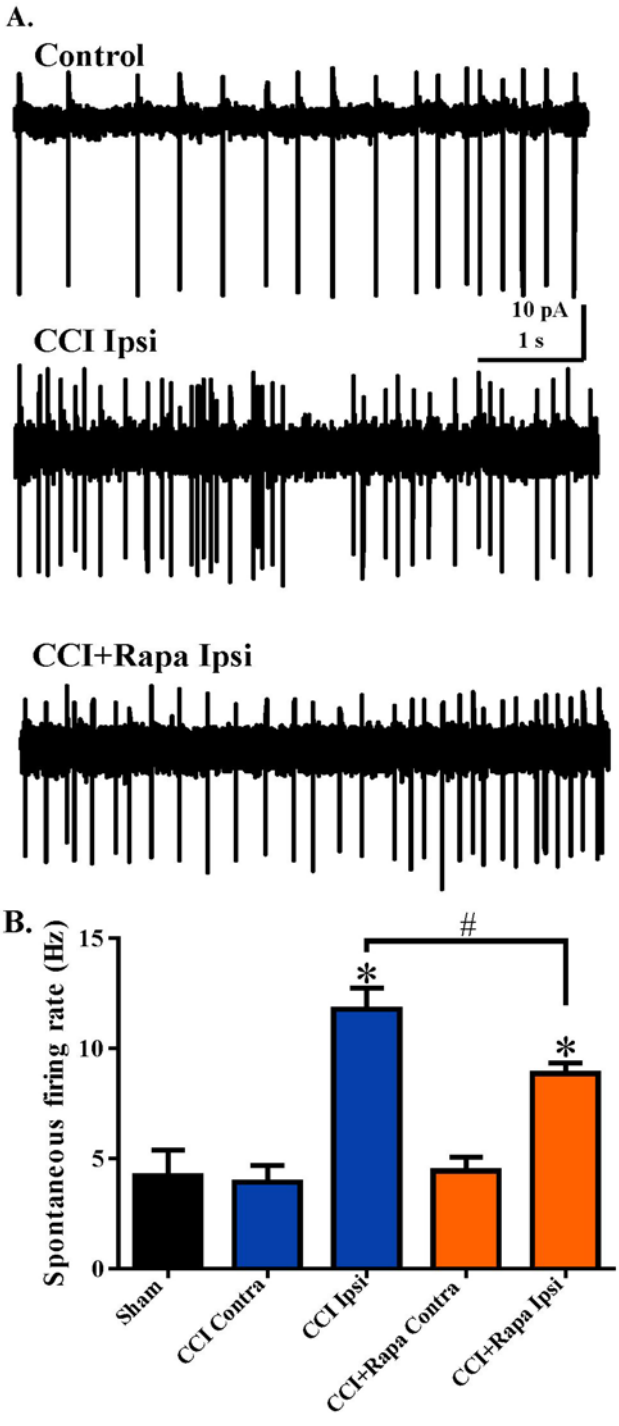

Figure 5.1. Rapamycin treatment reduces the increased activity of hilar inhibitory interneuron 8-12 weeks after CCI injury. A. Representative traces showing spontaneous action potential firing from three different treatment groups: control (i.e.

sham and contralateral neurons), ipsilateral to CCI injury + vehicle (CCI Ipsi), and ipsilateral to CCI injury + 3 mg/kg rapamycin (CCI+Rapa Ipsi). **B.** Mean spontaneous action potential firing in sham, CCI contra, CCI Ipsi, CCI+Rapa contra, and CCI+Rapa Ipsi groups. Error bars indicate SEM; asterisk (*) indicates $p < 0.05$ compared to sham and contralateral hemispheres; hashtag (#) indicates $p<0.05$ for CCI+vehicle Ipsi vs. CCI+Rapa Ipsi.

5.3.2 sEPSC frequency in eGFP-positive hilar interneurons

The sEPSC frequency in eGFP-positive hilar interneurons was determined using whole-cell patch-clamp recordings. Representative traces of sEPSC frequency are shown in Figure 5.2A from control (i.e. sham and contralateral hemisphere), ipsilateral to CCI injury with vehicle treatment, and ipsilateral to CCI injury with rapamycin treatment groups. A One-way ANOVA demonstrated that there was a change in sEPSC frequency of hilar eGFP-positive hilar interneurons among experimental groups (One-way ANOVA; $F(4,45)=9.478$, $p<0.0001$). Ipsilateral to CCI injury, eGFP-positive hilar interneurons exhibited increased sEPSC frequency relative to sham interneurons and interneurons contralateral to CCI (sham: 3.69 ±0.71 Hz, CCI contra= 3.65 ±0.73 Hz, CCI ipsi= 10.69 ±1.36 Hz; Tukey's, $p=0.0034$ sham vs CCI ipsi, $p=0.0003$ CCI contra vs CCI ipsi; Fig 5.2B). Rapamycin treatment reduced, but did not normalize, the increased sEPSC frequency in ipsilateral eGFP-positive neurons (CCI+Rapa contra=2.66 ±0.65 Hz, CCI+Rapa ipsi= 6.60 ±1.33 Hz; Tukey's, $p=0.0182$ sham vs CCI+Rapa ipsi, $p=0.0356$ CCI contra vs CCI+Rapa ipsi, $p=0.0127$ CCI+Rapa contra vs CCI+Rapa ipsi, $p=0.014$ CCI ipsi vs CCI+Rapa ipsi, Fig 5.2B). These results indicate rapamycin treatment after CCI reduced, but did not normalize, the increases in AP firing and sEPSC frequency in eGFP-positive interneurons ipsilateral to CCI injury.

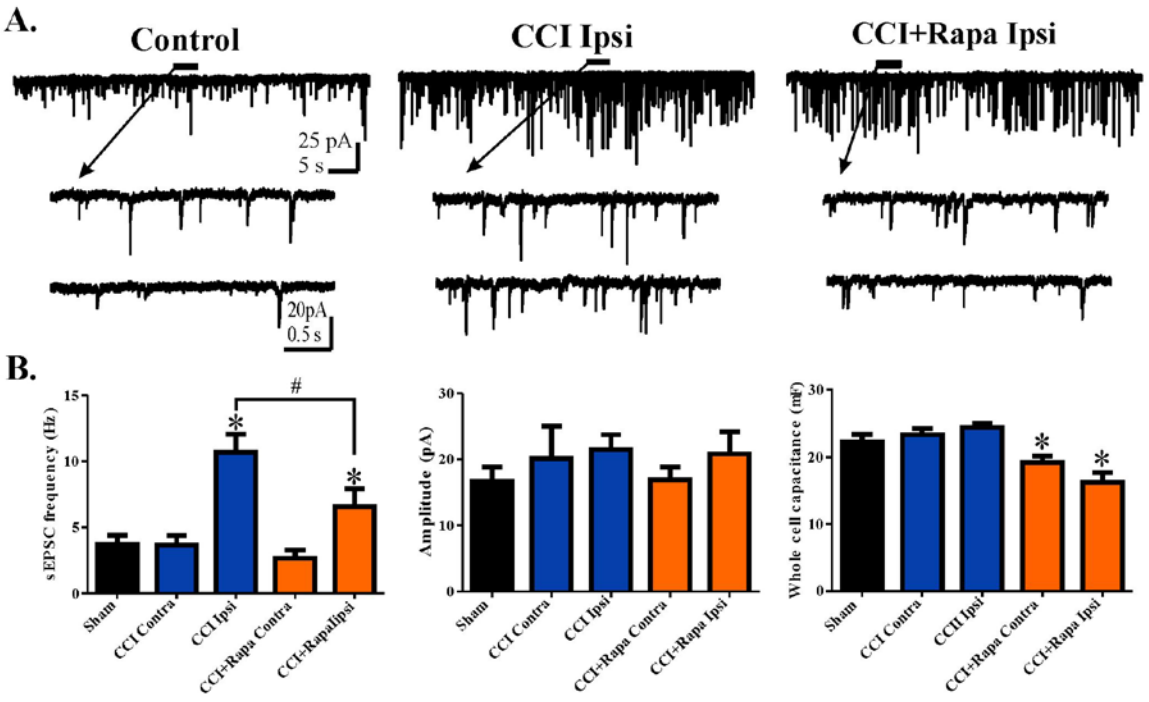

Figure 5.2. Rapamycin treatment reduces the increase in sEPSC frequency of hilar inhibitory interneurons 8-12 weeks after CCI injury. A. Representative traces showing sEPSCs in eGFP-positive neurons from three different treatment groups: control (i.e. sham and contralateral neurons), ipsilateral to CCI injury + vehicle (CCI Ipsi), and ipsilateral to CCI injury + 3 mg/kg rapamycin (CCI+Rapa Ipsi). Expanded sections of the trace under the black line indicated by arrow. **B.** Mean sEPSC frequency in sham, CCI contra, CCI Ipsi, CCI+Rapa contra, and CCI+Rapa Ipsi groups. Error bars indicate SEM; asterisk (*) indicates $p < 0.05$ compared to sham and contralateral hemispheres; hashtag (#) indicates $p<0.05$ for CCI Ipsi vs. CCI+Rapa Ipsi.

5.3.3 Whole cell capacitance and sEPSC amplitude of eGFP-positive hilar interneurons

In the pilocarpine-induced SE model of TLE an increase in soma size of surviving somatostatin+ hilar interneurons has been reported and rapamycin treatment resulted in reduced soma size relative to vehicle treatment (Buckmaster and Wen, 2011). As an indirect measurement of soma size, whole cell capacitance was measured from recorded eGFP-positive hilar interneurons to determine the effect of CCI and rapamycin treatment on capacitance. There was an overall effect of whole cell capacitance among

experimental groups (One-way ANOVA; $F(4,46)=8.187$; $p<0.0001$). We found that CCI injury did not result in an increase to whole cell capacitance of eGFP-positive hilar interneurons in the ipsilateral hemisphere relative to sham or contralateral controls (sham= 22.31 ±1.09 MΩ, CCI contra= 23.36 ±0.89 MΩ, CCI ipsi= 24.44 ±0.65 MΩ;; $p>0.05$, Fig 5.2B), but rapamycin treatment after CCI reduced whole cell capacitance of these neurons to a greater extent compared to CCI alone or sham injured groups (CCI+Rapa contra= 19.22 ±0.97 MΩ, CCI+Rapa ipsi= 16.21 ±1.52 MΩ; Tukey's, $p=0.0406$ sham vs CCI+Rapa contra, $p=0.0121$ sham vs CCI+Rapa ipsi, $p=0.0089$ CCI contra vs CCI+Rapa contra, $p=0.0017$ CCI ipsi vs CCI+Rapa contra, $p=0.001$ CCI ipsi vs CCI+Rapa ipsi, $p=0.0023$ CCI contra vs CCI+Rapa ipsi; Fig 5.2B). Additionally, amplitude measures from unitary sEPSCs in eGFP-positive hilar interneurons have been shown to be unaltered in CCI injured mice compared to the contralateral hemisphere and controls (Hunt et al., 2011). To assess the effect of rapamycin the amplitude of unitary sEPSC events was compared among sham and CCI injured mice. There was no difference in amplitude of sEPSCs among experimental groups using a One-way ANOVA (Sham= 16.65 ±2.18 pA, CCI contra= 20.14 ±4.89 pA, CCI ipsi= 21.49 ±2.25 pA, CCI+Rapa contra= 16.90 ±1.91 pA, CCI+Rapa ipsi= 20.86 ±3.30 pA; One-way ANOVA; $p>0.05$, Fig 5.2B). These results indicate that effects of rapamycin on sEPSC and AP firing frequency are not likely due to post-synaptic modification of synaptic glutamate responses but excitatory synaptic input may be altered by rapamycin.

5.3.4 Responses to glutamate photostimulation of local excitatory circuits

After CCI, surviving eGFP-positive hilar interneurons ipsilateral to injury exhibit increased input from both DGCs and CA3 pyramidal neurons (Hunt et al., 2011). Although MFS

connections among DGCs after CCI injury are reduced in mice treated with rapamycin (Guo et al., 2013;Butler et al., 2015), the effects of rapamycin have not been investigated in the context of synaptic input to hilar eGFP-positive neurons. Here, hilar interneuron recordings were performed during glutamate uncaging in either the DGC layer, or CA3, in order to test for reactive axonal plasticity between DGCs-to-hilar interneurons or between CA3 pyramidal cells-to-hilar interneurons respectively. Representative traces of evoked responses in eGFP-positive hilar interneurons during glutamate photostimulation applied to DGCs (Figure 5.3A) and CA3 pyramidal neurons (Figure 5.4A) are shown from control (i.e. sham and vehicle/rapamycin-treated contralateral hemispheres), ipsilateral to CCI injury with vehicle treatment, and ipsilateral to CCI injury with rapamycin treatment groups. To test for newly sprouted DGC- or CA3- to-hilar interneuron connections, the number of glutamate uncaging sites that responded with ≥1 evoked EPSC (eEPSC; post-stimulation frequency minus pre-stimulation frequency) were measured across groups (n= # of stimulation sites). Responses to glutamate photostimulation in both the DGC layer and CA3 were TTX sensitive (Fig 5.3C), indicating they originated subsequent to action potential generation in photostimulated DGCs and CA3 pyramidal cells.

Slices from sham-injured animals and slices from hemispheres contralateral to injury in CCI animals (vehicle or rapamycin treatment) did not significantly differ in the number of responsive sites during uncaging within the DGC layer (Kruskal-Wallis stat=3.079, p=0.2144) or during uncaging within CA3 (Kruskal-Wallis stat=2.523, p=0.2832). As a result, these eGFP-positive hilar interneuron recordings from sham treatment or contralateral to CCI were combined into a single control group for clarity of presentation. The number of responsive stimulation sites (9 cells; 5 mice) with sham eGFP-positive hilar interneuron recordings was 1/34 (DGC uncaging) and 0/18 (CA3 uncaging). The number of responsive stimulation sites (6 cells; 5 mice) with contralateral CCI+vehicle eGFP-positive hilar interneuron recordings was 3/36 (DGC uncaging) and 1/14 (CA3 uncaging). The number of responsive stimulation sites (5 cells; 5 mice) with

contralateral CCI+vehicle eGFP-positive hilar interneuron recordings was 1/26 (DGC uncaging) and 1/10 (CA3 uncaging).

There was a significant overall difference in the number of responsive stimulation sites between control recordings and recordings from the ipsilateral hemisphere of CCI-injured animals given either vehicle or rapamycin (Kruskal-Wallis stat=18.27, p=0.0001 for DG photostimulation; Kruskal-Wallis stat=13.86, p=0.001 for CA3 photostimulation). The number of responsive stimulation sites (10 cells; 6 mice) from the ipsilateral hemisphere of CCI+vehicle mice was 22/55 (DGC uncaging) and 10/25 (CA3 uncaging). Cells ipsilateral to CCI injury with vehicle treatment exhibited significantly larger numbers of responsive stimulation sites to glutamate uncaging applied to DGCs versus control recordings (Dunn's, $p<0.0001$). Similarly, cells ipsilateral to CCI injury exhibited significantly larger numbers of responsive stimulation sites to glutamate uncaging applied to CA3 versus control recordings (Dunn's, p=0.0009).

In this study, rapamycin treatment in CCI-injured mice reduced both sEPSC frequency and action potential firing of surviving eGFP-positive hilar interneurons located within the injured hemisphere. As a result, eGFP-positive recordings were performed during glutamate uncaging in DG and CA3 within slices from animals given CCI+rapamycin treatment to determine whether mTOR modulation alters the pattern of synaptic reorganization detected in CCI+vehicle mice. The number of responsive stimulation sites (8 cells; 7 mice) from the ipsilateral hemisphere of CCI injured mice given rapamycin was 7/40 (DGC uncaging) and 8/18 (CA3 uncaging). For uncaging within the DGC layer, the ipsilateral hemisphere of CCI-injured rapamycin treated mice displayed no increase in the number of responsive stimulation sites in comparison to control recordings (Dunn's, p=0.1381) and their number of responsive sites was significantly reduced relative to ipsilateral cells from CCI+vehicle mice (Dunn's, p=0.0054). For uncaging within CA3, the ipsilateral hemisphere of CCI-injured rapamycin treated mice exhibited a significantly larger number of responsive stimulation sites relative to controls (Dunn's,

p=0.0009) whereas there was no significant different versus ipsilateral slices from CCI+vehicle mice (Dunn's, p=0.8705). These results indicate that rapamycin treatment reduces the increased input to eGFP-positive neurons from DGCs, but not the increased input from CA3 pyramidal neurons after CCI injury based on the number of responsive sites.

In addition to the number of responsive stimulation sites, we also compared the mean normalized frequency of eEPSCs between all treatment groups. This analysis was undertaken to assess how the differences in the number of responsive sites affected the total number of eEPSCs. eEPSC frequency was again normalized by subtracting the pre-stimulation frequency from the post-stimulation frequency. Both pre-stimulation and post-stimulation measurements were performed within 200 millisecond bins of time that occurred on either side of photostimulation.

Slices from sham-injured animals and slices from hemispheres contralateral to injury in CCI animals (vehicle or rapamycin treatment) did not significantly differ in normalized frequency of eEPSCs during uncaging within the DGC layer (Kruskal-Wallis stat=2.823, p=0.2438) or during uncaging within CA3 (Kruskal-Wallis stat=1.112, p=0.5735). As a result, eGFP+ hilar interneuron recordings from sham treatment or contralateral to CCI were again combined into a single control group for clarity of presentation and consistency with analysis of the number of responsive stimulation sites. The mean normalized frequency of eEPSCs for eGFP hilar interneurons from sham injured mice was 0.1273 ±0.076 for DGC photostimulation and 0.089 ±0.108 for CA3 photostimulation. The mean normalized frequency of eEPSCs for eGFP-positive hilar interneurons from the contralateral hemisphere of CCI-injured mice given vehicle treatment was 0.3111 ±0.129 for DGC photostimulation and 0.280 ±0.136 for CA3 photostimulation. The mean normalized frequency of eEPSCs for eGFP-positive hilar interneurons from the contralateral hemisphere of CCI-injured mice given rapamycin treatment was 0.038 ±0.095 for DGC photostimulation and 0.025 ±0.377 for CA3 photostimulation.

There was a significant overall difference in the normalized eEPSC frequency between control recordings and recordings from the ipsilateral hemisphere of CCI-injured animals given either vehicle or rapamycin (Kruskal-Wallis stat=31.11, $p<0.0001$ for DG photostimulation; Kruskal-Wallis stat=13.74, $p=0.001$ for CA3 photostimulation). eGFP hilar interneurons from CCI-injured mice given vehicle treatment exhibited greater eEPSC frequency following glutamate photostimulation in the DGC layer compared to controls (mean normalized frequency: 0.898 ±0.189; Dunn's, $p<0.0001$; Fig. 5.3B). Additionally, these interneurons exhibited increased eEPSC frequency after glutamate photostimulation in CA3 compared to controls (mean normalized frequency: 1.308 ±0.428; Dunn's, $p=0.0022$; Fig. 5.4B)

eGFP-positive hilar inhibitory interneurons from the ipsilateral hemisphere of CCI-injured mice given rapamycin treatment failed to exhibit increased eEPSC frequency after DGC photostimulation compared to controls (mean normalized frequency: 0.332 ±0.108; Dunn's, $p=0.1381$; Fig. 5.3B), and was significantly reduced relative to eGFP cells from CCI-injured mice given vehicle treatment (Dunn's, $p=0.0114$). However, eGFP hilar interneurons from CCI-injured mice given rapamycin treatment exhibited an increase in eEPSC frequency after CA3 glutamate photostimulation compared to controls (1.267 ±0.440; Dunn's, $p=0.0027$; Fig. 5.4B) and this increase was not significantly different than the eEPSC frequency exhibited by CCI-injured mice given vehicle treatment (Dunn's, $p=0.9288$). Collectively these results indicate that rapamycin reduces aberrant connections between DGC-to-eGFP-positive hilar interneurons but fails to suppress aberrant connections between CA3-to- eGFP-positive hilar interneurons.

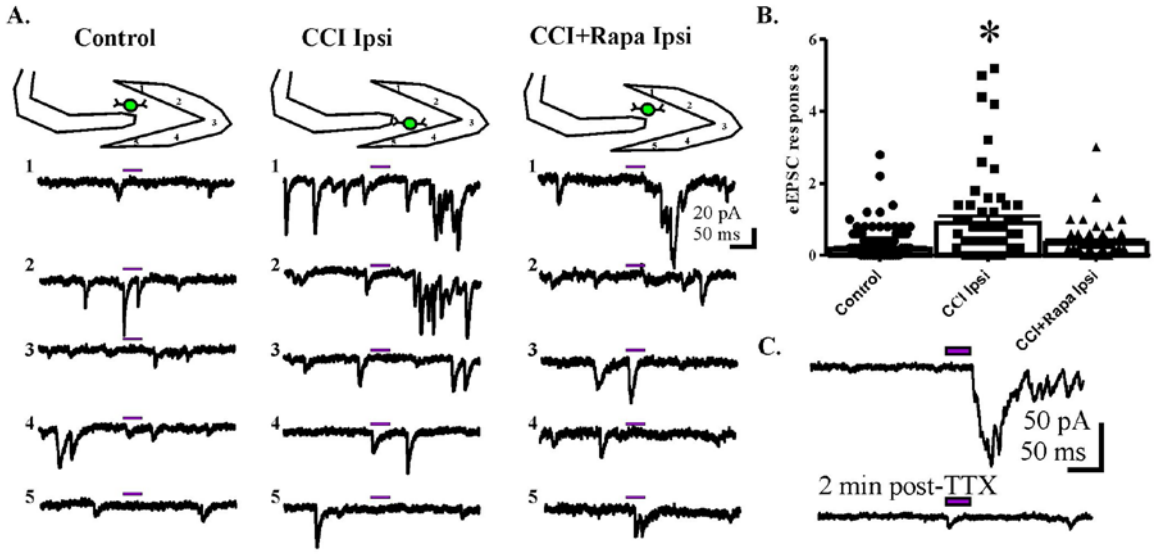

Figure 5.3. eEPSC responses in eGFP-positive hilar interneurons from glutamate photoactivation in dentate granule cells (DGCs) 8-12 weeks after injury in mice from control, CCI-injured with vehicle treatment, and CCI-injured with rapamycin treatment. A. Representative eEPSC responses in eGFP-positive interneurons to glutamate photostimulation applied to DGCs from three different treatment groups: control (i.e. sham and contralateral hemispheres), CCI+vehicle Ipsi, and CCI+Rapa Ipsi. **B.** Individual and mean of eEPSC responses in control, CCI+vehicle Ipsi, and CCI+Rapa Ipsi groups. Error bars indicate SEM; asterisk (*) indicates $p < 0.05$ for mean normalized eEPSC responses compared to control. **C.** Representative eEPSC response demonstrates TTX sensitivity.

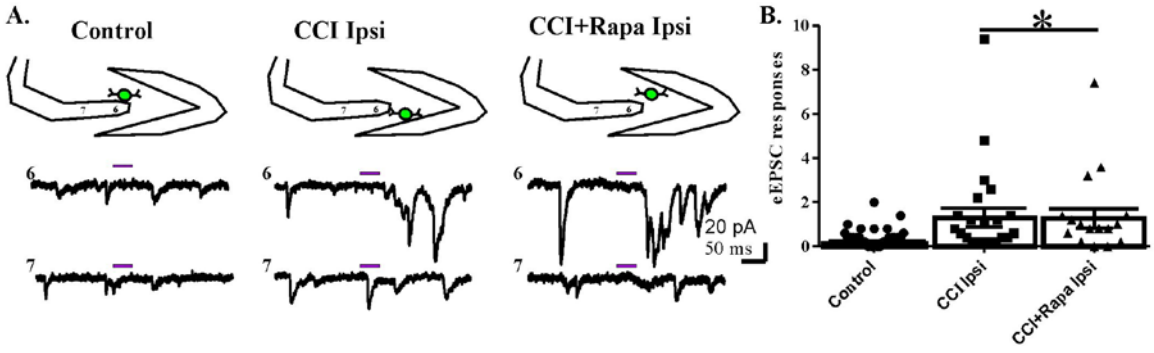

Figure 5.4. eEPSC responses in eGFP-positive hilar interneurons from glutamate photoactivation in CA3 pyramids 8-12 weeks after injury in mice from control, CCI-injured with vehicle treatment, and CCI-injured with rapamycin treatment. A. Representative traces of eEPSC responses of eGFP-positive interneurons to glutamate photoactivation applied to CA3 pyramids from three different treatment groups: control, CCI+vehicle Ipsi, and CCI+Rapa Ipsi. **B.** Individual and mean of eEPSC responses in

control, CCI+vehicle Ipsi, and CCI+Rapa Ipsi groups. Error bars indicate SEM; asterisk (*) indicates $p < 0.05$ for mean normalized eEPSC responses compared to control.

5.4 Discussion

This study investigated the effect of mTOR inhibition after CCI on the synaptic reorganization of a subset of hilar interneurons. In models of traumatic brain injury and TLE, the loss of these interneurons is significant (Lowenstein et al., 1992;Buckmaster and Wen, 2011), and Chapter 4 of this dissertation corroborated these previous reports. It has been theorized that these interneurons contribute to shunting excessive excitatory input through the DGC layer, and the loss of these neurons could contribute to seizure susceptibility (Buckmaster and Dudek, 1997b;Buckmaster and Wen, 2011;Hunt et al., 2011). Additionally, the transplant of immature inhibitory neurons into the hippocampus of mice after pilocarpine treatment alleviated seizures (Hunt et al., 2013b). Understanding the contribution of these interneurons to hippocampal excitability and how aberrant sprouting onto the surviving population impacts the hippocampal circuit, are important in our understanding of PTE and other forms of epilepsy. The main findings indicate mTOR inhibition reduces excitability of hilar inhibitory interneurons by inhibiting the increase in excitatory synaptic reorganization after CCI injury.

Although higher dose rapamycin treatment (10mg/kg) resulted in a regional reduction in FJB staining of the hippocampus (~1mm postior to injury epicenter), cell death was not reduced to control levels (Guo et al., 2013;Butler et al., 2015). Additionally, rapamycin treatment does not prevent eGFP-positive cell loss in the hilus after CCI injury, as demonstrated in Chapter 4 of this dissertation. Therefore, measures of

eGFP-positive neuron activity are likely not related to altered cell survival using rapamycin treatment after CCI injury.

After pilocarpine-induced SE, somatostatin interneurons increase in soma size compared to control and non-SE mice, and rapamycin treatment after pilocarpine induced SE reduced this increase in soma size (Buckmaster and Wen, 2011). While CCI injury did not significantly alter whole cell capacitance compared to sham controls, daily rapamycin treatment reduced both contralateral and ipsilateral whole cell capacitance of eGFP-positive interneurons 8-13 weeks after injury. By inference, reduced capacitance may reflect reduced soma size in eGFP-positive interneurons after rapamycin treatment, consistent with measurements in the pilocarpine treated mice (Buckmaster and Wen, 2011).

The surviving ipsilateral eGFP-positive hilar interneurons after CCI exhibit increased sEPSC frequency and spontaneous AP firing relative to the contralateral hemisphere and sham treated controls 8-12 weeks after injury. This result is consistent with previous work related to increased excitation of eGFP-positive interneurons in models of TLE and PTE (Halabisky et al., 2010;Hunt et al., 2011). Previous studies have shown rapamycin treatment in models of TLE and PTE reduced mossy fiber sprouting in the inner molecular layer of the dentate gyrus, but none have examined the effects of rapamycin on the CCI-associated increase in excitation of eGFP-positive hilar interneurons. In mice receiving daily rapamycin treatment for 8-12 weeks post injury, the sEPSC frequency and spontaneous AP firing rate of ipsilateral eGFP-positive hilar interneurons was reduced, but not normalized, with no change in the contralateral hemisphere. This result is consistent with the reduction in Timm staining (i.e. mossy fiber

sprouting) and recurrent excitation observed in previous studies of rapamycin's effect in PTE models (Guo et al., 2013;Butler et al., 2015) and after status epilepticus induced TLE (Buckmaster et al., 2009;Zeng et al., 2009). There was no change among groups in sEPSC amplitude or direct response to glutamate, which suggests a pre-synaptic mechanism (i.e. axonal sprouting) is a likely contributor to the change in excitability.

It is not known if rapamycin treatment reduces axonal sprouting ubiquitously or if the effect is preferential to only DGCs. After CCI injury or seizures, surviving ipsilateral eGFP-positive interneurons receive increased excitatory input which arises from axons of both DGCs, and CA3 pyramidal neurons (Halabisky et al., 2010;Hunt et al., 2011). We used caged glutamate to measure responses in eGFP-positive hilar interneurons to glutamate photostimulation applied to DGCs and CA3 pyramidal neurons. Input to eGFP-positive neurons arising from both DG and CA3 was increased ipsilateral to CCI injury, consistent with a previous report (Hunt et al., 2011). Rapamycin treatment reduced input arising from DGCs to control levels, consistent with effects of mTOR inhibition on mossy fiber sprouting and synaptic reorganization of DGCs. There was no reduction, however, in excitatory synaptic responses arising from CA3 pryamidal neurons. These results suggest that rapamycin reduced DGC axon sprouting, but did not suppress reactive axon sprouting of CA3 pyramidal cells after CCI injury. This preference could be related to the reduction of DGC neurogenesis after CCI in rapamycin treated mice (Butler et al., 2015) or effects of other factors such as serotonin, which can induce axonal plasticity (Busto et al., 1997). The sustained, rapamycin –resistant increase in input from CA3 neurons probably contributes to the sustained increase in sEPSC frequency in the eGFP-positive neurons.

This study as well as previous work examining excitatory plasticity of eGFP-positive interneurons suggests excitatory synaptic reorganization onto ipsilateral eGFP-positive interneurons occurs after injury from both DGC and CA3 cell sprouting. It is unclear if this increased sprouting onto surviving interneurons is compensatory, serving a potentially beneficial role in maintenance of synaptic inhibition of DGCs, or detrimental to overall hippocampal circuitry. Rapamycin treatment appears to preferentially inhibit synaptic reorganization from DGCs, but not CA3 pyramids onto ipsilateral eGFP-positive hilar interneurons following CCI injury. Continued synaptic excitation of hilar interneurons arising from CA3 could contribute to synaptic imbalance and altered excitability of ipsilateral hilar inhibitory interneurons, and therefore DGCs. The lack of effect on reorganization of CA3 inputs also suggests a different role for mTOR in CA3 pyramidal neuron plasticity than DGCs. Alternatively, maintained plasticity from CA3 could contribute to the reemergence of seizure susceptibility in models of TLE and PTE when rapamycin treatment is removed, even with no mossy fiber sprouting (Guo et al., 2013;Heng et al., 2013). Additionally, this study demonstrates that mTOR's role is not limited to excitatory circuits but has effects on both excitatory and inhibitory balance in the hippocampus. Further work on inhibitory modulation related to mTOR signaling will help develop our understanding of this complex system of excitatory and inhibitory balance.

Chapter 6: General Discussion

6.1 Summary of findings

The principal findings of this dissertation are that rapamycin treatment after CCI injury: 1) reduced seizure prevalence, 2) did not prevent overall FJB labeling or eGFP-positive cell death in the ipsilateral dentate gyrus, 3) reversed injury-induced neurogenesis in the ipsilateral hippocampus, 4) reduced synaptic reorganization of ipsilateral dentate granule cells, 5) further reduced synaptic inhibition of ipsilateral dentate granule cells 8-13 weeks post-injury, 6) prevented reduction in THIP-mediated tonic GABAergic inhibition of ipsilateral dentate granule cells at both 1-2 and 8-13 weeks post-injury, 7) prevented increased synaptic dentate granule cell-hilar GABAergic cell input in ipsilateral hemisphere, and 8) did not prevent the increased synaptic CA3-to-hilar GABAergic cell "back-projection" that is observed in the ipsilateral hemisphere with brain insult. This dissertation is the first detailed examination of rapamycin's effect on functional hippocampal cell signaling in mice given focal brain injury. The results indicate that mTOR signaling regulates hippocampal glutamatergic and GABAergic signaling at many synapses after brain injury and is not limited to reorganization of excitatory DGC synapses as previously described (Buckmaster et al., 2009;Zeng et al., 2009;Guo et al., 2013).

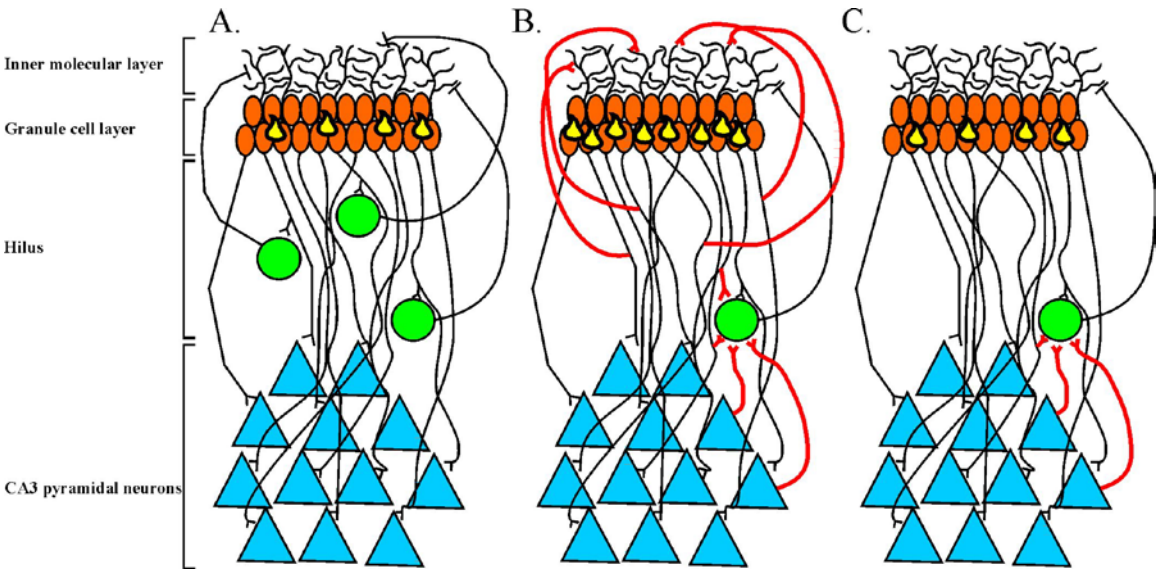

Figure 6.1 Illustration of effects of mTOR inhibition on dentate gyrus circuitry after CCI injury. A. Normal local dentate gyrus circuitry, yellow cells represent immature granule neurons. **B.** Dentate gyrus circuitry after CCI injury in ipsilateral hippocampus which includes loss of hilar inhibitory interneurons, increased immature neuron production, and axon sprouting of dentate granule cells and CA3 pyramidal neurons. **C.** Effects of chronic rapamycin treatment dentate gyrus circuitry includes reduced immature neuron production and axon sprouting of dentate granule cells, but no change in hilar inhibitory interneuron loss or CA3 pyramidal neuron axon sprouting.

6.2 Effect of mTOR inhibition on cell death after CCI injury

6.2.1 Fluoro-Jade B (FJB) labeling

Following brain injury, cell death by either mechanical forces of the injury or by programmed cell death through a cascade of events is a common feature (Graham et al., 2006). There are many ways of measuring dead or dying neurons following brain injury, and one of the more common techniques used is Fluoro-Jade staining. FJB is anion fluorescein stain used for histological staining of neurons undergoing degeneration (Schmued and Hopkins, 2000). Following CCI injury, FJB staining peaks in the ipsilateral hemisphere in the first 3 days and then gradually declines (Anderson et al.,

2005). Therefore to measure cell loss after CCI and the potential effect of rapamycin on this cell loss after CCI injury, FJB staining was performed.

A previous report demonstrated reduced FJB labeling in the ipsilateral hemisphere of CCI injured mice which received rapamycin treatment (6 mg/kg), but this was only measured in an area ~1 mm posterior to injury epicenter (Guo et al., 2013). FJB-positive cell density measures were therefore assessed using 180 μm regions across the septo-temporal axis. Using this regional analysis of FJB staining, two of the 180 μm regions ~1mm posterior to the injury epicenter demonstrated a significant reduction in the ipsilateral FJB-positive cell density of mice treated with rapamycin (10 mg/kg) compared to mice injured and given vehicle treatment. These findings show that overall FJB-positive cell death in the ipsilateral dentate gyrus following CCI injury is not altered by rapamycin treatment, but high dose (10 mg/kg) rapamycin treatment does have regional reduction of FJB-positive cell density compared to CCI injury alone. This would suggest that any antiepileptogenic properties of rapamycin treatment following CCI injury are not likely due to overall neuroprotective effects in the dentate gyrus. This is an important distinction considering previous work using rapamycin treatment has suggested this mechanism of action when only sampling from a similar specified 300 μm region ~1 mm posterior to injury epicenter in mice treated with rapamycin after CCI injury (Guo et al., 2013). However, it is unclear what role reduced cell death in a posterior region from the injury epicenter would have on the epileptogenic process.

6.2.2 Hilar eGFP-positive cell loss

Cell loss in selective regions such as the hilus, CA3, and CA1 area is a common feature of both TBI and epilepsy. Hilar inhibitory interneurons are particularly susceptible to cell death following brain injury (Lowenstein et al., 1992;Smith et al., 1995). One of the subsets of hilar inhibitory interneurons vulnerable to cell death after injury is the somatostatin-positive subset of hilar inhibitory interneurons (Buckmaster and Dudek, 1997b). The development of transgenic mice has greatly improved the ability to target specific genes of neuronal subtypes in disease state. FVB (i.e. GIN mice) which express enhanced green fluorescent protein (eGFP) in the somatostatin-positive neurons, have been used in models of TBI and epilepsy to better understand this vulnerable cell type in disease (Oliva et al., 2000;Buckmaster and Wen, 2011). In this dissertation loss of hilar eGFP-positive neurons in the hilus of the ipsilateral hemisphere of CCI injured mice given vehicle treatment was exhibited in the most dorsal two-thirds of the hippocampus examined compared to sham and contralateral controls. Rapamycin treatment after CCI injury did not alter the reduction of eGFP-positive hilar interneurons in the ipsilateral hemisphere. There was also no difference among any groups in the most ventral third of hippocampus examined in this study, suggesting that loss of these neurons occurs in regions of the brain closer to injury epicenter.

6.2.3 Additional future directions

mTOR inhibition after CCI injury did not alter overall FJB-positive cell density or eGFP-positive hilar inhibitory cell loss in the ipsilateral hemisphere in this study, as described in Chapters 3 and 4 of this dissertation. Based on these data inhibition of

mTOR is not a candidate for use as a neuroprotective therapy. Neuroprotection is typically thought of as the prevention of overall neuron loss in a region susceptible to neuron loss/death after injury. However, a recent study in the pilocarpine-induced status epilepticus model of TLE demonstrated that transplanted GABA progenitor neurons from the medial ganglionic eminence into mice after pilocarpine treatment reduced seizure frequency of the mice treated with the GABAergic progenitor neuron transplant (Hunt et al., 2013b). These data would suggest that overall neuron protection after injury is not the ideal target of PTE, but rather studies should focus on the protection of the hilar GABAergic interneurons. Although this study demonstrates great potential for use of transplantation of GABAergic precursor neurons as a therapeutic for epilepsy, there are still many obstacles to overcome before use of this therapeutic strategy in humans, such as generation of pure GABA progenitor neurons to avoid complications of tumor formation (Hunt and Baraban, 2015). In the meantime, alternative strategies to cell transplantation could prove to be useful tools in therapeutic targets for PTE.

One potential alternative to a pharmacological treatment for neuroprotection after injury would be hypothermia. It remains unclear the exact mechanism hypothermia modifies after brain injury, but one postulated mechanism involves reduced inflammatory signaling (Goss et al., 1995;Marion et al., 1997). Following brain injury, there is an increase in many cell signaling pathways and extracellular signaling molecules, including inflammatory cytokines (Yakovlev and Faden, 1995). Inflammatory cytokine production has also been associated with seizures and epilepsy (Nelson and Ellenberg, 1976;Pacifici et al., 1995;Crespel et al., 2002;Choi and Koh, 2008;Dedeurwaerdere et al., 2012). Hypothermia in experimental animal models of TBI has shown reduction in

inflammatory cytokines in the brain and improvement of cognitive and motor functions in these animals (Dietrich et al., 1994). One of the other notable improvements with hypothermia treatment following CCI injury in the ipsilateral hemisphere of rats is the increase of intact CA3 pyramidal neurons compared to normothermic CCI injured rats (Kline et al., 2002). The CA3 pyramidal cell layer and inhibitory interneurons in the hilus of the dentate gyrus have been similarly noted as vulnerable cell populations following brain injury (Lowenstein et al., 1992;Smith et al., 1995;Saatman et al., 2006). Although not yet tested, it is possible that hypothermia to CCI injured mice could reduce or prevent cell loss in the hilus, similar to reports from the CA3 region of rats. If shown to be an effective treatment option, this would potentially eliminate many of the obstacles currently limiting GABAergic cell transplant therapy, and would be a potential major step forward in TBI and PTE treatment.

6.3 Effects of mTOR inhibition on neurogenesis after CCI injury

6.3.1 Dentate granule cell area

Following CCI injury, there is a reduction in the cell density of select regions such as the hilus, CA3 and CA1 regions. One area which demonstrates a brief reduction shortly after injury (2 days; (Smith et al., 1995), but no change at later time points (7-14 days; (Grady et al., 2003;Witgen et al., 2005) is the dentate granule cell layer. To assess the effect of rapamycin treatment after CCI injury on this response of the dentate granule cell area, measurements using ImageJ softeware of dentate granule cell area were made at 14 days post-injury in CCI injured mice with daily vehicle or rapamycin (3 or 10 mg/kg) treatment and compared to sham injured controls. There were no changes in the

contralateral hemispheres of any of the treatment groups, and dentate granule cell area was not significantly different in the ipsilateral hemisphere of CCI injured mice with vehicle treatment compared to sham injured controls. Dentate granule cell area of CCI injured mice which received either 3 or 10 mg/kg rapamycin treatment was reduced relative to sham injured controls. These data would suggest that the processes underlying the maintanence of dentate granule cell area after CCI injury are affected by rapamycin treatment. One potential mechanism underlying this response could be the process of neurogenesis in the subgranular zone of the dentate gyrus. mTOR signaling is thought to contribute to cell proliferation and therefore this process of neurogenesis was tested.

6.3.2 Doublecortin expression

Doublecortin (DCX) is a microtubule associated protein and is expressed in immature neurons during development. Expression of DCX is transient and is only expressed in cells which are fated to become neurons following proliferation. This transient expression begins approximately 4-10 days after proliferation and continues up to 4 weeks following generation (Gage, 2002;Kempermann et al., 2004;Rikani et al., 2013). Following CCI injury there is an initial decrease in DCX expressing neurons in the ipsilateral hemisphere in the first 3 days, but then a gradual increase in expression in the ipsilateral hemisphere over the following 10-14 days post-injury (Dash et al., 2001;Chirumamilla et al., 2002;Barha et al., 2011;Carlson et al., 2014;Villasana et al., 2014;Butler et al., 2015;Villasana et al., 2015). Seizures have also been associated with increased expression of DCX-positive neurons in the dentate gyrus (Parent et al., 1997;Parent et al., 2006;Kron et al., 2010) and therefore the measurement of this peak region of DCX expression after CCI injury was the goal of this dissertation. Fourteen

days after CCI injury, in the ipsilateral hemisphere of CCI injured mice with vehicle treatment there was an increase in DCX-positive cell density in the dentate granule cell area compared to sham injured mice. Rapamycin treatment (3 or 10 mg/kg) following CCI injury resulted in reduced DCX-positive cell density in the ipsilateral hemisphere compared to the ipsilateral hemisphere of CCI injured mice and no significant difference compared to sham controls. There was no difference in DCX-positive cell density in the dentate granule cell areas of the contralateral hemisphere in any experimental group. This data demonstrates that neurogenesis is a process following CCI injury that is regulated by mTOR signaling. The relative contribution of mature versus immature neurons in creating abnormal circuitry of the dentate gyrus is unclear, but the reduction of immature neuron production in rapamycin treated mice following CCI injury could be beneficial in preventing some of the abnormal circuitry generated in the ipsilateral hemisphere of CCI injured mice. Also, increased neurogenesis following CCI injury has been proposed as a mechanism for improved cognition, and therefore, rapamycin treatment after CCI injury could negatively affect cognition following injury.

6.3.3 Additional future directions

Two of the remaining unknown questions associated with neurogenesis and PTE are: does neurogenesis remain upregulated in latent periods after TBI and do certain populations of newborn neurons contribute to the reorganization of the dentate gyrus differently? In the pilocarpine induced status epilepticus model of TLE, newborn neuron production increases in the first few weeks after insult, but reduces below control levels at later time points (15 weeks; (Hattiangady et al., 2004;Hattiangady and Shetty, 2010;Hu et al., 2015). To date no studies of newborn neuron production after CCI injury have been

done at later time points (i.e. months after injury), as with the pilocarpine model of TLE. Therefore it remains unknown if the noted increase of newborn neuron production in the ipsilateral hemisphere after CCI injury is maintained or reduces below control levels at later time points.

Another unknown feature of injury-induced neurogenesis is the contribution of different populations of newborn neurons either before, during, or following the initial insult. One report suggests that dentate granule cells, which are in an immature state, at the time of pilocarpine induced status epilepticus contribute more to synaptic reorganization (i.e. mossy fiber sprouting) than other populations of dentate granule cells generated before, during, or after pilocarpine-induced status epilepticus (Kron et al., 2010). It is untested whether this feature of the pilocarpine model of TLE holds true for the CCI model of PTE. The previous report of functional integration of newborn granule cells after CCI injury was all done from age matched dentate granule cells born after sham or CCI injury (Villasana et al., 2015). Although this report showed increased morphological changes to the dendrites of newly born neurons after CCI injury in the ipsilateral hemisphere, there were no functional changes in sEPSC or sIPSC frequency of these neurons (Villasana et al., 2015). The authors concluded that this demonstrated normal integration of these newly born neurons after CCI injury in the ipsilateral hippocampus, but even in robust models of status epilepticus seizures it is necessary to perturb the environment of dentate granule cells to “unmask” recurrent excitation (Cronin and Dudek, 1988;Wuarin and Dudek, 1996;Patrylo and Dudek, 1998;Molnar and Nadler, 1999;Lynch and Sutula, 2000;Winokur et al., 2004). Additionally the measurements of synaptic integration at 4 weeks post-injury would not likely reflect potential synaptic

reorganization associated with axonal sprouting, which generally takes longer to develop. Therefore, further tests are necessary to understand how these newborn neurons in the hippocampus contribute to the process of epileptogenesis.

6.4 Effects of mTOR inhibition on excitatory synaptic reorganization of dentate granule cells

6.4.1 Mossy fiber sprouting

Axons of dentate granule cells are known as mossy fibers. These axons are generally unidirectional and project from dentate granule cells to CA3 pyramidal neurons as part of the tri-synaptic circuit of the hippocampus. One of the hallmark features of resected tissue from patients with epilepsy is sprouting of the mossy fibers back into the inner molecular layer of the dentate granule cells and synapsing on the dendrites of neighboring dentate granule cells, called mossy fiber sprouting (de Lanerolle et al., 1989;Sutula et al., 1989;Babb et al., 1991;Houser, 1992). This form of axon sprouting is believed to contribute to recurrent excitation within the dentate gyrus and either lead to increased aberrant excitation of dentate granule cells or synchronization of populations of dentate granule cells, potentially leading to seizure generating foci within the hippocampus. Following CCI injury, mossy fiber sprouting occurs in the ipsilateral hemisphere in highest abundance near the site of injury, and may be affected by factors such as hippocampal distortion (Hunt et al., 2009; 2010;Hunt et al., 2012). Rapamycin treatment has demonstrated beneficial effects on abberant mossy fiber sprouting in this model of PTE and other models of TLE (Buckmaster et al., 2009;Zeng et al., 2009;Guo et al., 2013;Heng et al., 2013). However, using this model of PTE a previous report

demonstrated that when rapamycin treatment was removed after 4 weeks post-injury, mossy fiber sprouting at 12 weeks post-injury returned to CCI with vehicle treatment levels in the ipsilateral hemisphere. Therefore, this dissertation maintained daily rapamycin treatment over the entire timeframe of the study. Rapamycin treatment after CCI injury resulted in a dose dependent reduction in mossy fiber sprouting of the ipsilateral hemisphere, in which 10 mg/kg normalized mossy fiber sprouting to control levels. There was no change in mossy fiber sprouting among contralateral hemispheres of any experimental group.

This reduction in mossy fiber sprouting using rapamycin is consistent with previous work in models of epilepsy as well as the CCI model of PTE (Buckmaster et al., 2009;Zeng et al., 2009;Guo et al., 2013;Heng et al., 2013). In the studies run in this dissertation, all mice which demonstrated spontaneous seizures expressed at least portions of mossy fiber sprouting into at least the granule cell layer along the blades of the dentate gyrus. These data are consistent with a previous study using a high dose of rapamycin (10 mg/kg) in a robust model of epilepsy, pilocarpine-induced (Heng et al., 2013). Combined with previous work using rapamycin treatment, this data suggests that rapamycin treatment pauses the underlying processes associated with mossy fiber sprouting following CCI injury but does not eliminate this mechanism. Further studies in this dissertation were the first to demonstrate functional changes associated with this reduced anatomical measure of synaptic reorganization using rapamycin after CCI injury.

6.4.2 sEPSC frequency of dentate granule cells

Although the histological assessment of mossy fiber sprouting suggests the potential for recurrent excitation through the dentate gyrus, it does not functionally address this question. Therefore, the use of electrophysiology is a helpful tool to investigate functional changes to neurons in this region. One of the problems with determining aberrant excitation in dentate granule cells is the amount of inhibitory properties associated with this cell group. For this reason, methods to unmask recurrent excitatory circuits must be used to determine changes in these cells in disease states (Cronin et al., 1992;Patrylo and Dudek, 1998;Molnar and Nadler, 1999;Lynch and Sutula, 2000;Wuarin and Dudek, 2001;Winokur et al., 2004). One way to "unmask" changes in the excitatory circuit of the dentate gyrus is by measuring spontaneous excitatory post synaptic currents (sEPSCs) in the presence of a $GABA_AR$ blocker, bicuculline, and in nominally Mg^{2+} free artificial cerebrospinal fluid (ACSF). Dentate granule cells from CCI injured mice given vehicle treatment 8-13 weeks after injury in ACSF nominally free of Mg^{2+} and bicuculline added exhibited an increase in sEPSC frequency compared to dentate granule cells from sham injured mice and the contralateral hemisphere. The dentate granule cells from the ipsilateral hemisphere of CCI injured mice with vehicle treatment also demonstrated "bursts" of activity during the sEPSC frequency recordings. Rapamycin treatment in mice after CCI injury demonstrated a dose dependent reduction in sEPSC frequency of ipsilateral dentate granule cells, and high dose (10 mg/kg) rapamycin treatment resulted in normalized sEPSC frequency of ipsilateral dentate granule cells compared to sham injured mice. These data combined with results of mossy fiber sprouting and seizure expression in experimental mice suggest

that mossy fiber sprouting does contribute to seizure generation of CCI injured mice. However this connection is only part of the complex process of epileptogenesis and not likely the only causation for PTE. In order to corroborate these findings of functional changes to individually recorded neurons, extracellular recordings of dentate granule cell population response to electrical stimulation was also performed.

6.4.3 Antidromic stimulation of dentate granule cells

The use of whole cell patch-clamp recordings allows assessment of excitatory connections onto an individual neuron, but does not address the possibility of population synchrony or a population response to an individual stimulus. Antidromic stimulation is the use of stimulating downstream axons of a population of neurons to cause the synchronized action potential generation of a neuron population. Extracellular recordings of a neuron population exhibit the synchrony of the neuron population after stimulation and in cases of recurrent excitatory circuit formation (i.e. mossy fiber sprouting), secondary depolarizations after the initial population spike are thought to demonstrate the recurrent excitatory loop generated by excitatory synaptic reorganization. In this dissertation, vehicle injection after CCI injury replicated the previous report of secondary depolarization to antidromic stimulation in extracellular recordings of dentate granule cells from the ipsilateral hemisphere 8-13 weeks post-injury (Hunt et al., 2009). Rapamycin treatment after CCI injury reduced in a dose dependent manner these secondary depolarizations to antidromic stimulation in the ipsilateral dentate granule cells. This data corroborates the results of sEPSC frequency of ipsilateral dentate granule cells after CCI injury and the effect of rapamycin treatment. Reduced axon sprouting of dentate granule cells in the ipsilateral hemisphere of mice which received rapamycin

treatment after CCI injury suggests some role of mossy fiber sprouting in epileptogenesis after TBI.

6.4.4 Additional future directions

All of these data demonstrate that mossy fiber sprouting is at least part of the epileptogenic process. Interestingly, these data also correlate the effect of rapamycin after CCI injury on neurogenesis with rapamycin's effect on aberrant mossy fiber sprouting and hyperexcitability of the dentate gyrus after CCI injury. After CCI injury newborn neurons develop morphologically abnormal dendritic processes, but appear to integrate into the hippocampal circuit with normal excitatory and inhibitory synaptic input (Villasana et al., 2015). However, this previous work on functional integration of newborn dentate granule cells was performed with normal extracellular conditions. Based on the work done in robust seizure models and this dissertation, it could be important to perturb the extracellular environment to "unmask" the potential abnormalities of newborn neurons in the ipsilateral hemisphere after CCI injury. Future studies on the ability of these newborn neurons to respond normally to environmental strain, would further our understanding of the potential role these newborn neurons could play in the epileptogenic process.

6.5 Effects of mTOR inhibition on inhibitory synaptic reorganization of dentate granule cells

6.5.1 sIPSC frequency of dentate granule cells

Synaptic GABAergic inhibition can be measured using whole cell patch-clamp recordings of neurons and assessing the spontaneous inhibitory post-synaptic current

(sIPSC) frequency. In the CCI model, dentate granule cells in the ipsilateral hemisphere of CCI injured mice exhibit reduced sIPSC frequency at both an early (1-2 weeks post-injury) and late (8-12 weeks post-injury) time period compared to dentate granule cells in the contralateral hemisphere or sham controls (Hunt et al., 2011;Boychuk et al., 2016). This reduction in sIPSC frequency has been postulated as the result of cell death to hilar inhibitory interneurons in the ipsilateral hemisphere after injury (Hunt et al., 2011). Rapamycin treatment after pilocarpine-induced status epilepticus in GIN mice resulted in a reduction of axon sprouting of eGFP-positive hilar interneurons, but did not prevent the loss of these neurons in the pilocarpine induced status epilepticus model (Buckmaster and Wen, 2011) or in this dissertation. The primary target of these eGFP-positive hilar interneurons is the dendritic field of dentate granule cells. Reduced axon sprouting of these hilar inhibitory interneurons in mice treated with rapamycin after CCI injury could result in further reduced synaptic inhibition of dentate granule cells.

To test this possibility sIPSC frequency was measured. 1-2 weeks post-injury, sIPSC frequency of dentate granule cells from the ipsilateral hemisphere of CCI injured mice with vehicle or rapamycin treatment was reduced compared to sham control mice. However, there was no difference in sIPSC frequency between ipsilateral dentate granule cells of vehicle or rapamycin treated CCI-injured mice. At the later time point, 8-13 weeks post-injury, the sIPSC frequency of ipsilateral dentate granule cells from CCI injured mice with vehicle or rapamycin treatment was reduced relative to sham controls, and ipsilateral dentate granule cells from rapamycin treated mice exhibited further reduced sIPSC frequency compared to ipsilateral dentate granule cells from CCI injured mice with vehicle treatment. These data suggest that rapamycin treatment after CCI

injury reduces inhibitory synapse formation onto dentate granule cells, possibly through the inhibition of axon sprouting of hilar inhibitory interneurons. This form of reduced axon sprouting over time could be detrimental for the balance of excitation and inhibition in the hippocampus after injury.

6.5.2 Resting and THIP-induced tonic $GABA_AR$ currents

Synaptic inhibition of dentate granule cells is only one of the forms of inhibitory control of dentate granule cells. Tonic inhibition is another form of inhibitory control of dentate granule cells, and alterations of tonic inhibition after CCI have been reported previously (Mtchedlishvili et al., 2010;Boychuk et al., 2016). One of the key differences in one previous report of CCI-induced changes to $GABA_AR$ mediated tonic inhibition and both this dissertation as well as another study from the Smith lab, is the ability to record dentate granule cells from the ipsilateral hemisphere after CCI injury. In a previous report the ipsilateral hippocampus was extensively damaged and unsuitable for recording dentate granule cells, therefore differences in outcome measures are likely due to the severity of that CCI injury model (Mtchedlishvili et al., 2010). In this dissertation, whole cell patch clamp recordings were obtained from ipsilateral dentate granule cells as well as contralateral and sham controls.

Because mTOR inhibition after CCI injury had synaptic inhibitory effects at 8-13 weeks post-injury, this study tested the possible effects of rapamycin treatment after CCI on tonic $GABA_AR$ mediated currents. At both 1-2 and 8-13 weeks post-injury, ipsilateral dentate granule cells from CCI injured mice with vehicle treatment exhibited reduced THIP-induced tonic currents relative to sham controls, but ipsilateral dentate granule cells

from CCI injured mice with rapamycin treatment did not exhibit a reduced THIP-induced tonic current. The reduced THIP-induced tonic current amplitude in ipsilateral dentate granule cells of CCI injured mice with vehicle treatment corroborates previous work from the Smith lab (Boychuk et al., 2016). The reduced responsiveness of ipsilateral dentate granule cells to THIP was not due to reduced mRNA expression of either α4 or δ subunit containing $GABA_AR$'s (Boychuk et al., 2016). There are many possible explanations for this reduced responsiveness including; subunit reorganization, the number of receptors in the membrane, different activation state of $GABA_AR$'s, or the amount of agonist present in post-synaptic space. Based on the evidence for kinase mediated phosphorylation of $GABA_AR$'s and the potential relationship this process has with trafficking of $GABA_AR$'s, these possibilities are discussed below.

6.5.3 Additional future directions

Modulation of $GABA_AR$'s continues to be a subject of interest in both normal physiology as well as in disease states. Two kinases that have been most associated with altering phosphorylation state of $GABA_AR$'s are PKA and PKC (Browning et al., 1990;Porter et al., 1990;Moss et al., 1992a;Moss et al., 1992b). Another kinase which has been associated with increased phosphorylation of $GABA_AR$'s in cell culture is Akt (also known as PKB; (Wang et al., 2003). It is currently unclear what role phosphorylation of $GABA_AR$'s plays in modifying the function of these receptors. The work done by Boychuk and colleagues demonstrates reduced $GABA_AR$ function in a subset of receptors without altered mRNA expression in the ipsilateral dentate granule cells after CCI injury at both an early (1-2 weeks post-injury) and late (8-13 weeks post injury) time period. As previously stated there are many possible explanations for altered function of

phosphorylated $GABA_AR$'s. Although the work presented in this dissertation does not determine an exact mechanism of action, it would suggest that Akt/mTOR activity is involved in the process of this reduced function of $GABA_AR$'s in ipsilateral dentate granule cells. Due to Akt and mTOR being kinases, it is likely that the processes these proteins affect are related to phosphorylation events. These phosphorylation events could be either associated with the direct phosphorylation of $GABA_AR$'s or part of a cell signaling pathway which effects the phosphorylation state of $GABA_AR$'s. Improved understanding of the role of phosphorylation of $GABA_AR$'s in both normal physiology and disease state would benefit our understanding of the role altered function of $GABA_AR$'s due to phosphorylation events after CCI injury plays in the epileptogeneic process.

6.6 Effects of mTOR inhibition on synaptic reorganization of surviving hilar GABAergic interneurons

6.6.1 Action potential firing of eGFP-positive hilar interneurons

Neuron communication occurs by neurotransmission and action potentials. There are many factors which can increase action potential firing of a neuron such as reduced inhibition, internal polarity properties of the neuron, or sprouting of excitatory synapses onto a neuron. Increased excitatory inputs onto a neuron can cause an increase in the frequency of action potentials generated in that neuron. More active neurons therefore have higher frequencies of action potentials than less active neurons. Increased activity of the same neuron populations can result in maintained or strengthening of synaptic contacts for that neuron population (i.e. long-term potentiation). In some disease states,

such as PTE, axon sprouting is a common feature and could alter the activity level of different neuron populations (Hunt et al., 2009; 2010; 2011). In the CCI model, 8-12 weeks after injury mossy fiber sprouting in the ipsilateral hemisphere is a hallmark feature, but mossy fibers do not only sprout into the inner molecular layer. One of the prominent connections of dentate granule cells is with hilar inhibitory interneurons (Amaral, 1979;Amaral and Dent, 1981;Claiborne et al., 1986;Zhang and Houser, 1999). These axons can also sprout within their normal projection pathway onto surviving inhibitory interneurons in the hilus (Halabisky et al., 2010;Hunt et al., 2011). Rapamycin has been shown in models of epilepsy and the CCI model to reduce mossy fiber sprouting, but what effect this could have with the reorganization of the hippocampal inhibitory circuit had not been previously tested.

Therefore action potential firing and sEPSC frequency of surviving hilar eGFP neurons was measured using cell-attached and whole cell patch clamp recordings to determine changed in activity of surviving hilar inhibitory interneurons. 8-12 weeks after CCI injury, this dissertation shows that surviving hilar eGFP-positive neurons in GIN mice fire more action potentials than sham and contralateral eGFP-positive neurons hilar interneurons, similar to a previous report (Hunt et al., 2011). Daily rapamycin treatment (3 mg/kg) for 8-13 weeks post-CCI injury reduced action potential firing of surviving eGFP-positive hilar neurons compared to ipsilateral eGFP-positive neurons in CCI injured mice with vehicle treatment, but did not normalize the firing frequency to sham levels. Although this data indicates reduced activity of surviving ipsilateral eGFP-positive hilar interneurons of rapamycin treated mice after CCI injury, it does not demonstrate that this is due to a reduction in excitatory synaptic plasiticity.

6.6.2 sEPSC frequency of eGFP-positive hilar interneurons

This study used sEPSC frequency to test if the effect of rapamycin treatment after CCI injury on action potential firing of hilar interneurons was due to reduced excitatory synaptic reorganization of ipsilateral hilar interneurons after CCI injury. eGFP-positive hilar interneurons from the ipsilateral hemisphere of CCI injured mice which received vehicle treatment exhibited increased sEPSC frequency compared to eGFP-positive hilar neurons from the contralateral hemisphere or sham controls, similar to the previous report from the Smith lab (Hunt et al., 2011). Rapamycin treatment after CCI injury did not alter sEPSC frequency in eGFP-positive neurons of the contralateral hemisphere, but eGFP-positive hilar interneurons from the ipsilateral hemisphere exhibited reduced sEPSC frequency compared to eGFP-positive neurons of the ipsilateral hemisphere of CCI injured animals but did not normalize to sham control levels. These data suggest rapamycin treatment after CCI injury reduces synaptic reorganization in the hilus as well as the abberant mossy fiber sprouting and synaptic reorganization into the inner molecular layer previously discussed. The increase in excitation of surviving ipsilateral hilar interneurons of CCI-injured mice has been proposed as a compensatory mechanism for maintaining the inhibition of dentate granule cells after the loss of hilar interneurons following brain injury (Hunt et al., 2011). Therefore, this reduced excitation could also be detrimental for inhibition of the dentate granule cells. However it was also noted that increased excitation onto surviving hilar inhibitory interneurons in the ipsilateral hemisphere after CCI injury could causes these surviving hilar interneurons to be more susceptible to entering a state of depolarizing block (Hunt et al., 2011). So this reduction in excitatory drive of eGFP-positive hilar interneurons could be beneficial in reducing the

potential risk of these neurons entering a depolarizing block state during excessive excitation. It remains unclear how altered excitation of surviving hilar interneurons contributes to the epileptogenic process and the beneficial/detrimental nature of this synaptic reorganization.

6.6.3 Cell size of surviving eGFP-positive hilar interneurons

In the pilocarpine-induced model of status epilepticus, increased soma size was observed in eGFP-positive hilar interneurons from GIN mice which underwent pilocarpine-induced status epilepticus compared to saline controls (Buckmaster and Wen, 2011). This suggests that cell size for this subset of neurons could potentially change in injury states such as the ipsilateral hemisphere of CCI injured mice, and rapamycin treatment after CCI injury could modify this response to injury. An indirect measure of cell soma size is the whole cell capacitance measure of neurons during whole cell patch clamp electrophysiology recordings. However, this has not been previously tested in the CCI model. After CCI injury, eGFP-positive hilar interneurons exhibited no change in whole cell capacitance in either the contralateral or ipsilateral hemisphere of CCI injured mice with vehicle treatment compared to sham controls 8-13 weeks post-injury. However, eGFP-positive hilar interneurons from both the contralateral and ipsilateral hemispheres of CCI injured mice with rapamycin treatment displayed reduced whole cell capacitance compared to sham controls. The theory of increased soma size in pilocarpine induced status-epilepticus mice was that increased size was due to the increased energy demands of the neurons in these mice, and that rapamycin treatment reduced the energy demands for these neurons (Buckmaster and Wen, 2011). Although the CCI model does not exhibit the increase in cell size measured in the pilocarpine model of status

epilepticus, rapamycin treatment after CCI injury did demonstrate reduced cell size in both hemispheres. However, there is a caveat of no rapamycin treated sham-injured mice to compare this change in cell size. If energy demand is the driving force in soma size, it could be beneficial to maintain lowered energy demand on an already reduced neuron population such as the eGFP-positive hilar interneurons after CCI injury.

6.7 Effects of mTOR inhibition on glutamate photoactivation responses in the dentate gyrus

6.7.1 Photoactivation responses from dentate granule cells

Use of caged glutamate to stimulate cell populations is a useful tool for mapping out circuitry in a region of the brain and avoids the use of large electrodes which can kill neurons during electrophysiology experiments. Based on the work from Chapter 5 of this dissertation, rapamycin treatment after CCI injury reduces excitatory inputs onto surviving hilar eGFP-positive neurons. However, after CCI injury there are two neuron populations in the ipsilateral hemisphere that this aberrant excitatory sprouting can occur. These two neuron populations are dentate granule cells and CA3 pyramidal neurons (Halabisky et al., 2010;Hunt et al., 2011;Zhang et al., 2012). Based on the work from Chapter 3 of this dissertation, mossy fiber sprouting of dentate granule cells is reduced in mice treated with rapamycin after CCI injury. However, eGFP-positive hilar inhibitory interneurons in the ipsilateral hemisphere of CCI injured mice treated with rapamycin still have increased excitatory input and fire more action potentials than eGFP-positive hilar inhibitory interneurons from the contralateral hemisphere or sham controls. Therefore, glutamate photostimulation applied to both dentate granule cells and CA3

pyramidal neurons was used while recording from eGFP-positive hilar inhibitory interneurons to determine if rapamycin treatment was preferential toward axon sprouting of dentate granule cells or CA3 pyramidal neurons.

There was no difference in the responses to applied glutamate photostimulation in dentate granule cells from the contralateral hemisphere onto recorded eGFP-positive hilar interneurons 8-12 weeks post-injury. eGFP-positive hilar interneurons in the ipsilateral hemisphere of CCI injured mice with vehicle treatment exhibited increased evoked responses when glutamate photostimulation was applied to the dentate granule cell layer compared to controls. Ipsilateral eGFP-positive hilar interneurons from CCI injured mice which received rapamycin treatment did not exhibit increased evoked responses after glutamate photostimulation in dentate granule cells, seen in CCI injured mice with vehicle treatment. This data confirms the effects previously reported in this dissertation of rapamycin treatment after CCI injury on aberrant mossy fiber sprouting. This is the first report of functional changes associated with reduced mossy fiber sprouting within the hilus, and therefore leads to the following question: does rapamycin also reduce aberrant sprouting of CA3 pyramidal neurons onto surviving hilar inhibitory interneurons?

6.7.2 Glutamate photostimulation in CA3 pyramidal neurons

The effect of rapamycin on CA3 backprojections is untested. To test the potential effect of rapamycin on this aberrant sprouting of CA3 pyramidal neurons, whole cell patch-clamp recordings of sEPSCs were made of eGFP-positive hilar interneurons, and then caged glutamate was released in the CA3 pyramidal cell layer 8-12 weeks post-

injury. eGFP-positive hilar interneurons in the ipsilateral hemisphere of CCI injured mice with vehicle treatment exhibited increased responses to glutamate photostimulation applied to CA3 pyramidal cell layer compared to controls. Ipsilateral eGFP-positive hilar interneurons from CCI injured mice which received rapamycin treatment also exhibited the observed increase in evoked responses to glutamate photostimulation of CA3 pyramidal neurons, seen in CCI injured mice with vehicle treatment. This data suggests rapamycin treatment preferentially inhibits hilar sprouting of mossy fibers onto surviving eGFP-positive interneurons, but does not inhibit CA3 backprojections. Based on the data in this study, CA3 pyramids undergo axon sprouting in an mTOR independent manner. It remains unclear what role these backprojections play in disease states such as epilepsy.

6.7.3 Additional future directions

Little is understood about the sprouting of CA3 pyramidal neurons in normal physiology or disease states. In normal physiology CA3 pyramidal neurons will synapse back into the hilus onto GABAergic hilar inhibitory interneurons and excitatory mossy cells (Scharfman, 1993;Scharfman, 1994;Kneisler and Dingledine, 1995). The input onto recorded dentate granule cells after CA3 pyramid stimulation is one of inhibition, which suggests the primary contribution of the CA3 pyramidal neuron back-projection is one of synapsing onto GABAergic hilar inhibitory interneurons (Scharfman, 1993;Kneisler and Dingledine, 1995). This has led to the theory that CA3 pyramidal neurons contribute to a secondary dentate filter of inhibition for dentate granule cells (Scharfman, 2007). After CCI and in models of TLE the synaptic input of CA3 pyramidal neurons onto surviving hilar inhibitory interneurons in the ipsilateral hemisphere increases (Halabisky et al., 2010;Hunt et al., 2011), which this dissertation confirms. The work from Chapter 5 of

this dissertation demonstrates that these increased synaptic connections with surviving hilar inhibitory interneurons in the ipsilateral hemisphere are not rapamycin sensitive. This is different than the increase in excitatory synaptic connections from dentate granule cells onto surviving hilar inhibitory interneurons, which are sensitive to rapamycin treatment after CCI injury. It remains unclear if this is a beneficial or detrimental effect of TBI. Both the CA3 pyramidal cells and hilar inhibitory interneurons are lost after CCI injury in the ipsilateral hippocampus (Lowenstein et al., 1992;Hicks et al., 1993;Smith et al., 1995;Saatman et al., 2006). If the back-projection of CA3 pyramidal neurons is part of a secondary dentate filter, then sprouting of surviving CA3 pyramidal neurons would be beneficial in the maintenance of this inhibitory filter.

There are several possible explanations for this difference in excitatory axon sprouting of dentate granule cells and CA3 pyramidal neurons. Some of the possibilities are: different growth cues for axon sprouting, different cell membrane receptor populations, and different activity levels of neuron populations. One of the possibilities is that different neuron populations respond to various extracellular signaling molecules such as hormones differently. It is possible that CA3 pyramidal neuron sprouting is the result of one of the hormones released after TBI in the ipsilateral hemisphere which dentate granule cells are insensitive to but CA3 pyramidal neurons respond to strongly. A recent report in pilocarpine induced status epilepticus mice demonstrated a substantial reduction in seizure generation when mice were treated with an inhibitor of TrkB (Liu et al., 2013). Loss of CA3 pyramidal neurons is a common feature of animal models of TLE, and interestingly the treatment of pilocarpine induced TLE mice with this TrkB kinase inhibitor reduced the percent of cell loss in the CA3 region. This would suggest

that the CA3 pyramidal neurons are very important to the epileptogenic process. One may even conclude that a focus on changes to CA3 pyramidal neurons, as opposed to a dentate-centric view of epilepsy, could be very beneficial in our understanding of epileptogenesis.

However, work done in the pilocarpine-induced status epilepticus mouse model of TLE suggests CA3 pyramidal neuron sprouting is not only to hilar interneurons and mossy cells, but also increased sprouting directly onto dentate granule cells was observed in mice which underwent status epilepticus (Zhang et al., 2012). There is no evidence of direct CA3 pyramidal neuron connections onto dentate granule cells in CCI injured mice yet, but evidence from the Smith lab (Hunt et al., 2011) and Chapter 5 of this dissertation suggest that this form of sprouting could happen in the ipsilateral hemisphere of CCI injured mice. If this form of sprouting is also insensitive to rapamycin treatment, then this could be another potentially maintained form of excitatory synaptic reorganization in CCI injured mice given rapamycin treatment. This aberrant synaptic reorganization of CA3 pyramidal neurons directly onto dentate granule cells could lead to reemergence of phenotypes associated with epilepsy and potentially seizures after rapamycin treatment is removed, by becoming a focus of aberrant circuitry within the hippocampus. Investigation into the existence of these aberrant connections between CA3 pyramidal neurons and dentate granule cells within the ipsilateral hemisphere of CCI injured mice, as well as potential treatments to prevent this aberrant sprouting would help in understanding the role of CA3 backprojections to epileptogenesis.

6.8 Final conclusions

The findings in this dissertation greatly improve our understanding of the effects of rapamycin treatment following CCI injury on many cellular mechanisms associated with epileptogenesis. Previously the only outcome measures used in studies testing rapamycin as an antiepileptogenic therapy were mossy fiber sprouting and seizure generation (Buckmaster et al., 2009;Zeng et al., 2009;Guo et al., 2013;Heng et al., 2013). However the role of mossy fiber sprouting in the process of epileptogenesis has become controversial (Heng et al., 2013). This dissertation research shows that rapamycin treatment does not prevent the initiation of epileptogenesis, but rather modifies the process and so modifies the disease. The experimental outcomes from these studies should be used to help guide future work toward the development of an antiepileptogenic therapy for PTE. Rapamycin may still have some clinical relevance for other forms of epilepsy such as tuberous sclerosis complex disorder, a genetic form of epilepsy in which the inhibitory molecules which control mTOR signaling are dysfunctional and lead to excessive activity of mTOR (Zeng et al., 2008). Even in this case caution should be observed before the use of rapamycin in the human population with potential impact on all cell types if treatment is given broadly. Drug delivery would be very important to avoid complications in these other tissues and organ systems.

Additionally, increased mTOR activity is not limited to neurons within the hippocampus, but is also present in glia (Zhu et al., 2014). Rapamycin treatment also reduces microglia activation after TBI injury in mice (Erlich et al., 2007). This dissertation work did not focus on changes in glia after CCI injury or how rapamycin treatment would modify these changes. The electrophysiological measurements made

here are expected to be most sensitive to changes in neuronal synaptic reorganization. For example, the stimulation protocols used here to assess cell connectivity, such as antidromic stimulation of DGC axons or glutamate photoactivation within the DGC and CA3 neuron layers, are expected to preferentially activate neurons. Additionally, the mossy fiber sprouting observed with Timm stain indicates that axonal reorganization of DGCs is occurring after brain injury. That being said, it remains possible that astrocytes or microglia are participating in some of the observed changes following brain injury and/or are sensitive to the rapamycin treatment used here. There is evidence that glia can indirectly modify neuronal excitability and axonal plasticity through the release of various transmitters and factors. The present projects did not attempt to isolate the effects of glia on hippocampal signaling after brain injury.

Appendix 1

Lists of immunohistochemical protocols

A1.1 Doublecortin protocol

First Day:

-10% blocking/permeabilization step for 30 minutes at room temperature

-2% goat serum, 0.15% triton 100 in TBS with 1:5000 primary rabbit anti-doublecortin antibody overnight at 4^{o}C

Second Day: All done at room temperature

-3 X 5 minute washes with 2% goat serum, 0.15 triton 100 in TBS

-1 hour in goat anti-rabbit alexa fluor (488; 1:1000)

-3 X 5 minute washes with TBS

-Mount tissue on Superfrost slides using vectashield with DAPI

A1.2 Fluoro Jade B protocol

- 5 minutes in 1% NaOH in 80% ethanol, gently shake at room temp

- 2 minutes in 70% ethanol

- 2 minutes in DDH_2O

- 10 minutes in 0.06% potassium permanganate solution (60 mg in 100 mL DDH_2O), cover in aluminum foil

- Short rinse in DDH_2O

- 1 minute DDH_2O

- 1 minute DDH_2O

- 1 minute DDH_2O

- 10 minutes in Fluoro Jade B solution (1 mL from 0.01% FJB in 99 mL of 0.1% acetic acid H_2O)

- 1 minute DDH2O

- 1 minute DDH2O

- 1 minute DDH2O

- 1 minute DDH2O

- 1 minute DDH2O

- Dry excess water from slide

- Dry slides on slide warmer at 50 oC for 30 minutes, protect from light

- 10 minutes in Xylene

- 10 minutes in Xylene

A1.5 Sodium phosphate buffer (0.3 M) protocol

Chemical	For 500 mL	For 1000 mL
Sodium phosphate monobasic ($NaH_2PO_4*H_2O$, FW= 137.99)	4.755 g	9.51 g
Sodium phosphate dibasic (Na_2HPO_4, FW= 141.96)	16.395 g	32.79 g

Appendix 2

Electrophysiology protocols/setup

A2.1 ACSF protocol

Chemical	0.5 L	1 L	1.5 L	2 L	Final concentration
NaCl	3.6235 g	7.247 g	10.8705 g	14.494 g	124 mM
$NaHCO_3$	1.09 g	2.18 g	3.27 g	4.36 g	26 mM
NaH_2PO_4	0.086 g	0.172 g	0.258 g	0.344 g	1.4 mM
Glucose	0.99 g	1.98 g	2.97 g	3.96 g	11 mM
KCl	0.75 mL	1.5 mL	2.25 mL	3 mL	3 mM
$MgCl_2$	0.65 mL	1.3 mL	1.95 mL	2.6 mL	1.3 mM
$CaCl_2$	0.65- 1 mL	1.3- 2 mL	1.95- 3 mL	2.6- 4 mL	1.3- 2 mM

A2.2 Internal solutions protocols

A2.2.1 Cs-gluconate 140

Chemical	200 mL	100 mL	mM	mOSM
Gluconic acid	8.81 mL	4.405 mL	130	140
HEPES	0.4766 g	0.2383 g	10	10
NaCl	200 μL	100 μL	1	2
$MgCl_2$	200 μL	100 μL	1	3
$CaCl_2$	200 μL	100 μL	1	3
Titrate to pH=7.2 with CsOH				

Add EGTA	0.38048 g	0.19024 g	5	5

-Spin until EGTA dissolves <30 minutes total, then titrate to pH=7.2 again

A2.2.2 K-gluconate 130

Chemical	200 mL	100 mL	mM	mOSM
K gluconate	6.0892 g	3.0446 g	130	260
HEPES	0.4766 g	0.2383 g	10	10
NaCl	200 μL	100 μL	1	2
$MgCl_2$	200 μL	100 μL	1	3
$CaCl_2$	200 μL	100 μL	1	3
Titrate to pH=7.2 with KOH				
Add EGTA	0.38048 g	0.19024 g	5	5

-Spin until EGTA dissolves <30 minutes total, then titrate to pH=7.2 again

A2.3 Diagram of electrophysiology connections for Axon 200B

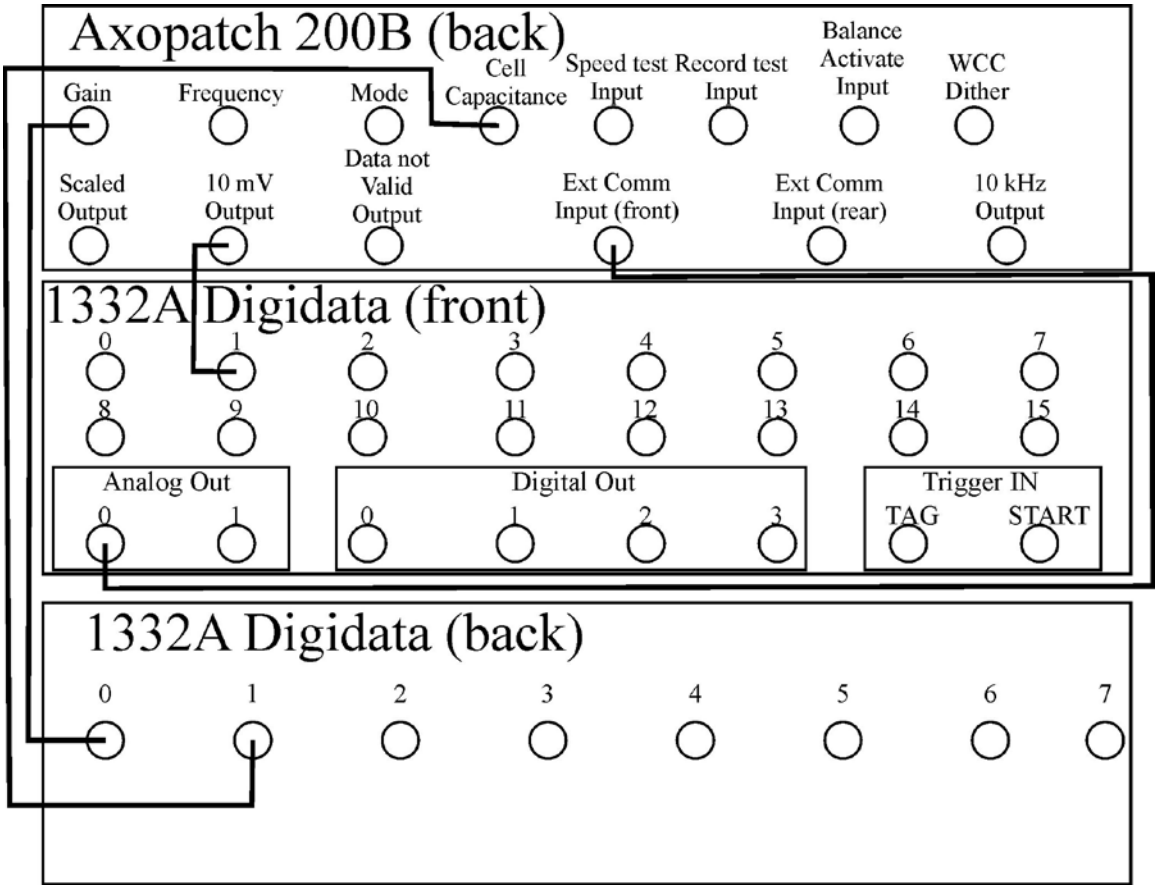

A2.4 Diagram of electrophysiology connections for Multiclamp 700B

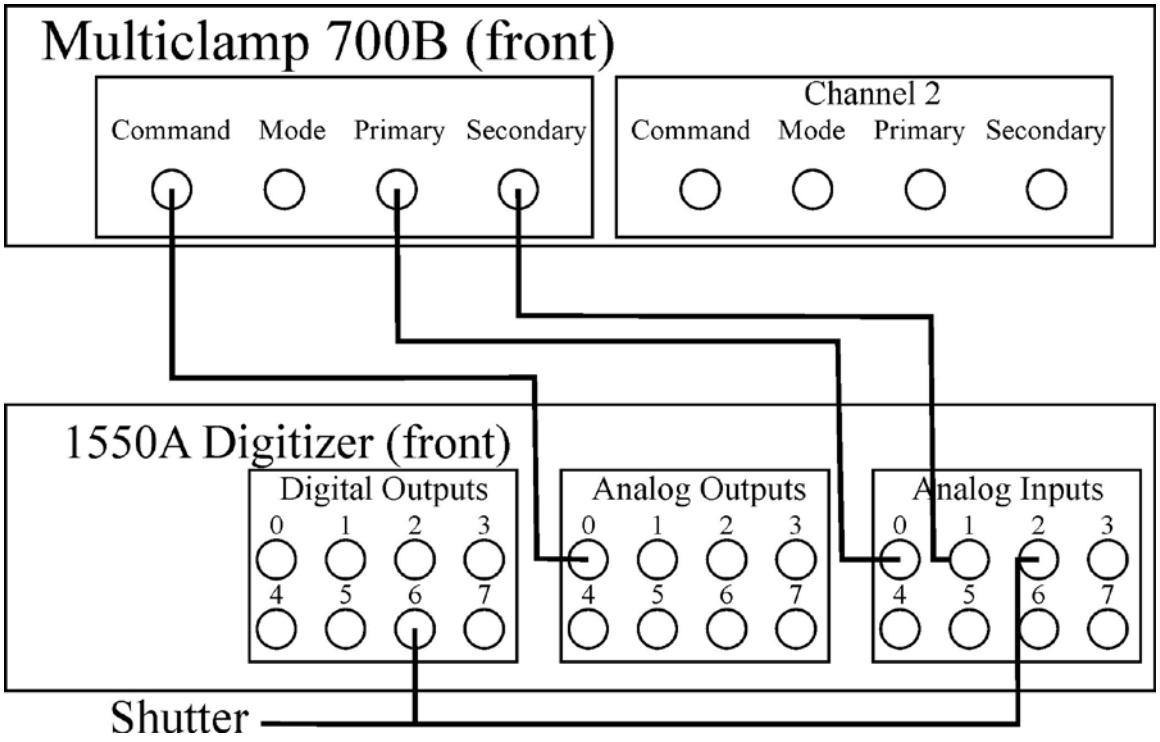

A2.5 List of tubing used for electrophysiology

Fisherbrand Manifold pump tubing (1.30 mm x 16”)

Dow corning Silastic (<0.040in x 50 ft.)

Nalgene tubing products (0.25in x 3 ft.)

References:

Abou-Khalil, B. (2008). Levetiracetam in the treatment of epilepsy. *Neuropsychiatr Dis Treat* 4**,** 507-523.

Aimone, J.B., Wiles, J., and Gage, F.H. (2006). Potential role for adult neurogenesis in the encoding of time in new memories. *Nat Neurosci* 9**,** 723-727.

Altman, J., and Das, G.D. (1965a). Autoradiographic and histological evidence of postnatal hippocampal neurogenesis in rats. *J Comp Neurol* 124**,** 319-335.

Altman, J., and Das, G.D. (1965b). Post-natal origin of microneurones in the rat brain. *Nature* 207**,** 953-956.

Alvarez-Buylla, A., Ling, C.Y., and Kirn, J.R. (1990). Cresyl violet: a red fluorescent Nissl stain. *J Neurosci Methods* 33**,** 129-133.

Amaral, D.G. (1979). Synaptic extensions from the mossy fibers of the fascia dentata. *Anat Embryol (Berl)* 155**,** 241-251.

Amaral, D.G., and Dent, J.A. (1981). Development of the mossy fibers of the dentate gyrus: I. A light and electron microscopic study of the mossy fibers and their expansions. *J Comp Neurol* 195**,** 51-86.

Amiri, A., Cho, W., Zhou, J., Birnbaum, S.G., Sinton, C.M., Mckay, R.M., and Parada, L.F. (2012). Pten deletion in adult hippocampal neural stem/progenitor cells causes cellular abnormalities and alters neurogenesis. *J Neurosci* 32**,** 5880-5890.

Andersen, P., Bliss, T.V., and Skrede, K.K. (1971). Lamellar organization of hippocampal pathways. *Exp Brain Res* 13**,** 222-238.

Anderson, K.J., Miller, K.M., Fugaccia, I., and Scheff, S.W. (2005). Regional distribution of fluoro-jade B staining in the hippocampus following traumatic brain injury. *Exp Neurol* 193**,** 125-130.

Annegers, J.F., Hauser, W.A., Coan, S.P., and Rocca, W.A. (1998). A population-based study of seizures after traumatic brain injuries. *N Engl J Med* 338**,** 20-24.

Ansari, M.A., Roberts, K.N., and Scheff, S.W. (2008). A time course of contusion-induced oxidative stress and synaptic proteins in cortex in a rat model of TBI. *J Neurotrauma* 25**,** 513-526.

Arvidsson, A., Collin, T., Kirik, D., Kokaia, Z., and Lindvall, O. (2002). Neuronal replacement from endogenous precursors in the adult brain after stroke. *Nat Med* 8**,** 963-970.

Atkins, C.M., Truettner, J.S., Lotocki, G., Sanchez-Molano, J., Kang, Y., Alonso, O.F., Sick, T.J., Dietrich, W.D., and Bramlett, H.M. (2010). Post-traumatic seizure susceptibility is attenuated by hypothermia therapy. *Eur J Neurosci* 32**,** 1912-1920.

Babb, T.L., Kupfer, W.R., Pretorius, J.K., Crandall, P.H., and Levesque, M.F. (1991). Synaptic reorganization by mossy fibers in human epileptic fascia dentata. *Neuroscience* 42**,** 351-363.

Bakst, I., Avendano, C., Morrison, J.H., and Amaral, D.G. (1986). An experimental analysis of the origins of somatostatin-like immunoreactivity in the dentate gyrus of the rat. *J Neurosci* 6**,** 1452-1462.

Barha, C.K., Ishrat, T., Epp, J.R., Galea, L.A., and Stein, D.G. (2011). Progesterone treatment normalizes the levels of cell proliferation and cell death in the dentate gyrus of the hippocampus after traumatic brain injury. *Exp Neurol* 231**,** 72-81.

Bhaskaran, M., and Smith, B. (2010). Effects of TRPV1 activation on synaptic excitation in the dentate gyrus of a mouse model of temporal lobe epilepsy. *Exp Neurol* PMID: 20144892.

Blasco-Ibanez, J.M., Martinez-Guijarro, F.J., and Freund, T.F. (2000). Recurrent mossy fibers preferentially innervate parvalbumin-immunoreactive interneurons in the granule cell layer of the rat dentate gyrus. *Neuroreport* 11**,** 3219-3225.

Bolkvadze, T., and Pitkanen, A. (2012). Development of post-traumatic epilepsy after controlled cortical impact and lateral fluid-percussion-induced brain injury in the mouse. *J Neurotrauma* 29**,** 789-812.

Boychuk, J.A., Butler, C.R., Halmos, K.C., and Smith, B.N. (2016). Enduring changes in tonic GABAA receptor signaling in dentate granule cells after controlled cortical impact brain injury in mice. *Experimental Neurology*.

Bramlett, H.M., Dietrich, W.D., Green, E.J., and Busto, R. (1997). Chronic histopathological consequences of fluid-percussion brain injury in rats: effects of post-traumatic hypothermia. *Acta Neuropathol* 93**,** 190-199.

Brandt, C., Glien, M., Gastens, A.M., Fedrowitz, M., Bethmann, K., Volk, H.A., Potschka, H., and Loscher, W. (2007). Prophylactic treatment with levetiracetam after status epilepticus: lack of effect on epileptogenesis, neuronal damage, and behavioral alterations in rats. *Neuropharmacology* 53**,** 207-221.

Brooks-Kayal, A.R., Raol, Y.H., and Russek, S.J. (2009). Alteration of epileptogenesis genes. *Neurotherapeutics* 6**,** 312-318.

Brooks-Kayal, A.R., Shumate, M.D., Jin, H., Lin, D.D., Rikhter, T.Y., Holloway, K.L., and Coulter, D.A. (1999). Human neuronal gamma-aminobutyric acid(A) receptors: coordinated subunit mRNA expression and functional correlates in individual dentate granule cells. *J Neurosci* 19**,** 8312-8318.

Brooks-Kayal, A.R., Shumate, M.D., Jin, H., Rikhter, T.Y., and Coulter, D.A. (1998). Selective changes in single cell GABA(A) receptor subunit expression and function in temporal lobe epilepsy. *Nat Med* 4**,** 1166-1172.

Brown, N., Kerby, J., Bonnert, T.P., Whiting, P.J., and Wafford, K.A. (2002). Pharmacological characterization of a novel cell line expressing human alpha(4)beta(3)delta GABA(A) receptors. *Br J Pharmacol* 136**,** 965-974.

Browning, M.D., Bureau, M., Dudek, E.M., and Olsen, R.W. (1990). Protein kinase C and cAMP-dependent protein kinase phosphorylate the beta subunit of the purified gamma-aminobutyric acid A receptor. *Proc Natl Acad Sci U S A* 87**,** 1315-1318.

Buckmaster, P.S. (2012). Mossy Fiber Sprouting in the Dentate Gyrus.

Buckmaster, P.S., and Dudek, F.E. (1997a). Network properties of the dentate gyrus in epileptic rats with hilar neuron loss and granule cell axon reorganization. *J Neurophysiol* 77**,** 2685-2696.

Buckmaster, P.S., and Dudek, F.E. (1997b). Neuron loss, granule cell axon reorganization, and functional changes in the dentate gyrus of epileptic kainate-treated rats. *J Comp Neurol* 385**,** 385-404.

Buckmaster, P.S., Ingram, E.A., and Wen, X. (2009). Inhibition of the mammalian target of rapamycin signaling pathway suppresses dentate granule cell axon sprouting in a rodent model of temporal lobe epilepsy. *J Neurosci* 29**,** 8259-8269.

Buckmaster, P.S., Kunkel, D.D., Robbins, R.J., and Schwartzkroin, P.A. (1994). Somatostatin-immunoreactivity in the hippocampus of mouse, rat, guinea pig, and rabbit. *Hippocampus* 4**,** 167-180.

Buckmaster, P.S., and Lew, F.H. (2011). Rapamycin suppresses mossy fiber sprouting but not seizure frequency in a mouse model of temporal lobe epilepsy. *J Neurosci* 31**,** 2337-2347.

Buckmaster, P.S., and Schwartzkroin, P.A. (1994). Hyperexcitability in the dentate gyrus of the epileptic Mongolian gerbil. *Epilepsy Res* 18**,** 23-28.

Buckmaster, P.S., and Schwartzkroin, P.A. (1995). Interneurons and inhibition in the dentate gyrus of the rat in vivo. *J Neurosci* 15**,** 774-789.

Buckmaster, P.S., and Wen, X. (2011). Rapamycin suppresses axon sprouting by somatostatin interneurons in a mouse model of temporal lobe epilepsy. *Epilepsia* 52**,** 2057-2064.

Buckmaster, P.S., Zhang, G.F., and Yamawaki, R. (2002). Axon sprouting in a model of temporal lobe epilepsy creates a predominantly excitatory feedback circuit. *J Neurosci* 22**,** 6650-6658.

Busto, R., Dietrich, W.D., Globus, M.Y., Alonso, O., and Ginsberg, M.D. (1997). Extracellular release of serotonin following fluid-percussion brain injury in rats. *J Neurotrauma* 14**,** 35-42.

Butler, C.R., Boychuk, J.A., and Smith, B.N. (2015). Effects of Rapamycin Treatment on Neurogenesis and Synaptic Reorganization in the Dentate Gyrus after Controlled Cortical Impact Injury in Mice. *Front Syst Neurosci* 9**,** 163. doi: 10.3389/fnsys.2015.00163.

Carloni, S., Buonocore, G., and Balduini, W. (2008). Protective role of autophagy in neonatal hypoxia–ischemia induced brain injury. *Neurobiology of disease* 32**,** 329-339.

Carlson, S.W., Madathil, S.K., Sama, D.M., Gao, X., Chen, J., and Saatman, K.E. (2014). Conditional overexpression of insulin-like growth factor-1 enhances hippocampal neurogenesis and restores immature neuron dendritic processes after traumatic brain injury. *J Neuropathol Exp Neurol* 73**,** 734-746.

Caveness, W.F., Meirowsky, A.M., Rish, B.L., Mohr, J.P., Kistler, J.P., Dillon, J.D., and Weiss, G.H. (1979). The nature of posttraumatic epilepsy. *J Neurosurg* 50**,** 545-553.

Chepreganova-Changovska, T., Petrovska-Cvetkovska, D., Srceva-Jovanovski, M., and Filipce, V. (2014). Symptomatic Epileptogenic Lesions. *PRILOZI* 35**,** 45-52.

Chiolero, R., Schutz, Y., Lemarchand, T., Felber, J.-P., De Tribolet, N., Freeman, J., and Jéquier, E. (1989). Hormonal and metabolic changes following severe head injury or noncranial injury. *Journal of Parenteral and Enteral Nutrition* 13**,** 5-12.

Chirumamilla, S., Sun, D., Bullock, M.R., and Colello, R.J. (2002). Traumatic brain injury induced cell proliferation in the adult mammalian central nervous system. *J Neurotrauma* 19**,** 693-703.

Choi, J., and Koh, S. (2008). Role of brain inflammation in epileptogenesis. *Yonsei Med J* 49**,** 1-18.

Christensen, K.V., Leffers, H., Watson, W.P., Sanchez, C., Kallunki, P., and Egebjerg, J. (2010). Levetiracetam attenuates hippocampal expression of synaptic plasticity-

related immediate early and late response genes in amygdala-kindled rats. *BMC Neurosci* 11**,** 9.

Chrzaszcz, M., Venkatesan, C., Dragisic, T., Watterson, D.M., and Wainwright, M.S. (2010). Minozac treatment prevents increased seizure susceptibility in a mouse "two-hit" model of closed skull traumatic brain injury and electroconvulsive shock-induced seizures. *J Neurotrauma* 27**,** 1283-1295.

Claiborne, B.J., Amaral, D.G., and Cowan, W.M. (1986). A light and electron microscopic analysis of the mossy fibers of the rat dentate gyrus. *J Comp Neurol* 246**,** 435-458.

Clifton, G.L., Allen, S., Barrodale, P., Plenger, P., Berry, J., Koch, S., Fletcher, J., Hayes, R.L., and Choi, S.C. (1993). A phase II study of moderate hypothermia in severe brain injury. *J Neurotrauma* 10**,** 263-271.

Clifton, G.L., Miller, E.R., Choi, S.C., Levin, H.S., Mccauley, S., Smith, K.R., Jr., Muizelaar, J.P., Wagner, F.C., Jr., Marion, D.W., Luerssen, T.G., Chesnut, R.M., and Schwartz, M. (2001). Lack of effect of induction of hypothermia after acute brain injury. *N Engl J Med* 344**,** 556-563.

Conti, A.C., Raghupathi, R., Trojanowski, J.Q., and Mcintosh, T.K. (1998). Experimental brain injury induces regionally distinct apoptosis during the acute and delayed post-traumatic period. *J Neurosci* 18**,** 5663-5672.

Corradetti, M., and Guan, K. (2006). Upstream of the mammalian target of rapamycin: do all roads pass through mTOR? *Oncogene* 25**,** 6347-6360.

Cortez, S.C., Mcintosh, T.K., and Noble, L.J. (1989). Experimental fluid percussion brain injury: vascular disruption and neuronal and glial alterations. *Brain Res* 482**,** 271-282.

Coulter, D.A., and Carlson, G.C. (2007). Functional regulation of the dentate gyrus by GABA-mediated inhibition. *Prog Brain Res* 163**,** 235-243.

Crawford, I.L., and Connor, J.D. (1972). Zinc in maturing rat brain: hippocampal concentration and localization. *J Neurochem* 19**,** 1451-1458.

Crespel, A., Coubes, P., Rousset, M.C., Brana, C., Rougier, A., Rondouin, G., Bockaert, J., Baldy-Moulinier, M., and Lerner-Natoli, M. (2002). Inflammatory reactions in human medial temporal lobe epilepsy with hippocampal sclerosis. *Brain Res* 952**,** 159-169.

Cronin, J., and Dudek, F.E. (1988). Chronic seizures and collateral sprouting of dentate mossy fibers after kainic acid treatment in rats. *Brain Res* 474**,** 181-184.

Cronin, J., Obenaus, A., Houser, C.R., and Dudek, F.E. (1992). Electrophysiology of dentate granule cells after kainate-induced synaptic reorganization of the mossy fibers. *Brain Res* 573**,** 305-310.

D'ambrosio, R., Fairbanks, J.P., Fender, J.S., Born, D.E., Doyle, D.L., and Miller, J.W. (2004). Post-traumatic epilepsy following fluid percussion injury in the rat. *Brain* 127**,** 304-314.

D'ambrosio, R., Fender, J.S., Fairbanks, J.P., Simon, E.A., Born, D.E., Doyle, D.L., and Miller, J.W. (2005). Progression from frontal-parietal to mesial-temporal epilepsy after fluid percussion injury in the rat. *Brain* 128**,** 174-188.

D'ambrosio, R., Hakimian, S., Stewart, T., Verley, D.R., Fender, J.S., Eastman, C.L., Sheerin, A.H., Gupta, P., Diaz-Arrastia, R., Ojemann, J., and Miller, J.W. (2009).

Functional definition of seizure provides new insight into post-traumatic epileptogenesis. *Brain* 132**,** 2805-2821.

Danscher, G., Howell, G., Perez-Clausell, J., and Hertel, N. (1985). The dithizone, Timm's sulphide silver and the selenium methods demonstrate a chelatable pool of zinc in CNS. A proton activation (PIXE) analysis of carbon tetrachloride extracts from rat brains and spinal cords intravitally treated with dithizone. *Histochemistry* 83**,** 419-422.

Danscher, G., Shipley, M.T., and Andersen, P. (1975). Persistent function of mossy fibre synapses after metal chelation with DEDTC (Antabuse). *Brain Res* 85**,** 522-526.

Dash, P.K., Mach, S.A., and Moore, A.N. (2001). Enhanced neurogenesis in the rodent hippocampus following traumatic brain injury. *J Neurosci Res* 63**,** 313-319.

De Lanerolle, N.C., Kim, J.H., Robbins, R.J., and Spencer, D.D. (1989). Hippocampal interneuron loss and plasticity in human temporal lobe epilepsy. *Brain Res* 495**,** 387-395.

Dedeurwaerdere, S., Friedman, A., Fabene, P.F., Mazarati, A., Murashima, Y.L., Vezzani, A., and Baram, T.Z. (2012). Finding a better drug for epilepsy: antiinflammatory targets. *Epilepsia* 53**,** 1113-1118.

Diamond, M.L., Ritter, A.C., Failla, M.D., Boles, J.A., Conley, Y.P., Kochanek, P.M., and Wagner, A.K. (2015). IL-1beta associations with posttraumatic epilepsy development: A genetics and biomarker cohort study. *Epilepsia* 56**,** 991-1001.

Diaz-Arrastia, R., Agostini, M.A., Frol, A.B., Mickey, B., Fleckenstein, J., Bigio, E., and Van Ness, P.C. (2000). Neurophysiologic and neuroradiologic features of intractable epilepsy after traumatic brain injury in adults. *Arch Neurol* 57**,** 1611-1616.

Dietrich, W.D., Alonso, O., Busto, R., Globus, M.Y., and Ginsberg, M.D. (1994). Post-traumatic brain hypothermia reduces histopathological damage following concussive brain injury in the rat. *Acta Neuropathol* 87**,** 250-258.

Dixon, C.E., Clifton, G.L., Lighthall, J.W., Yaghmai, A.A., and Hayes, R.L. (1991). A controlled cortical impact model of traumatic brain injury in the rat. *J Neurosci Methods* 39**,** 253-262.

Dixon, C.E., Lyeth, B.G., Povlishock, J.T., Findling, R.L., Hamm, R.J., Marmarou, A., Young, H.F., and Hayes, R.L. (1987). A fluid percussion model of experimental brain injury in the rat. *J Neurosurg* 67**,** 110-119.

Djebaili, M., Guo, Q., Pettus, E.H., Hoffman, S.W., and Stein, D.G. (2005). The neurosteroids progesterone and allopregnanolone reduce cell death, gliosis, and functional deficits after traumatic brain injury in rats. *J Neurotrauma* 22**,** 106-118.

Doetsch, F., and Hen, R. (2005). Young and excitable: the function of new neurons in the adult mammalian brain. *Curr Opin Neurobiol* 15**,** 121-128.

Don, A.S., Tsang, C.K., Kazdoba, T.M., D'arcangelo, G., Young, W., and Zheng, X.F. (2012). Targeting mTOR as a novel therapeutic strategy for traumatic CNS injuries. *Drug Discov Today* 17**,** 861-868.

Drexel, M., Puhakka, N., Kirchmair, E., Hortnagl, H., Pitkanen, A., and Sperk, G. (2015). Expression of GABA receptor subunits in the hippocampus and thalamus after experimental traumatic brain injury. *Neuropharmacology* 88**,** 122-133.

Duan, X., Kang, E., Liu, C.Y., Ming, G.L., and Song, H. (2008). Development of neural stem cell in the adult brain. *Curr Opin Neurobiol* 18**,** 108-115.

Dudek, F.E., and Spitz, M. (1997). Hypothetical mechanisms for the cellular and neurophysiologic basis of secondary epileptogenesis: proposed role of synaptic reorganization. *J Clin Neurophysiol* 14**,** 90-101.

Ebert, B., Wafford, K.A., Whiting, P.J., Krogsgaard-Larsen, P., and Kemp, J.A. (1994). Molecular pharmacology of gamma-aminobutyric acid type A receptor agonists and partial agonists in oocytes injected with different alpha, beta, and gamma receptor subunit combinations. *Mol Pharmacol* 46**,** 957-963.

Echegoyen, J., Armstrong, C., Morgan, R.J., and Soltesz, I. (2009). Single application of a CB1 receptor antagonist rapidly following head injury prevents long-term hyperexcitability in a rat model. *Epilepsy Res* 85**,** 123-127.

Eckenhoff, M.F., and Rakic, P. (1988). Nature and fate of proliferative cells in the hippocampal dentate gyrus during the life span of the rhesus monkey. *J Neurosci* 8**,** 2729-2747.

Englander, J., Bushnik, T., Duong, T.T., Cifu, D.X., Zafonte, R., Wright, J., Hughes, R., and Bergman, W. (2003). Analyzing risk factors for late posttraumatic seizures: a prospective, multicenter investigation. *Arch Phys Med Rehabil* 84**,** 365-373.

Epsztein, J., Represa, A., Jorquera, I., Ben-Ari, Y., and Crepel, V. (2005). Recurrent mossy fibers establish aberrant kainate receptor-operated synapses on granule cells from epileptic rats. *J Neurosci* 25**,** 8229-8239.

Eriksson, P.S., Perfilieva, E., Bjork-Eriksson, T., Alborn, A.M., Nordborg, C., Peterson, D.A., and Gage, F.H. (1998). Neurogenesis in the adult human hippocampus. *Nat Med* 4**,** 1313-1317.

Erlich, S., Alexandrovich, A., Shohami, E., and Pinkas-Kramarski, R. (2007). Rapamycin is a neuroprotective treatment for traumatic brain injury. *Neurobiol Dis* 26**,** 86-93.

Esclapez, M., Hirsch, J.C., Ben-Ari, Y., and Bernard, C. (1999). Newly formed excitatory pathways provide a substrate for hyperexcitability in experimental temporal lobe epilepsy. *J Comp Neurol* 408**,** 449-460.

Farrant, M., and Nusser, Z. (2005). Variations on an inhibitory theme: phasic and tonic activation of GABA(A) receptors. *Nat Rev Neurosci* 6**,** 215-229.

Foster, K.G., and Fingar, D.C. (2010). Mammalian target of rapamycin (mTOR): conducting the cellular signaling symphony. *J Biol Chem* 285**,** 14071-14077.

Franck, J.E., Pokorny, J., Kunkel, D.D., and Schwartzkroin, P.A. (1995). Physiologic and morphologic characteristics of granule cell circuitry in human epileptic hippocampus. *Epilepsia* 36**,** 543-558.

Frederickson, C.J., Howell, G.A., and Frederickson, M.H. (1981). Zinc dithizonate staining in the cat hippocampus: relationship to the mossy-fiber neuropil and postnatal development. *Exp Neurol* 73**,** 812-823.

Freund, T.F., and Buzsaki, G. (1996). Interneurons of the hippocampus. *Hippocampus* 6**,** 347-470.

Gage, F.H. (2002). Neurogenesis in the adult brain. *The Journal of Neuroscience* 22**,** 612-613.

Glotzner, F.L., Haubitz, I., Miltner, F., Kapp, G., and Pflughaupt, K.W. (1983). [Seizure prevention using carbamazepine following severe brain injuries]. *Neurochirurgia (Stuttg)* 26**,** 66-79.

Glykys, J., Mann, E.O., and Mody, I. (2008). Which GABA(A) receptor subunits are necessary for tonic inhibition in the hippocampus? *J Neurosci* 28**,** 1421-1426.

Glykys, J., and Mody, I. (2007a). Activation of GABAA receptors: views from outside the synaptic cleft. *Neuron* 56**,** 763-770.

Glykys, J., and Mody, I. (2007b). The main source of ambient GABA responsible for tonic inhibition in the mouse hippocampus. *J Physiol* 582**,** 1163-1178.

Goodman, J.C., Robertson, C.S., Grossman, R.G., and Narayan, R.K. (1990). Elevation of tumor necrosis factor in head injury. *Journal of neuroimmunology* 30**,** 213-217.

Goss, J.R., Styren, S.D., Miller, P.D., Kochanek, P.M., Palmer, A.M., Marion, D.W., and Dekosky, S.T. (1995). Hypothermia attenuates the normal increase in interleukin 1 beta RNA and nerve growth factor following traumatic brain injury in the rat. *J Neurotrauma* 12**,** 159-167.

Gould, E., and Tanapat, P. (1997). Lesion-induced proliferation of neuronal progenitors in the dentate gyrus of the adult rat. *Neuroscience* 80**,** 427-436.

Grabenstatter, H.L., Del Angel, Y.C., Carlsen, J., Wempe, M.F., White, A.M., Cogswell, M., Russek, S.J., and Brooks-Kayal, A.R. (2014). The effect of STAT3 inhibition on status epilepticus and subsequent spontaneous seizures in the pilocarpine model of acquired epilepsy. *Neurobiol Dis* 62**,** 73-85.

Grady, M.S., Charleston, J.S., Maris, D., Witgen, B.M., and Lifshitz, J. (2003). Neuronal and glial cell number in the hippocampus after experimental traumatic brain injury: analysis by stereological estimation. *J Neurotrauma* 20**,** 929-941.

Graham, D.I., Raghupathi, R., Saatman, K.E., Meaney, D., and Mcintosh, T.K. (2000). Tissue tears in the white matter after lateral fluid percussion brain injury in the rat: relevance to human brain injury. *Acta Neuropathol* 99**,** 117-124.

Graham, D.I., Saatman, K.E., Marklund, N., Conte, V., Morales, D., Royo, N., and Mcintosh, T.K. (2006). The neuropathology of trauma. *Neurology and trauma* 2**,** 45-94.

Gueneau, G., Privat, A., Drouet, J., and Court, L. (1982). Subgranular zone of the dentate gyrus of young rabbits as a secondary matrix. A high-resolution autoradiographic study. *Dev Neurosci* 5**,** 345-358.

Guo, D., Zeng, L., Brody, D.L., and Wong, M. (2013). Rapamycin attenuates the development of posttraumatic epilepsy in a mouse model of traumatic brain injury. *PLoS One* 8**,** e64078.

Gupta, A., Elgammal, F.S., Proddutur, A., Shah, S., and Santhakumar, V. (2012). Decrease in tonic inhibition contributes to increase in dentate semilunar granule cell excitability after brain injury. *J Neurosci* 32**,** 2523-2537.

Gurkoff, G.G., Giza, C.C., Shin, D., Auvin, S., Sankar, R., and Hovda, D.A. (2009). Acute neuroprotection to pilocarpine-induced seizures is not sustained after traumatic brain injury in the developing rat. *Neuroscience* 164**,** 862-876.

Hadfield, J., Little, R., and Jones, R. (1992). Measured energy expenditure and plasma substrate and hormonal changes after severe head injury. *Injury* 23**,** 177-182.

Halabisky, B., Parada, I., Buckmaster, P., and Prince, D. (2010). Excitatory input onto hilar somatostatin interneurons is increased in a chronic model of epilepsy. *J Neurophysiol.* 104**,** 2214-2223.

Halasy, K., and Somogyi, P. (1993). Distribution of GABAergic synapses and their targets in the dentate gyrus of rat: a quantitative immunoelectron microscopic analysis. *J Hirnforsch* 34**,** 299-308.

Hall, E.D., Bryant, Y.D., Cho, W., and Sullivan, P.G. (2008). Evolution of post-traumatic neurodegeneration after controlled cortical impact traumatic brain injury in mice and rats as assessed by the de Olmos silver and fluorojade staining methods. *J Neurotrauma* 25**,** 235-247.

Hall, E.D., Sullivan, P.G., Gibson, T.R., Pavel, K.M., Thompson, B.M., and Scheff, S.W. (2005). Spatial and temporal characteristics of neurodegeneration after controlled cortical impact in mice: more than a focal brain injury. *J Neurotrauma* 22**,** 252-265.

Han, Z.S., Buhl, E.H., Lorinczi, Z., and Somogyi, P. (1993). A high degree of spatial selectivity in the axonal and dendritic domains of physiologically identified local-circuit neurons in the dentate gyrus of the rat hippocampus. *Eur J Neurosci* 5**,** 395-410.

Hattiangady, B., Rao, M.S., and Shetty, A.K. (2004). Chronic temporal lobe epilepsy is associated with severely declined dentate neurogenesis in the adult hippocampus. *Neurobiol Dis* 17**,** 473-490.

Hattiangady, B., and Shetty, A.K. (2010). Decreased neuronal differentiation of newly generated cells underlies reduced hippocampal neurogenesis in chronic temporal lobe epilepsy. *Hippocampus* 20**,** 97-112.

Hauptmann, A. (1912). Luminal bei epilepsie. *Munch Med Wochenschr* 59**,** 1907-1909.

Hauser, W.A., Annegers, J.F., and Kurland, L.T. (1993). Incidence of epilepsy and unprovoked seizures in Rochester, Minnesota: 1935-1984. *Epilepsia* 34**,** 453-468.

Hayes, R.L., Stalhammar, D., Povlishock, J.T., Allen, A.M., Galinat, B.J., Becker, D.P., and Stonnington, H.H. (1987). A new model of concussive brain injury in the cat produced by extradural fluid volume loading: II. Physiological and neuropathological observations. *Brain Inj* 1**,** 93-112.

Heinemann, U., Beck, H., Dreier, J., Ficker, E., Stabel, J., and Zhang, C. (1991). The dentate gyrus as a regulated gate for the propagation of epileptiform activity. *Epilepsy research. Supplement* 7**,** 273-280.

Heng, K., Haney, M.M., and Buckmaster, P.S. (2013). High-dose rapamycin blocks mossy fiber sprouting but not seizures in a mouse model of temporal lobe epilepsy. *Epilepsia* 54**,** 1535-1541.

Hesse, G.W. (1979). Chronic zinc deficiency alters neuronal function of hippocampal mossy fibers. *Science* 205**,** 1005-1007.

Hester, M.S., and Danzer, S.C. (2013). Accumulation of abnormal adult-generated hippocampal granule cells predicts seizure frequency and severity. *J Neurosci* 33**,** 8926-8936.

Hicks, R.R., Baldwin, S.A., and Scheff, S.W. (1997). Serum extravasation and cytoskeletal alterations following traumatic brain injury in rats. Comparison of lateral fluid percussion and cortical impact models. *Mol Chem Neuropathol* 32**,** 1-16.

Hicks, R.R., Smith, D.H., Lowenstein, D.H., Saint Marie, R., and Mcintosh, T.K. (1993). Mild experimental brain injury in the rat induces cognitive deficits associated with regional neuronal loss in the hippocampus. *J Neurotrauma* 10**,** 405-414.

Hoff, H., and Hoff, H. (1947). Progresses in the treatment of epilepsy. *Monatsschrift fur psychiatrie und neurologie* 114**,** 105-118.

Houser, C.R. (1992). Morphological changes in the dentate gyrus in human temporal lobe epilepsy. *Epilepsy Res Suppl* 7**,** 223-234.

Houser, C.R. (2007). Interneurons of the dentate gyrus: an overview of cell types, terminal fields and neurochemical identity. *Prog Brain Res* 163**,** 217-232.

Houser, C.R., and Esclapez, M. (1996). Vulnerability and plasticity of the GABA system in the pilocarpine model of spontaneous recurrent seizures. *Epilepsy Res* 26**,** 207-218.

Hu, M., Zhu, K., Chen, X.L., Zhang, Y.J., Zhang, J.S., Xiao, X.L., Liu, J.X., and Liu, Y. (2015). Newly generated neurons at 2 months post-status epilepticus are functionally integrated into neuronal circuitry in mouse hippocampus. *Exp Neurol* 273**,** 273-287.

Hu, Y., Lund, I.V., Gravielle, M.C., Farb, D.H., Brooks-Kayal, A.R., and Russek, S.J. (2008). Surface expression of GABAA receptors is transcriptionally controlled by the interplay of cAMP-response element-binding protein and its binding partner inducible cAMP early repressor. *J Biol Chem* 283**,** 9328-9340.

Huang, X., Zhang, H., Yang, J., Wu, J., Mcmahon, J., Lin, Y., Cao, Z., Gruenthal, M., and Huang, Y. (2010). Pharmacological inhibition of the mammalian target of rapamycin pathway suppresses acquired epilepsy. *Neurobiol Dis* 40**,** 193-199.

Hudak, A.M., Trivedi, K., Harper, C.R., Booker, K., Caesar, R.R., Agostini, M., Van Ness, P.C., and Diaz-Arrastia, R. (2004). Evaluation of seizure-like episodes in survivors of moderate and severe traumatic brain injury. *J Head Trauma Rehabil* 19**,** 290-295.

Hughes, J.T. (1988). The Edwin Smith Surgical Papyrus: an analysis of the first case reports of spinal cord injuries. *Spinal Cord* 26**,** 71-82.

Hunt, R.F., and Baraban, S.C. (2015). Interneuron Transplantation as a Treatment for Epilepsy. *Cold Spring Harb Perspect Med* 5.

Hunt, R.F., Boychuk, J.A., and Smith, B.N. (2013a). Neural circuit mechanisms of post-traumatic epilepsy. *Front Cell Neurosci* 7**,** 89.

Hunt, R.F., Girskis, K.M., Rubenstein, J.L., Alvarez-Buylla, A., and Baraban, S.C. (2013b). GABA progenitors grafted into the adult epileptic brain control seizures and abnormal behavior. *Nat Neurosci* 16**,** 692-697.

Hunt, R.F., Haselhorst, L.A., Schoch, K.M., Bach, E.C., Rios-Pilier, J., Scheff, S.W., Saatman, K.E., and Smith, B.N. (2012). Posttraumatic mossy fiber sprouting is related to the degree of cortical damage in three mouse strains. *Epilepsy Res* 99**,** 167-170.

Hunt, R.F., Scheff, S.W., and Smith, B.N. (2009). Posttraumatic epilepsy after controlled cortical impact injury in mice. *Exp Neurol* 215**,** 243-252.

Hunt, R.F., Scheff, S.W., and Smith, B.N. (2010). Regionally localized recurrent excitation in the dentate gyrus of a cortical contusion model of posttraumatic epilepsy. *J Neurophysiol* 103**,** 1490-1500.

Hunt, R.F., Scheff, S.W., and Smith, B.N. (2011). Synaptic reorganization of inhibitory hilar interneuron circuitry after traumatic brain injury in mice. *J Neurosci* 31**,** 6880-6890.

Jensen, F.E. (2011). Epilepsy as a spectrum disorder: implications from novel clinical and basic neuroscience. *Epilepsia* 52**,** 1-6.

Jin, X., Huguenard, J.R., and Prince, D.A. (2011). Reorganization of inhibitory synaptic circuits in rodent chronically injured epileptogenic neocortex. *Cereb Cortex* 21**,** 1094-1104.

Katona, I., Acsady, L., and Freund, T.F. (1999). Postsynaptic targets of somatostatin-immunoreactive interneurons in the rat hippocampus. *Neuroscience* 88**,** 37-55.

Kelly, K.M., Miller, E.R., Lepsveridze, E., Kharlamov, E.A., and Mchedlishvili, Z. (2015). Posttraumatic seizures and epilepsy in adult rats after controlled cortical impact. *Epilepsy Res* 117**,** 104-116.

Kempermann, G., Jessberger, S., Steiner, B., and Kronenberg, G. (2004). Milestones of neuronal development in the adult hippocampus. *Trends Neurosci* 27**,** 447-452.

Kharatishvili, I., Nissinen, J., Mcintosh, T., and Pitkänen, A. (2006). A model of posttraumatic epilepsy induced by lateral fluid-percussion brain injury in rats. *Neuroscience* 140**,** 685-697.

Kim, J.E., Choi, H.C., Song, H.K., Jo, S.M., Kim, D.S., Choi, S.Y., Kim, Y.I., and Kang, T.C. (2010). Levetiracetam inhibits interleukin-1 beta inflammatory responses in the hippocampus and piriform cortex of epileptic rats. *Neurosci Lett* 471**,** 94-99.

Kline, A.E., Bolinger, B.D., Kochanek, P.M., Carlos, T.M., Yan, H.Q., Jenkins, L.W., Marion, D.W., and Dixon, C.E. (2002). Acute systemic administration of interleukin-10 suppresses the beneficial effects of moderate hypothermia following traumatic brain injury in rats. *Brain Res* 937**,** 22-31.

Kneisler, T.B., and Dingledine, R. (1995). Synaptic input from CA3 pyramidal cells to dentate basket cells in rat hippocampus. *J Physiol* 487 (Pt 1)**,** 125-146.

Knoblach, S.M., and Faden, A.I. (2002). Administration of either anti-intercellular adhesion molecule-1 or a nonspecific control antibody improves recovery after traumatic brain injury in the rat. *J Neurotrauma* 19**,** 1039-1050.

Kobayashi, M., and Buckmaster, P.S. (2003). Reduced inhibition of dentate granule cells in a model of temporal lobe epilepsy. *J Neurosci* 23**,** 2440-2452.

Kron, M.M., Zhang, H., and Parent, J.M. (2010). The developmental stage of dentate granule cells dictates their contribution to seizure-induced plasticity. *J Neurosci* 30**,** 2051-2059.

Lasarge, C.L., Santos, V.R., and Danzer, S.C. (2015). PTEN deletion from adult-generated dentate granule cells disrupts granule cell mossy fiber axon structure. *Neurobiology of Disease*.

Lehmann, T.N., Gabriel, S., Kovacs, R., Eilers, A., Kivi, A., Schulze, K., Lanksch, W.R., Meencke, H.J., and Heinemann, U. (2000). Alterations of neuronal connectivity in area CA1 of hippocampal slices from temporal lobe epilepsy patients and from pilocarpine-treated epileptic rats. *Epilepsia* 41 Suppl 6**,** S190-194.

Lighthall, J.W. (1988). Controlled cortical impact: a new experimental brain injury model. *J Neurotrauma* 5**,** 1-15.

Liu, G., Gu, B., He, X.P., Joshi, R.B., Wackerle, H.D., Rodriguiz, R.M., Wetsel, W.C., and Mcnamara, J.O. (2013). Transient inhibition of TrkB kinase after status epilepticus prevents development of temporal lobe epilepsy. *Neuron* 79**,** 31-38.

Liu, J., Solway, K., Messing, R.O., and Sharp, F.R. (1998). Increased neurogenesis in the dentate gyrus after transient global ischemia in gerbils. *J Neurosci* 18**,** 7768-7778.

Longo, B.M., and Mello, L.E. (1997). Blockade of pilocarpine- or kainate-induced mossy fiber sprouting by cycloheximide does not prevent subsequent epileptogenesis in rats. *Neurosci Lett* 226**,** 163-166.

Loscher, W., Honack, D., and Rundfeldt, C. (1998). Antiepileptogenic effects of the novel anticonvulsant levetiracetam (ucb L059) in the kindling model of temporal lobe epilepsy. *J Pharmacol Exp Ther* 284**,** 474-479.

Löscher, W., and Schmidt, D. (2006). Experimental and clinical evidence for loss of effect (tolerance) during prolonged treatment with antiepileptic drugs. *Epilepsia* 47**,** 1253-1284.

Lothman, E.W., Bertram, E.H., 3rd, and Stringer, J.L. (1991). Functional anatomy of hippocampal seizures. *Prog Neurobiol* 37**,** 1-82.

Lowenstein, D.H., Thomas, M.J., Smith, D.H., and Mcintosh, T.K. (1992). Selective vulnerability of dentate hilar neurons following traumatic brain injury: a potential mechanistic link between head trauma and disorders of the hippocampus. *J Neurosci* 12**,** 4846-4853.

Lu, D., Mahmood, A., Qu, C., Goussev, A., Schallert, T., and Chopp, M. (2005). Erythropoietin enhances neurogenesis and restores spatial memory in rats after traumatic brain injury. *J Neurotrauma* 22**,** 1011-1017.

Lu, D., Qu, C., Goussev, A., Jiang, H., Lu, C., Schallert, T., Mahmood, A., Chen, J., Li, Y., and Chopp, M. (2007). Statins increase neurogenesis in the dentate gyrus, reduce delayed neuronal death in the hippocampal CA3 region, and improve spatial learning in rat after traumatic brain injury. *J Neurotrauma* 24**,** 1132-1146.

Lucas, S.M., Rothwell, N.J., and Gibson, R.M. (2006). The role of inflammation in CNS injury and disease. *Br J Pharmacol* 147 Suppl 1**,** S232-240.

Lund, I.V., Hu, Y., Raol, Y.H., Benham, R.S., Faris, R., Russek, S.J., and Brooks-Kayal, A.R. (2008). BDNF selectively regulates GABAA receptor transcription by activation of the JAK/STAT pathway. *Sci Signal* 1**,** ra9.

Lynch, M., and Sutula, T. (2000). Recurrent excitatory connectivity in the dentate gyrus of kindled and kainic acid-treated rats. *J Neurophysiol* 83**,** 693-704.

Magiorkinis, E., Diamantis, A., Sidiropoulou, K., and Panteliadis, C. (2014). Highights in the history of epilepsy: the last 200 years. *Epilepsy Res Treat* 2014**,** 582039.

Magiorkinis, E., Sidiropoulou, K., and Diamantis, A. (2010). Hallmarks in the history of epilepsy: epilepsy in antiquity. *Epilepsy & Behavior* 17**,** 103-108.

Magnuson, B., Ekim, B., and Fingar, D.C. (2012). Regulation and function of ribosomal protein S6 kinase (S6K) within mTOR signalling networks. *Biochem J* 441**,** 1-21.

Manaka, S. (1992). Cooperative prospective study on posttraumatic epilepsy: risk factors and the effect of prophylactic anticonvulsant. *Jpn J Psychiatry Neurol* 46**,** 311-315.

Marion, D.W., Penrod, L.E., Kelsey, S.F., Obrist, W.D., Kochanek, P.M., Palmer, A.M., Wisniewski, S.R., and Dekosky, S.T. (1997). Treatment of traumatic brain injury with moderate hypothermia. *N Engl J Med* 336**,** 540-546.

Matveeva, E.A., Vanaman, T.C., Whiteheart, S.W., and Slevin, J.T. (2008). Levetiracetam prevents kindling-induced asymmetric accumulation of hippocampal 7S SNARE complexes. *Epilepsia* 49**,** 1749-1758.

Maxwell, W.L., Dhillon, K., Harper, L., Espin, J., Macintosh, T.K., Smith, D.H., and Graham, D.I. (2003). There is differential loss of pyramidal cells from the human

hippocampus with survival after blunt head injury. *J Neuropathol Exp Neurol* 62**,** 272-279.

Mazzeo, A.T., Beat, A., Singh, A., and Bullock, M.R. (2009). The role of mitochondrial transition pore, and its modulation, in traumatic brain injury and delayed neurodegeneration after TBI. *Exp Neurol* 218**,** 363-370.

Mcclain, C.J., Cohen, D., Ott, L., Dinarello, C.A., and Young, B. (1987). Ventricular fluid interleukin-1 activity in patients with head injury. *The Journal of laboratory and clinical medicine* 110**,** 48-54.

Mcclain, C.J., Twyman, D.L., Ott, L.G., Rapp, R.P., Tibbs, P.A., Norton, J.A., Kasarskis, E.J., Dempsey, R.J., and Young, B. (1986). Serum and urine zinc response in head-injured patients. *Journal of neurosurgery* 64**,** 224-230.

Mccormick, D.A., and Contreras, D. (2001). On the cellular and network bases of epileptic seizures. *Annu Rev Physiol* 63**,** 815-846.

Mcintosh, T.K., Noble, L., Andrews, B., and Faden, A.I. (1987). Traumatic brain injury in the rat: characterization of a midline fluid-percussion model. *Cent Nerv Syst Trauma* 4**,** 119-134.

Mcintosh, T.K., Vink, R., Noble, L., Yamakami, I., Fernyak, S., Soares, H., and Faden, A.L. (1989). Traumatic brain injury in the rat: characterization of a lateral fluid-percussion model. *Neuroscience* 28**,** 233-244.

Mcqueen, J.K., Blackwood, D.H., Harris, P., Kalbag, R.M., and Johnson, A.L. (1983). Low risk of late post-traumatic seizures following severe head injury: implications for clinical trials of prophylaxis. *J Neurol Neurosurg Psychiatry* 46**,** 899-904.

Ming, G.L., and Song, H. (2005). Adult neurogenesis in the mammalian central nervous system. *Annu Rev Neurosci* 28**,** 223-250.

Mody, I. (2001). Distinguishing between GABA(A) receptors responsible for tonic and phasic conductances. *Neurochem Res* 26**,** 907-913.

Mody, I., Kohr, G., Otis, T.S., and Staley, K.J. (1992a). The electrophysiology of dentate gyrus granule cells in whole-cell recordings. *Epilepsy Res Suppl* 7**,** 159-168.

Mody, I., Otis, T.S., Staley, K., and Köhr, G. (1992b). "The balance between excitation and inhibition in dentate granule cells and its role in epilepsy. In: Molecular neurobiology of epilepsy," in *Molecular neurobiology of epilepsy*. Epilepsy− Res.− Suppl.), 331-339.

Mody, I., and Pearce, R.A. (2004). Diversity of inhibitory neurotransmission through GABA(A) receptors. *Trends Neurosci* 27**,** 569-575.

Molnar, P., and Nadler, J.V. (1999). Mossy fiber-granule cell synapses in the normal and epileptic rat dentate gyrus studied with minimal laser photostimulation. *J Neurophysiol* 82**,** 1883-1894.

Morganti-Kossmann, M.C., Rancan, M., Otto, V.I., Stahel, P.F., and Kossmann, T. (2001). Role of cerebral inflammation after traumatic brain injury: a revisited concept. *Shock* 16**,** 165-177.

Moss, S.J., Doherty, C.A., and Huganir, R.L. (1992a). Identification of the cAMP-dependent protein kinase and protein kinase C phosphorylation sites within the major intracellular domains of the beta 1, gamma 2S, and gamma 2L subunits of the gamma-aminobutyric acid type A receptor. *J Biol Chem* 267**,** 14470-14476.

Moss, S.J., Smart, T.G., Blackstone, C.D., and Huganir, R.L. (1992b). Functional modulation of GABAA receptors by cAMP-dependent protein phosphorylation. *Science* 257**,** 661-665.

Mtchedlishvili, Z., and Kapur, J. (2006). High-affinity, slowly desensitizing GABAA receptors mediate tonic inhibition in hippocampal dentate granule cells. *Mol Pharmacol* 69**,** 564-575.

Mtchedlishvili, Z., Lepsveridze, E., Xu, H., Kharlamov, E.A., Lu, B., and Kelly, K.M. (2010). Increase of GABA A receptor-mediated tonic inhibition in dentate granule cells after traumatic brain injury. *Neurobiology of disease* 38**,** 464-475.

Muller-Schwarze, A.B., Tandon, P., Liu, Z., Yang, Y., Holmes, G.L., and Stafstrom, C.E. (1999). Ketogenic diet reduces spontaneous seizures and mossy fiber sprouting in the kainic acid model. *Neuroreport* 10**,** 1517-1522.

Nadler, J.V. (2003). The recurrent mossy fiber pathway of the epileptic brain. *Neurochem Res* 28**,** 1649-1658.

Nadler, J.V., Perry, B.W., and Cotman, C.W. (1980). Selective reinnervation of hippocampal area CA1 and the fascia dentata after destruction of CA3-CA4 afferents with kainic acid. *Brain Res* 182**,** 1-9.

Nadler, J.V., Perry, B.W., Gentry, C., and Cotman, C.W. (1981). Fate of the hippocampal mossy fiber projection after destruction of its postsynaptic targets with intraventricular kainic acid. *J Comp Neurol* 196**,** 549-569.

Nave, B.T., Ouwens, M., Withers, D.J., Alessi, D.R., and Shepherd, P.R. (1999). Mammalian target of rapamycin is a direct target for protein kinase B: identification of a convergence point for opposing effects of insulin and amino-acid deficiency on protein translation. *Biochem J* 344 Pt 2**,** 427-431.

Nelson, K.B., and Ellenberg, J.H. (1976). Predictors of epilepsy in children who have experienced febrile seizures. *N Engl J Med* 295**,** 1029-1033.

Newcomb, J.K., Kampfl, A., Posmantur, R.M., Zhao, X., Pike, B.R., Liu, S.J., Clifton, G.L., and Hayes, R.L. (1997). Immunohistochemical study of calpain-mediated breakdown products to alpha-spectrin following controlled cortical impact injury in the rat. *J Neurotrauma* 14**,** 369-383.

Nusser, Z., Sieghart, W., and Somogyi, P. (1998). Segregation of different GABAA receptors to synaptic and extrasynaptic membranes of cerebellar granule cells. *J Neurosci* 18**,** 1693-1703.

O'reilly, K.E., Rojo, F., She, Q.B., Solit, D., Mills, G.B., Smith, D., Lane, H., Hofmann, F., Hicklin, D.J., Ludwig, D.L., Baselga, J., and Rosen, N. (2006). mTOR inhibition induces upstream receptor tyrosine kinase signaling and activates Akt. *Cancer Res* 66**,** 1500-1508.

Oliva, A.A., Jr., Jiang, M., Lam, T., Smith, K.L., and Swann, J.W. (2000). Novel hippocampal interneuronal subtypes identified using transgenic mice that express green fluorescent protein in GABAergic interneurons. *J Neurosci* 20**,** 3354-3368.

Oliveira, A.A., Almeida, J.P., Freitas, R.M., Nascimento, V.S., Aguiar, L.M., Junior, H.V., Fonseca, F.N., Viana, G.S., Sousa, F.C., and Fonteles, M.M. (2007). Effects of levetiracetam in lipid peroxidation level, nitrite-nitrate formation and antioxidant enzymatic activity in mice brain after pilocarpine-induced seizures. *Cell Mol Neurobiol* 27**,** 395-406.

Pacifici, R., Paris, L., Di Carlo, S., Bacosi, A., Pichini, S., and Zuccaro, P. (1995). Cytokine production in blood mononuclear cells from epileptic patients. *Epilepsia* 36**,** 384-387.

Paradiso, B., Zucchini, S., Su, T., Bovolenta, R., Berto, E., Marconi, P., Marzola, A., Navarro Mora, G., Fabene, P.F., and Simonato, M. (2011). Localized overexpression of FGF-2 and BDNF in hippocampus reduces mossy fiber sprouting and spontaneous seizures up to 4 weeks after pilocarpine-induced status epilepticus. *Epilepsia* 52**,** 572-578.

Parent, J.M., Elliott, R.C., Pleasure, S.J., Barbaro, N.M., and Lowenstein, D.H. (2006). Aberrant seizure-induced neurogenesis in experimental temporal lobe epilepsy. *Ann Neurol* 59**,** 81-91.

Parent, J.M., Janumpalli, S., Mcnamara, J.O., and Lowenstein, D.H. (1998). Increased dentate granule cell neurogenesis following amygdala kindling in the adult rat. *Neurosci Lett* 247**,** 9-12.

Parent, J.M., and Lowenstein, D.H. (1997). Mossy fiber reorganization in the epileptic hippocampus. *Curr Opin Neurol* 10**,** 103-109.

Parent, J.M., Yu, T.W., Leibowitz, R.T., Geschwind, D.H., Sloviter, R.S., and Lowenstein, D.H. (1997). Dentate granule cell neurogenesis is increased by seizures and contributes to aberrant network reorganization in the adult rat hippocampus. *J Neurosci* 17**,** 3727-3738.

Patrylo, P.R., and Dudek, F.E. (1998). Physiological unmasking of new glutamatergic pathways in the dentate gyrus of hippocampal slices from kainate-induced epileptic rats. *J Neurophysiol* 79**,** 418-429.

Pavlov, I., Huusko, N., Drexel, M., Kirchmair, E., Sperk, G., Pitkänen, A., and Walker, M. (2011). Progressive loss of phasic, but not tonic, GABA A receptor-mediated inhibition in dentate granule cells in a model of post-traumatic epilepsy in rats. *Neuroscience* 194**,** 208-219.

Paxinos, G., and Franklin, K.B.J. (2001). *The mouse brain in stereotaxic coordinates 2nd edition.* Academic press.

Pearce, P.S., Friedman, D., Lafrancois, J.J., Iyengar, S.S., Fenton, A.A., Maclusky, N.J., and Scharfman, H.E. (2014). Spike-wave discharges in adult Sprague-Dawley rats and their implications for animal models of temporal lobe epilepsy. *Epilepsy Behav* 32**,** 121-131.

Peng, Z., Huang, C.S., Stell, B.M., Mody, I., and Houser, C.R. (2004). Altered expression of the delta subunit of the GABAA receptor in a mouse model of temporal lobe epilepsy. *J Neurosci* 24**,** 8629-8639.

Peng, Z., Zhang, N., Wei, W., Huang, C.S., Cetina, Y., Otis, T.S., and Houser, C.R. (2013). A reorganized GABAergic circuit in a model of epilepsy: evidence from optogenetic labeling and stimulation of somatostatin interneurons. *J Neurosci* 33**,** 14392-14405.

Penry, J.K., and Newmark, M.E. (1979). The use of antiepileptic drugs. *Ann Intern Med* 90**,** 207-218.

Perez, Y., Morin, F., Beaulieu, C., and Lacaille, J.C. (1996). Axonal sprouting of CA1 pyramidal cells in hyperexcitable hippocampal slices of kainate-treated rats. *Eur J Neurosci* 8**,** 736-748.

Pierce, J.E., Smith, D.H., Trojanowski, J.Q., and Mcintosh, T.K. (1998). Enduring cognitive, neurobehavioral and histopathological changes persist for up to one year following severe experimental brain injury in rats. *Neuroscience* 87**,** 359-369.

Pitkanen, A., Nissinen, J., Jolkkonen, E., Tuunanen, J., and Halonen, T. (1999). Effects of vigabatrin treatment on status epilepticus-induced neuronal damage and mossy fiber sprouting in the rat hippocampus. *Epilepsy Res* 33**,** 67-85.

Pleasant, J.M., Carlson, S.W., Mao, H., Scheff, S.W., Yang, K.H., and Saatman, K.E. (2011). Rate of neurodegeneration in the mouse controlled cortical impact model is influenced by impactor tip shape: implications for mechanistic and therapeutic studies. *J Neurotrauma* 28**,** 2245-2262.

Plum, L., Schubert, M., and Bruning, J.C. (2005). The role of insulin receptor signaling in the brain. *Trends Endocrinol Metab* 16**,** 59-65.

Popek, K., and Musil, F. (1969). [Clinical attempt to prevent post-traumatic epilepsy following severe brain injuries in adults]. *Cas Lek Cesk* 108**,** 133-147.

Porter, N.M., Twyman, R.E., Uhler, M.D., and Macdonald, R.L. (1990). Cyclic AMP-dependent protein kinase decreases GABAA receptor current in mouse spinal neurons. *Neuron* 5**,** 789-796.

Pun, R.Y., Rolle, I.J., Lasarge, C.L., Hosford, B.E., Rosen, J.M., Uhl, J.D., Schmeltzer, S.N., Faulkner, C., Bronson, S.L., Murphy, B.L., Richards, D.A., Holland, K.D., and Danzer, S.C. (2012). Excessive activation of mTOR in postnatally generated granule cells is sufficient to cause epilepsy. *Neuron* 75**,** 1022-1034.

Racine, R.J. (1972). Modification of seizure activity by electrical stimulation. II. Motor seizure. *Electroencephalogr Clin Neurophysiol* 32**,** 281-294.

Raible, D.J., Frey, L.C., Cruz Del Angel, Y., Russek, S.J., and Brooks-Kayal, A.R. (2012). GABA(A) receptor regulation after experimental traumatic brain injury. *J Neurotrauma* 29**,** 2548-2554.

Raible, D.J., Frey, L.C., Del Angel, Y.C., Carlsen, J., Hund, D., Russek, S.J., Smith, B., and Brooks-Kayal, A.R. (2015). JAK/STAT pathway regulation of GABAA receptor expression after differing severities of experimental TBI. *Exp Neurol* 271**,** 445-456.

Raichle, M.E., and Gusnard, D.A. (2002). Appraising the brain's energy budget. *Proc Natl Acad Sci U S A* 99**,** 10237-10239.

Raol, Y.H., Lund, I.V., Bandyopadhyay, S., Zhang, G., Roberts, D.S., Wolfe, J.H., Russek, S.J., and Brooks-Kayal, A.R. (2006). Enhancing GABA(A) receptor alpha 1 subunit levels in hippocampal dentate gyrus inhibits epilepsy development in an animal model of temporal lobe epilepsy. *J Neurosci* 26**,** 11342-11346.

Rashid, K., Van Der Zee, C.E., Ross, G.M., Chapman, C.A., Stanisz, J., Riopelle, R.J., Racine, R.J., and Fahnestock, M. (1995). A nerve growth factor peptide retards seizure development and inhibits neuronal sprouting in a rat model of epilepsy. *Proc Natl Acad Sci U S A* 92**,** 9495-9499.

Rikani, A.A., Choudhry, Z., Choudhry, A.M., Zenonos, G., Tariq, S., and Mobassarah, N.J. (2013). Spatially regulated adult neurogenesis. *Ann Neurosci* 20**,** 67-70.

Rink, A., Fung, K.M., Trojanowski, J.Q., Lee, V.M., Neugebauer, E., and Mcintosh, T.K. (1995). Evidence of apoptotic cell death after experimental traumatic brain injury in the rat. *Am J Pathol* 147**,** 1575-1583.

Roberts, D.S., Raol, Y.H., Bandyopadhyay, S., Lund, I.V., Budreck, E.C., Passini, M.A., Wolfe, J.H., Brooks-Kayal, A.R., and Russek, S.J. (2005). Egr3 stimulation of GABRA4 promoter activity as a mechanism for seizure-induced up-regulation of GABA(A) receptor alpha4 subunit expression. *Proc Natl Acad Sci U S A* 102**,** 11894-11899.

Robertson, C.S., Clifton, G.L., and Grossman, R.G. (1984). Oxygen utilization and cardiovascular function in head-injured patients. *Neurosurgery* 15**,** 307-314.

Rodgers, K.M., Dudek, F.E., and Barth, D.S. (2015). Progressive, Seizure-Like, Spike-Wave Discharges Are Common in Both Injured and Uninjured Sprague-Dawley Rats: Implications for the Fluid Percussion Injury Model of Post-Traumatic Epilepsy. *J Neurosci* 35**,** 9194-9204.

Rola, R., Mizumatsu, S., Otsuka, S., Morhardt, D.R., Noble-Haeusslein, L.J., Fishman, K., Potts, M.B., and Fike, J.R. (2006). Alterations in hippocampal neurogenesis following traumatic brain injury in mice. *Exp Neurol* 202**,** 189-199.

Rossi, D.J., and Hamann, M. (1998). Spillover-mediated transmission at inhibitory synapses promoted by high affinity alpha6 subunit GABA(A) receptors and glomerular geometry. *Neuron* 20**,** 783-795.

Saatman, K.E., Contreras, P.C., Smith, D.H., Raghupathi, R., Mcdermott, K.L., Fernandez, S.C., Sanderson, K.L., Voddi, M., and Mcintosh, T.K. (1997). Insulin-like growth factor-1 (IGF-1) improves both neurological motor and cognitive outcome following experimental brain injury. *Exp Neurol* 147**,** 418-427.

Saatman, K.E., Feeko, K.J., Pape, R.L., and Raghupathi, R. (2006). Differential behavioral and histopathological responses to graded cortical impact injury in mice. *J Neurotrauma* 23**,** 1241-1253.

Saatman, K.E., Graham, D.I., and Mcintosh, T.K. (1998). The neuronal cytoskeleton is at risk after mild and moderate brain injury. *J Neurotrauma* 15**,** 1047-1058.

Santhakumar, V., Bender, R., Frotscher, M., Ross, S.T., Hollrigel, G.S., Toth, Z., and Soltesz, I. (2000). Granule cell hyperexcitability in the early post-traumatic rat dentate gyrus: the 'irritable mossy cell' hypothesis. *J Physiol* 524 Pt 1**,** 117-134.

Scharfman, H.E. (1993). Activation of dentate hilar neurons by stimulation of the fimbria in rat hippocampal slices. *Neurosci Lett* 156**,** 61-66.

Scharfman, H.E. (1994). Evidence from simultaneous intracellular recordings in rat hippocampal slices that area CA3 pyramidal cells innervate dentate hilar mossy cells. *J Neurophysiol* 72**,** 2167-2180.

Scharfman, H.E. (2007). The CA3 "backprojection" to the dentate gyrus. *Prog Brain Res* 163**,** 627-637.

Scheff, S.W., Baldwin, S.A., Brown, R.W., and Kraemer, P.J. (1997). Morris water maze deficits in rats following traumatic brain injury: lateral controlled cortical impact. *J Neurotrauma* 14**,** 615-627.

Schmued, L.C., and Hopkins, K.J. (2000). Fluoro-Jade B: a high affinity fluorescent marker for the localization of neuronal degeneration. *Brain Res* 874**,** 123-130.

Semah, F., Picot, M.-C., Adam, C., Broglin, D., Arzimanoglou, A., Bazin, B., Cavalcanti, D., and Baulac, M. (1998). Is the underlying cause of epilepsy a major prognostic factor for recurrence? *Neurology* 51**,** 1256-1262.

Semyanov, A., Walker, M.C., Kullmann, D.M., and Silver, R.A. (2004). Tonically active GABA A receptors: modulating gain and maintaining the tone. *Trends Neurosci* 27**,** 262-269.

Sengupta, S., Peterson, T.R., and Sabatini, D.M. (2010). Regulation of the mTOR complex 1 pathway by nutrients, growth factors, and stress. *Mol Cell* 40**,** 310-322.

Seri, B., Garcia-Verdugo, J.M., Collado-Morente, L., Mcewen, B.S., and Alvarez-Buylla, A. (2004). Cell types, lineage, and architecture of the germinal zone in the adult dentate gyrus. *J Comp Neurol* 478**,** 359-378.

Shao, L.R., and Dudek, F.E. (2005). Changes in mIPSCs and sIPSCs after kainate treatment: evidence for loss of inhibitory input to dentate granule cells and possible compensatory responses. *J Neurophysiol* 94**,** 952-960.

Shetty, A.K. (2013). Prospects of levetiracetam as a neuroprotective drug against status epilepticus, traumatic brain injury, and stroke. *Front Neurol* 4**,** 172.

Shibley, H., and Smith, B.N. (2002). Pilocarpine-induced status epilepticus results in mossy fiber sprouting and spontaneous seizures in C57BL/6 and CD-1 mice. *Epilepsy Res* 49**,** 109-120.

Sidiropoulou, K., Diamantis, A., and Magiorkinis, E. (2010). Hallmarks in 18th- and 19th-century epilepsy research. *Epilepsy Behav* 18**,** 151-161.

Smith, B.N., and Dudek, F.E. (1997). Enhanced population responses in the basolateral amygdala of kainate-treated, epileptic rats in vitro. *Neurosci Lett* 222**,** 1-4.

Smith, B.N., and Dudek, F.E. (2001). Short- and long-term changes in CA1 network excitability after kainate treatment in rats. *J Neurophysiol* 85**,** 1-9.

Smith, B.N., and Dudek, F.E. (2002). Network interactions mediated by new excitatory connections between CA1 pyramidal cells in rats with kainate-induced epilepsy. *J Neurophysiol* 87**,** 1655-1658.

Smith, D.H., Soares, H.D., Pierce, J.S., Perlman, K.G., Saatman, K.E., Meaney, D.F., Dixon, C.E., and Mcintosh, T.K. (1995). A model of parasagittal controlled cortical impact in the mouse: cognitive and histopathologic effects. *J Neurotrauma* 12**,** 169-178.

Sokoloff, L. (1999). Energetics of functional activation in neural tissues. *Neurochem Res* 24**,** 321-329.

Sokoloff, L., Mangold, R., Wechsler, R.L., Kenney, C., and Kety, S.S. (1955). The effect of mental arithmetic on cerebral circulation and metabolism. *J Clin Invest* 34**,** 1101-1108.

Staley, K.J., and Mody, I. (1992). Shunting of excitatory input to dentate gyrus granule cells by a depolarizing GABAA receptor-mediated postsynaptic conductance. *J Neurophysiol* 68**,** 197-212.

Staley, K.J., Otis, T.S., and Mody, I. (1992). Membrane properties of dentate gyrus granule cells: comparison of sharp microelectrode and whole-cell recordings. *J Neurophysiol* 67**,** 1346-1358.

Stalhammar, D., Galinat, B.J., Allen, A.M., Becker, D.P., Stonnington, H.H., and Hayes, R.L. (1987). A new model of concussive brain injury in the cat produced by extradural fluid volume loading: I. Biomechanical properties. *Brain Inj* 1**,** 73-91.

Statler, K.D., Alexander, H., Vagni, V., Holubkov, R., Dixon, C.E., Clark, R.S., Jenkins, L., and Kochanek, P.M. (2006). Isoflurane exerts neuroprotective actions at or near the time of severe traumatic brain injury. *Brain Res* 1076**,** 216-224.

Statler, K.D., Scheerlinck, P., Pouliot, W., Hamilton, M., White, H.S., and Dudek, F.E. (2009). A potential model of pediatric posttraumatic epilepsy. *Epilepsy Res* 86**,** 221-223.

Staubli, U., Gall, C., and Lynch, G. (1984). The distribution of the commissural-associational afferents of the dentate gyrus after perforant path lesions in one-day-old rats. *Brain Res* 292**,** 156-159.

Steward, O. (1992). Lesion-induced synapse reorganization in the hippocampus of cats: sprouting of entorhinal, commissural/associational, and mossy fiber projections after unilateral entorhinal cortex lesions, with comments on the normal organization of these pathways. *Hippocampus* 2**,** 247-268.

Steward, O., Cotman, C., and Lynch, G. (1976). A quantitative autoradiographic and electrophysiological study of the reinnervation of the dentate gyrus by the contralateral entorhinal cortex following ipsilateral entorhinal lesions. *Brain Res* 114**,** 181-200.

Steward, O., Cotman, C.W., and Lynch, G.S. (1973). Re-establishment of electrophysiologically functional entorhinal cortical input to the dentate gyrus deafferented by ipsilateral entorhinal lesions: innervation by the contralateral entorhinal cortex. *Exp Brain Res* 18**,** 396-414.

Steward, O., Cotman, C.W., and Lynch, G.S. (1974). Growth of a new fiber projection in the brain of adult rats: Re-innervation of the dentate gyrus by the contralateral entorhinal cortex following ipsilateral entorhinal lesions. *Exp Brain Res* 20**,** 45-66.

Steward, O., and Messenheimer, J.A. (1978). Histochemical evidence for a post-lesion reorganization of cholinergic afferents in the hippocampal formation of the mature cat. *J Comp Neurol* 178**,** 697-709.

Sugaya, Y., Maru, E., Kudo, K., Shibasaki, T., and Kato, N. (2010). Levetiracetam suppresses development of spontaneous EEG seizures and aberrant neurogenesis following kainate-induced status epilepticus. *Brain Res* 1352**,** 187-199.

Suh, H., Deng, W., and Gage, F.H. (2009). Signaling in adult neurogenesis. *Annu Rev Cell Dev Biol* 25**,** 253-275.

Sun, D., Bullock, M.R., Mcginn, M.J., Zhou, Z., Altememi, N., Hagood, S., Hamm, R., and Colello, R.J. (2009). Basic fibroblast growth factor-enhanced neurogenesis contributes to cognitive recovery in rats following traumatic brain injury. *Exp Neurol* 216**,** 56-65.

Sunnen, C.N., Brewster, A.L., Lugo, J.N., Vanegas, F., Turcios, E., Mukhi, S., Parghi, D., D'arcangelo, G., and Anderson, A.E. (2011). Inhibition of the mammalian target of rapamycin blocks epilepsy progression in NS-Pten conditional knockout mice. *Epilepsia* 52**,** 2065-2075.

Surges, R., Volynski, K.E., and Walker, M.C. (2008). Is levetiracetam different from other antiepileptic drugs? Levetiracetam and its cellular mechanism of action in epilepsy revisited. *Ther Adv Neurol Disord* 1**,** 13-24.

Sutula, T., Cascino, G., Cavazos, J., Parada, I., and Ramirez, L. (1989). Mossy fiber synaptic reorganization in the epileptic human temporal lobe. *Ann Neurol* 26**,** 321-330.

Sutula, T., Koch, J., Golarai, G., Watanabe, Y., and Mcnamara, J.O. (1996). NMDA receptor dependence of kindling and mossy fiber sprouting: evidence that the

NMDA receptor regulates patterning of hippocampal circuits in the adult brain. *J Neurosci* 16**,** 7398-7406.

Sutula, T., Zhang, P., Lynch, M., Sayin, U., Golarai, G., and Rod, R. (1998). Synaptic and axonal remodeling of mossy fibers in the hilus and supragranular region of the dentate gyrus in kainate-treated rats. *J Comp Neurol* 390**,** 578-594.

Tabernero, J., Rojo, F., Calvo, E., Burris, H., Judson, I., Hazell, K., Martinelli, E., Ramon Y Cajal, S., Jones, S., Vidal, L., Shand, N., Macarulla, T., Ramos, F.J., Dimitrijevic, S., Zoellner, U., Tang, P., Stumm, M., Lane, H.A., Lebwohl, D., and Baselga, J. (2008). Dose- and schedule-dependent inhibition of the mammalian target of rapamycin pathway with everolimus: a phase I tumor pharmacodynamic study in patients with advanced solid tumors. *J Clin Oncol* 26**,** 1603-1610.

Taft, W.C., Yang, K., Dixon, C.E., Clifton, G.L., and Hayes, R.L. (1993). Hypothermia attenuates the loss of hippocampal microtubule-associated protein 2 (MAP2) following traumatic brain injury. *J Cereb Blood Flow Metab* 13**,** 796-802.

Tanaka, Y., Matsuwaki, T., Yamanouchi, K., and Nishihara, M. (2013). Increased lysosomal biogenesis in activated microglia and exacerbated neuronal damage after traumatic brain injury in progranulin-deficient mice. *Neuroscience* 250**,** 8-19.

Tauck, D., and Nadler, J. (1985). Evidence of functional mossy fiber sprouting in hippocampal formation of kainic acid-treated rats. *J Neurosci.* 5**,** 1016-1022.

Taylor, C.P. (1997). Mechanisms of action of gabapentin. *Rev Neurol (Paris)* 153 Suppl 1**,** S39-45.

Temkin, N.R. (2009). Preventing and treating posttraumatic seizures: the human experience. *Epilepsia* 50 Suppl 2**,** 10-13.

Temkin, N.R., Anderson, G.D., Winn, H.R., Ellenbogen, R.G., Britz, G.W., Schuster, J., Lucas, T., Newell, D.W., Mansfield, P.N., Machamer, J.E., Barber, J., and Dikmen, S.S. (2007). Magnesium sulfate for neuroprotection after traumatic brain injury: a randomised controlled trial. *Lancet Neurol* 6**,** 29-38.

Temkin, N.R., Corrigan, J.D., Dikmen, S.S., and Machamer, J. (2009). Social functioning after traumatic brain injury. *J Head Trauma Rehabil* 24**,** 460-467.

Temkin, N.R., Dikmen, S.S., Anderson, G.D., Wilensky, A.J., Holmes, M.D., Cohen, W., Newell, D.W., Nelson, P., Awan, A., and Winn, H.R. (1999). Valproate therapy for prevention of posttraumatic seizures: a randomized trial. *J Neurosurg* 91**,** 593-600.

Temkin, N.R., Dikmen, S.S., Wilensky, A.J., Keihm, J., Chabal, S., and Winn, H.R. (1990). A randomized, double-blind study of phenytoin for the prevention of post-traumatic seizures. *N Engl J Med* 323**,** 497-502.

Temkin, N.R., Dikmen, S.S., and Winn, H.R. (1998). Clinical trials for seizure prevention. *Adv Neurol* 76**,** 179-188.

Temkin, N.R., Haglund, M.M., and Winn, H.R. (1995). Causes, prevention, and treatment of post-traumatic epilepsy. *New Horiz* 3**,** 518-522.

Temkin, N.R., Jarell, A.D., and Anderson, G.D. (2001). Antiepileptogenic agents: how close are we? *Drugs* 61**,** 1045-1055.

Timm, F. (1958). [Histochemistry of zinc]. *Dtsch Z Gesamte Gerichtl Med* 47**,** 428-431.

Toth, Z., Hollrigel, G.S., Gorcs, T., and Soltesz, I. (1997). Instantaneous perturbation of dentate interneuronal networks by a pressure wave-transient delivered to the neocortex. *J Neurosci* 17**,** 8106-8117.

Van Der Zee, C.E., Rashid, K., Le, K., Moore, K.A., Stanisz, J., Diamond, J., Racine, R.J., and Fahnestock, M. (1995). Intraventricular administration of antibodies to nerve growth factor retards kindling and blocks mossy fiber sprouting in adult rats. *J Neurosci* 15**,** 5316-5323.

Van Praag, H., Schinder, A.F., Christie, B.R., Toni, N., Palmer, T.D., and Gage, F.H. (2002). Functional neurogenesis in the adult hippocampus. *Nature* 415**,** 1030-1034.

Villasana, L.E., Kim, K.N., Westbrook, G.L., and Schnell, E. (2015). Functional integration of adult-born hippocampal neurons after traumatic brain injury. *eneuro* 2**,** ENEURO. 0056-0015.2015.

Villasana, L.E., Westbrook, G.L., and Schnell, E. (2014). Neurologic impairment following closed head injury predicts post-traumatic neurogenesis. *Exp Neurol* 261**,** 156-162.

Wall, M.J., and Usowicz, M.M. (1997). Development of action potential-dependent and independent spontaneous GABAA receptor-mediated currents in granule cells of postnatal rat cerebellum. *Eur J Neurosci* 9**,** 533-548.

Wang, H., Gao, J., Lassiter, T.F., Mcdonagh, D.L., Sheng, H., Warner, D.S., Lynch, J.R., and Laskowitz, D.T. (2006). Levetiracetam is neuroprotective in murine models of closed head injury and subarachnoid hemorrhage. *Neurocrit Care* 5**,** 71-78.

Wang, H., Lynch, J.R., Song, P., Yang, H.J., Yates, R.B., Mace, B., Warner, D.S., Guyton, J.R., and Laskowitz, D.T. (2007). Simvastatin and atorvastatin improve behavioral outcome, reduce hippocampal degeneration, and improve cerebral blood flow after experimental traumatic brain injury. *Exp Neurol* 206**,** 59-69.

Wang, Q., Liu, L., Pei, L., Ju, W., Ahmadian, G., Lu, J., Wang, Y., Liu, F., and Wang, Y.T. (2003). Control of synaptic strength, a novel function of Akt. *Neuron* 38**,** 915-928.

Wei, W., Zhang, N., Peng, Z., Houser, C.R., and Mody, I. (2003). Perisynaptic localization of delta subunit-containing GABA(A) receptors and their activation by GABA spillover in the mouse dentate gyrus. *J Neurosci* 23**,** 10650-10661.

Werner, C., and Engelhard, K. (2007). Pathophysiology of traumatic brain injury. *British journal of anaesthesia* 99**,** 4-9.

Willner, P. (1984). The validity of animal models of depression. *Psychopharmacology (Berl)* 83**,** 1-16.

Winokur, R.S., Kubal, T., Liu, D., Davis, S.F., and Smith, B.N. (2004). Recurrent excitation in the dentate gyrus of a murine model of temporal lobe epilepsy. *Epilepsy Res* 58**,** 93-105.

Witgen, B.M., Lifshitz, J., Smith, M.L., Schwarzbach, E., Liang, S.L., Grady, M.S., and Cohen, A.S. (2005). Regional hippocampal alteration associated with cognitive deficit following experimental brain injury: a systems, network and cellular evaluation. *Neuroscience* 133**,** 1-15.

Wuarin, J.P., and Dudek, F.E. (1996). Electrographic seizures and new recurrent excitatory circuits in the dentate gyrus of hippocampal slices from kainate-treated epileptic rats. *J Neurosci* 16**,** 4438-4448.

Wuarin, J.P., and Dudek, F.E. (2001). Excitatory synaptic input to granule cells increases with time after kainate treatment. *J Neurophysiol* 85**,** 1067-1077.

Xiong, Y., Zhang, Y., Mahmood, A., Meng, Y., Zhang, Z.G., Morris, D.C., and Chopp, M. (2012). Neuroprotective and neurorestorative effects of thymosin beta4 treatment initiated 6 hours after traumatic brain injury in rats. *J Neurosurg* 116**,** 1081-1092.

Yakovlev, A.G., and Faden, A.I. (1995). Molecular biology of CNS injury. *J Neurotrauma* 12**,** 767-777.

Yamawaki, R., Thind, K., and Buckmaster, P.S. (2015). Blockade of excitatory synaptogenesis with proximal dendrites of dentate granule cells following rapamycin treatment in a mouse model of temporal lobe epilepsy. *Journal of Comparative Neurology* 523**,** 281-297.

Yan, H.D., Ji-Qun, C., Ishihara, K., Nagayama, T., Serikawa, T., and Sasa, M. (2005). Separation of antiepileptogenic and antiseizure effects of levetiracetam in the spontaneously epileptic rat (SER). *Epilepsia* 46**,** 1170-1177.

York Iii, G.K. (2005). The 'falling-down disease'–epilepsy first described in ancient Babylonia. *Neurology Today* 5**,** 33-34.

Young, A.B., Ott, L.G., Beard, D., Dempsey, R.J., Tibbs, P.A., and Mcclain, C.J. (1988). The acute-phase response of the brain-injured patient. *Journal of neurosurgery* 69**,** 375-380.

Young, B., Rapp, R.P., Norton, J.A., Haack, D., and Walsh, J.W. (1983). Failure of prophylactically administered phenytoin to prevent post-traumatic seizures in children. *Childs Brain* 10**,** 185-192.

Zacco, A., Togo, J., Spence, K., Ellis, A., Lloyd, D., Furlong, S., and Piser, T. (2003). 3-hydroxy-3-methylglutaryl coenzyme A reductase inhibitors protect cortical neurons from excitotoxicity. *J Neurosci* 23**,** 11104-11111.

Zeng, L.H., Rensing, N.R., and Wong, M. (2009). The mammalian target of rapamycin signaling pathway mediates epileptogenesis in a model of temporal lobe epilepsy. *J Neurosci* 29**,** 6964-6972.

Zeng, L.H., Xu, L., Gutmann, D.H., and Wong, M. (2008). Rapamycin prevents epilepsy in a mouse model of tuberous sclerosis complex. *Ann Neurol* 63**,** 444-453.

Zhan, R.Z., and Nadler, J.V. (2009). Enhanced tonic GABA current in normotopic and hilar ectopic dentate granule cells after pilocarpine-induced status epilepticus. *J Neurophysiol* 102**,** 670-681.

Zhang, N., and Houser, C.R. (1999). Ultrastructural localization of dynorphin in the dentate gyrus in human temporal lobe epilepsy: a study of reorganized mossy fiber synapses. *J Comp Neurol* 405**,** 472-490.

Zhang, N., Wei, W., Mody, I., and Houser, C.R. (2007). Altered localization of GABA(A) receptor subunits on dentate granule cell dendrites influences tonic and phasic inhibition in a mouse model of epilepsy. *J Neurosci* 27**,** 7520-7531.

Zhang, W., Huguenard, J.R., and Buckmaster, P.S. (2012). Increased excitatory synaptic input to granule cells from hilar and CA3 regions in a rat model of temporal lobe epilepsy. *J Neurosci* 32**,** 1183-1196.

Zhao, C., Deng, W., and Gage, F.H. (2008). Mechanisms and functional implications of adult neurogenesis. *Cell* 132**,** 645-660.

Zhu, X., Park, J., Golinski, J., Qiu, J., Khuman, J., Lee, C.C., Lo, E.H., Degterev, A., and Whalen, M.J. (2014). Role of Akt and mammalian target of rapamycin in functional outcome after concussive brain injury in mice. *J Cereb Blood Flow Metab* 34**,** 1531-1539.

Zipp, F., Nitsch, R., Soriano, E., and Frotscher, M. (1989). Entorhinal fibers form synaptic contacts on parvalbumin-immunoreactive neurons in the rat fascia dentata. *Brain Res* 495**,** 161-166.

Zou, H., Brayer, S.W., Hurwitz, M., Niyonkuru, C., Fowler, L.E., and Wagner, A.K. (2013). Neuroprotective, neuroplastic, and neurobehavioral effects of daily treatment with levetiracetam in experimental traumatic brain injury. *Neurorehabil Neural Repair* 27**,** 878-888.

Vita

Corwin R. Butler

Born: Louisville, KY

EDUCATION

2006-2009 Bachelors of Arts (Biology), Asbury University, Wilmore, KY

2010-present PhD candidate, University of Kentucky College of Medicine, Lexington, KY

SELECTED HONORS & AWARDS

08/06-12/09: Presidential Scholarship (Academic Merit); Asbury University

08/08-05-10: Sigma Zeta; Asbury University

2011-2015 Travel Award; University of Kentucky Graduate School

PUBLICATIONS

Manuscripts

Butler C.R., Boychuk J.A., and Smith B.N. (2015). Effects of rapamycin treatment after controlled cortical impact injury on neurogenesis and synaptic reorganization in the mouse dentate gyrus. *Front. Syst. Neurosci.* 9:163. doi: 10.3389/fnsys.2015.00163

Boychuk, J.A., **Butler, C.R.**, Smith, B.N. Enduring Changes in Tonic GABAA Receptor Signaling in Dentate Granule Cells After Controlled Cortical Impact Brain Injury in Mice Corresponding . *Exp Neurol.* 277:178-189 doi:10.1016/j.expneurol.2016.01.005.

Submitted

Butler, C.R., Boychuk, J.A., Smith, B.N., Differential effects of rapamycin treatment on GABAergic inhibition in mouse dentate granule cells after focal TBI. Submitted to *Exp Neurol*.

In Preparation

Boychuk, J.A., **Butler, C.R.**, Frey, L., Brooks-Kayal, A., and Smith, B.N. Inhibitory Signaling to Dentate Granule Cells Following Traumatic Brain Injury. In Preparation for *J Neurophys*.

Butler, C.R., Boychuk, J.A., Smith, B.N., Rapamycin treatment after controlled cortical impact reduces excitatory synaptic reorganization onto somatostatin interneurons from dentate granule cells but not CA3 pyramids. In Preparation for *J Neurosci*.

Abstracts

Butler, C.R., Joseph, J.E., Baldridge, B.R., (2008) Variability in face recognition for adults and children in the fusiform and inferior occipital regions. Kentucky Academy of Science (KAS), November 1, Lexington, KY

Butler, C.R., Joseph, J.E., Baldridge, B.R., (2009) The ability of adults to distinguish similarity between pairs of house images and face images both in the upright and inverted position. Kentucky Academy of Science (KAS), November 14, Highland Heights, KY

Butler, C.R., Boychuk, J.A., Smith, B.N., (2012). Jak/stat activation and gaba neuron loss after focal traumatic brain injury in mice. Society for Neuroscience (SFN), October 14, New Orleans, LA.

Boychuk, J.A., **Butler, C.R.**, Raible, D.J., Frey, L.C., Brooks-Kayal, A.R., Smith, B.N., (2012). Focal traumatic brain damage results in localized GABA neuron loss and JAK/STAT activation early following injury. American Epilepsy Society (AES), December 2, San Diego, CA

Butler, C.R., Boychuk, J.A., Smith, B.N., (2013) Inhibitory signaling to dentate granule cells following traumatic brain injury. Society for Neuroscience, Nov.12, San Diego, CA

Boychuk, J.A., **Butler, C.R.**, Smith, B.N., (2013) A role for cytokine interleukin-6 in posttraumatic epileptogenesis. American Epilepsy Society, Dec. 7, Washington DC

Raible, D.J., Boychuk, J.A., **Butler, C.R.**, Cruz del Angel, Y., Russek, S., Smith, B.N., Frey, L., Brooks-Kayal, A., (2013) Jak/STAT inhibition to prevent post-traumatic epileptogenesis. American Epilepsy Society, Dec. 7, Washington DC

Butler, C.R., Boychuk, J.A., Smith, B.N., (2014) mTOR inhibition after traumatic brain injury alters hilar interneuron excitability. Society for Neuroscience, Nov. 17, Washington DC

Boychuk, J.A., **Butler, C.R.**, Smith, B.N. (2014) Tonic GABAergic inhibitory signaling to dentate granule cell in mice following controlled cortical impact. American Epilepsy Society, Dec.6, Seattle, WA

Butler, C.R., Boychuk, J.A., Smith, B.N. (2015) mTOR inhibition after controlled cortical impact alters hilar interneuron excitability. Society for Neuroscience, Oct. 20, Chicago, IL

Boychuk, J.A., **Butler, C.R.,** Smith, B.N. (2016) Effects of controlled cortical impact brain injury on cell loss and neurogenesis in the mouse dentate gyrus. Winter Brain, Jan. 26, Breckinridge, CO

SEMINARS

Apr 2013 "Modulation of epileptogenesis after traumatic brain injury."

Department of Physiology, University of Kentucky Medical College.

PROFESSIONAL EXPERIENCES

05/08-08/08	Research Assistant, University of Kentucky, Department of Anatomy and Neurobiology, Dr. Jane Joseph Lab
05/09-08/09	Research Assistant, University of Kentucky, Department of Anatomy and Neurobiology, Dr. Jane Joseph Lab
08/10-10/10	Graduate rotation, University of Kentucky, Department of Microbiology, Immunology, and Molecular Genetics, Dr. Francesc Marti Lab
10/10-12-10	Graduate rotation, University of Kentucky, Department of Physiology, Dr. Kathryn Saatman Lab
01/11-05/11	Graduate rotation, University of Kentucky, Department of Physiology, Dr. Bret Smith Lab
05/11-present	Graduate Research Assistant, University of Kentucky, Department of Physiology, Dr. Bret Smith Lab

Professional Memberships

2011-present Society for Neuroscience

2011-present Bluegrass Chapter Society for Neuroscience